USAARL-TECH-TR--2023-17

UNITED STATES ARMY AEROMEDICAL RESEARCH LABORATORY

Impact of Transport Forces and Immobilization Practices on Patient Physiology: Evaluate Effect of Strapping Tension

Amy Lloyd, Rachel Kinsler, Kerri Caruso, Laura Kroening, & Jeffrey Molles

Notice

Qualified Requesters

Qualified requesters may obtain copies from the Defense Technical Information Center (DTIC), Fort Belvoir, Virginia 22060. Orders will be expedited if placed through the librarian or other person designated to request documents from DTIC.

Change of Address

Organizations receiving reports from the U.S. Army Aeromedical Research Laboratory on automatic mailing lists should confirm correct address when corresponding about laboratory reports.

Disposition

Destroy this document when it is no longer needed. Do not return it to the originator.

Disclaimer

The views, opinions, and/or findings contained in this report are those of the author(s) and should not be construed as an official Department of the Army position, policy, or decision, unless so designated by other official documentation. Citation of trade names in this report does not constitute an official Department of the Army endorsement or approval of the use of such commercial items.

Human Subjects Use Statement

In the conduct of research involving human subjects, the investigator(s) adhered to the policies regarding the protection of human subjects as prescribed by Department of Defense Instruction 3216.02 (Protection of Human Subjects and Adherence to Ethical Standards in Department of Defense (DoD)-Supported Research) dated 8 November 2011.

IRB Determination and Number

This study, USAARL 2021-006, was approved by the U.S. Army Medical Research and Development Command Institutional Review Board on 28 May 2021.

REPORT DOCUMENTATION PAGE	*Form Approved* *OMB No. 0704-0188*

1. REPORT DATE *(DD-MM-YYYY)*	2. REPORT TYPE	3. DATES COVERED *(From - To)*
13-02-2023	Technical Report	October 2016 - April 2022

4. TITLE AND SUBTITLE
Impact of Transport Forces and Immobilization Practices on Patient Physiology: Evaluate Effect of Strapping Tension

5a. CONTRACT NUMBER

5b. GRANT NUMBER
DM167047

5c. PROGRAM ELEMENT NUMBER
6.3/373000

6. AUTHOR(S)
Lloyd, A.[1,2], Kinsler, R.[1], Caruso, K.[1,2], Kroening, L.[1,2], & Molles, J.[1,2]

5d. PROJECT NUMBER
2021-006

5e. TASK NUMBER

5f. WORK UNIT NUMBER

7. PERFORMING ORGANIZATION NAME(S) AND ADDRESS(ES)
U.S. Army Aeromedical Research Laboratory
P.O. Box 620577
Fort Rucker, AL 36362

8. PERFORMING ORGANIZATION REPORT NUMBER
USAARL-TECH-TR--2023-17

9. SPONSORING/MONITORING AGENCY NAME(S) AND ADDRESS(ES)
Defense Health Program

10. SPONSOR/MONITOR'S ACRONYM(S)
DHP

11. SPONSOR/MONITOR'S REPORT NUMBER(S)

12. DISTRIBUTION/AVAILABILITY STATEMENT
DISTRIBUTION STATEMENT A. Approved for public release: distribution is unlimited.

13. SUPPLEMENTARY NOTES
[1]U.S. Army Aeromedical Research Laboratory, [2]Goldbelt Frontier, LLC

14. ABSTRACT
The goal of the study was to evaluate how litter strap tension affects patient biodynamics during transport. The hypothesis that strap tension has significant effects on transmitted vibration during transport was tested during three phases of testing. In Phase 1, standard tension practices were observed by having medics strap a manikin to a litter. This phase determined average litter strapping tension. Phase 2 consisted of test setup validation using an instrumented vibration manikin. The simulated patient manikin was tested on a ride simulation platform in several configurations while vibration data was collected. In Phase 3, data was collected using 25 human subject participants with varying body weights. The weight of each participant was between 102 and 275 pounds. The human subject participants were secured to a litter on the ride simulator and subjected to multiple vibration profiles. The level of strap tension did significantly affect the biodynamics of the supine patient. The effects of strap location and strap tension varied by segment because of the difference in strap proximity to and placement on each segment. Results from this project will provide significant information and strategies that can be used toward increasing patient safety, reducing discomfort, and developing vibration mitigation systems.

15. SUBJECT TERMS
Patient weight, immobilization, vibration, acceleration, rotational velocity, MEDEVAC, helicopter, ground vehicle, enroute care, vibration mitigation, vibration transmissibility, litter strap, strapping tension

16. SECURITY CLASSIFICATION OF: a. REPORT	b. ABSTRACT	c. THIS PAGE	17. LIMITATION OF ABSTRACT	18. NUMBER OF PAGES	19a. NAME OF RESPONSIBLE PERSON
					Loraine St. Onge, PhD
UNCLAS	UNCLAS	UNCLAS	SAR	98	19b. TELEPHONE NUMBER *(Include area code)* 334-255-6906

This page is intentionally blank.

Summary

Recent surveys from health care providers in the field have reported severe discomfort and pain experienced by casualties during military transport, with the pain attributed to vehicle vibration and shock. The method and degree of strapping tension varies depending on patient injuries. The level of tension may play a role in the severity of the motion transmitted to the patient's body segments. Results from this project will provide significant information and tools that can be used to increase patient safety, reduce patient discomfort, and develop vibration mitigation systems. Specifically, this project evaluated the effect of strapping tensions applied by expert medics on patients.

The hypothesis that the strap tension has a significant effect on the characteristics of transfer functions during transport was tested in three phases. In phase 1, standard tension practices were observed by having experienced medics strap a manikin to a litter and measuring the strap tension. This phase determined the average litter strapping tension. Phase 2 consisted of a test setup validation using an instrumented vibration manikin. The manikin was tested in several configurations and vibration data was collected. In phase 3, human subject data was collected using 25 human subjects with different body weights. The weight of each subject was between 46.27 and 124.74 kilograms (kg). The weight range is based on the most recent U.S. Army general population anthropometric Survey, a 5% female is 46.27 kg and a 95% male is 124.74 kg. Participants were secured to a litter on the multi-axis ride simulator (MARS) and subjected to different vibration profiles. The MARS was used to simulate real-field ride profiles from ground and air transport vehicles, and a laboratory-created vibration profile that includes vibration and repeated shock of different magnitudes and frequencies. The effect of the interaction between the two strapping tension conditions (standard tension and a low strap tension) from the magnitude of the transmitted motion to the different body segments and the resulting relative motion between the body segments were evaluated.

The results showed that under the low-tension condition, high frequency input vibration (air profile) slightly decreased overall energy transfer (area under the transmissibility curve was ~3% lower overall) but tended to increase relative segment motions and chest maximum transmissibility, while decreasing pelvis maximum transmissibility. For the under low tension conditions, low frequency input vibration (ground and white noise profiles) shifted energy from the chest and pelvis segment into the head segment. This resulted in a significant increase in the head transmissibility (up to a 19% increase) but a slight decrease and in the chest and pelvis transmissibilities. Relative segment motion was increased in the vertical direction but decreased in the horizontal directions. This was true of both the head and pelvis segments with respect to the chest, though the effects were more pronounced in the head's relative motion.

Based off the results, the use of the standard tension straps is generally preferable to the low-tension straps. The standard tension produced less absolute and relative body motion. Less motion to trauma patients would theoretically produce the best outcome.

This page is intentionally blank.

Acknowledgements

The authors would like to express sincere gratitude to the following people for their valuable contributions to this test program:

- The Dustoff Training Complex who allowed us to conduct phase 1 testing at the Dustoff Training Complex.
- The Flatiron Detachment who allowed us to conduct phase 1 testing at the Flatiron Detachment.
- ActiBioMotion for collaborating on the project and completing the data analysis.

This page is intentionally blank.

Table of Contents

List of Figures

Table of Contents (continued)

List of Tables

Introduction

A survey of active-duty U.S. Army, Reserve, and National Guard enroute care medical providers in the field have reported severe discomfort and pain experienced by casualties during military ground and air transport; pain which was attributed to vibration and repeated shock associated with the transport (Kinsler et al., 2015). The transmitted forces and vibrations to the patient's body through the transport system can have severe consequences, especially for neurotrauma patients, who are sensitive to increased intracranial pressure (Ratanalert, 2004; Reno, 2010). Prior to transport, casualties with serious injuries, such as head and back injuries, are required to be immobilized to prevent movement that may lead to further complications. Immobilization equipment includes the use of litter straps to secure the patient to the litter, and in some cases, the use of a backboard and head blocks.

Subjective observations during field evacuation of patients have indicated that cases where patients undergo unexpected mechanical shocks and motions during loading/unloading may include situations in which the litter is dropped. The transmitted severe forces/motions may have dramatic consequences on the patient health outcome and wellbeing. While motion transmitted to the human body is the main focus in most transmitted-vibration analysis studies (Meusch & Rahmatalla, 2014a, 2014b; DeShaw & Rahmatalla, 2016), the measurement of the forces transmitted to the different body segments of the supine patient during transport has not been reported in the literature.

Besides the transmitted forces to the human body, patients may also suffer from discomfort/pain resulting from the formation of pressure sores at the contact points between the patient's body and the transport system. Strapping of the patient and the degree of strapping tension varies depending on patient condition and injuries and may play an effective role in the formation of pressure sores. It may also affect the severity of the motion transmitted to the patient's neck and lower back areas. Due to the effect of inertia, it is expected that the severity of the resulting motion is proportional to the patient's body mass.

The complexity of the biodynamic response of different body segments presents a challenging task for analysis. Unexpected large body motion can dramatically change the directions of the sensors attached on the body and the transport system which can generate significant assessment and conclusion errors. However, with the current advances in new motion measurement technologies, recent publications have outlined effective methodologies to deal with such complicated environments (DeShaw & Rahmatalla, 2012). Little work has been reported in the literature regarding the effects of whole-body vibration on supine humans (DeShaw & Rahmatalla, 2015; Rahmatalla et al., 2015; Wang & Rahmatalla, 2012) compared to seated transport.

A recent study was completed by the U.S. Army Aeromedical Research Laboratory (USAARL) to evaluate the effect of patient weight as a factor when using an immobilization system versus no immobilization system (litter only) during patient transport. Significant differences were found between weight groups and immobilization configurations within weight groups, with regards to z-axis transmissibility, area under z-axis transmissibility curve, z-axis transmissibility resonance frequency, root-mean-square (RMS) z-axis acceleration, and RMS rotational velocity (Conti et al., 2020).

Military Relevance

One of the primary medical evacuation (MEDEVAC) tasks of large scale combat operations is to treat and stabilize the patient during transport and provide enroute care as required (Department of the Army, 2014). Studies reported in the literature and observations from Operation Enduring Freedom/Operation Iraqi Freedom indicate that repeated shock and vibration due to aeromedical and ground transport can cause considerable patient motion that may lead to discomfort and pain, and may be adversely affecting patients' medical outcome. Surveys of military enroute care providers stated that patients with spinal immobilization required additional sedation when transported by ground vehicles. Casualties with spinal cord injury (SCI), a tramuatic brain injury (TBI), and/or other severe neurologic injuries are the most vulnerable to vehicle repeated shock and vibration. Medical evacuation of Warfighters with head and spinal injuries, or other severe neurologic injuries, is often essential to obtain life- and function-saving treatment in a medical facility with neurosurgical capabilities. Vehicle shock and vibration during ground and air medical evacuation makes it challenging to restrict the patients' body movements during transport. When vehicle shock and vibrations act on the body, they can cause fracture destabilization and aggravation of SCI and TBI.

Patient management during military enroute care is a complex process due to numerous patient clinical conditions, patient sizes, various vehicle configurations, patient transport systems, securing methods (e.g., strapping positions and tensions), and changing vibration environments associated with transport. This project investigates the effect of strapping tension on the biodynamic response of the supine human. The project outcome is mathematical models that can be used to understand the ever-changing patient enroute care management methodology in relation to the biodynamic response of the supine human.

The long-term outcome from this work is to develop guidelines for effective best practices that can reduce secondary damages to patients during transport. Materiel designers and developers will have assessment tools for developing better vibration mitigation technologies and more effective transport systems. In the future, non-traditional casualty evacuation (CASEVAC) may be used to transport patients away from combat zones. One such technology being explored is Unmanned Aerial Systems (UAS) that could transport patients with no onboard provider, in which case it is important to ensure that patients are secure.

Objectives

The overall objective was to evaluate the effect of the strapping tension on patient vibration biodynamic response during simulated transport. The hypothesis that the tension at which the straps securing the patients to the litter produce different biodynamical responses will be tested under two strapping tension conditions including the standard strapping tension (two fingers inserted under the strap), and a low strap tension (half the tension of the standard tension).

Specific Aims

The study consisted of three phases. Phases 1 and 2 were test setup validations for phase 3. Phase 1 provided the research team with a measurement of the standard tension used to secure patient to a litter by qualified U.S. Army 68W Health Care Specialists, referred to as medics from this point forward. Specific aim 1 was accomplished in phase 1. Phase 2 consisted of test design setup evaluation and vibration profile collection using an instrumented manikin. Specific aim 2 was accomplished in phase 2. Phase 3 consisted of collecting data with human subjects using the standard tension found in phase 1 and a low strap tension, and specific aims 3 and 4 were accomplished during this phase. Any participants in phase 3 will be refer to as subjects from this point onward.

Specific Aim 1:

The team will evaluate the strapping methods and tension of medics to determine the average standard strapping tension used when securing patients to a litter.

Specific Aim 2:

The team will use the Instrumented Supine Manikin (ISMv1.2) (Deshaw et al., 2019) to validate the test setup for the phase 3 human subject testing. The ISMv1.2 will also be used to gather vibration data for test configurations in which it is unfeasible or unsafe for human subjects in phase 3.

Specific Aim 3:

The team will measure vibration in healthy humans while subjected to ride profiles on the multi-axis ride simulator while lying supine on a U.S. Army Decontaminable (Decon) litter using the standard strapping method of two finger tightness and a low strap tension (half the tension of the standard method).

Specific Aim 4:

The team will characterize the biodynamic response due to strapping tension for the standard strapping tension and the low strap tension in terms of the transmissibility function. The transmissibility concept is a very well-established biodynamical measure in the field of whole-body vibration (Griffin, 1990). It has been effectively used to quantify vibration transmitted to mechanical and biological systems, as an effective approach for designing vibration suppression systems, and as a guide for safety standards.

Hypotheses:

Null Hypothesis, H_0: Vibration transmissibility values are not significantly different between supine humans secured with the standard strap tension versus supine humans secured using a low strap tension.

Alternate Hypothesis, H_1: Vibration transmissibility values are significantly different between supine humans secured with the standard strap tension versus supine humans secured using a low strap tension.

Materials

Litter (Decon Litter) and National Industries for the Blind Canvas Webbing Patient Securing Cargo Straps (litter straps) (Figures 1 and 2).

Figure 1. Decon Litter (National Stock Number: 6530-01-380-7309).

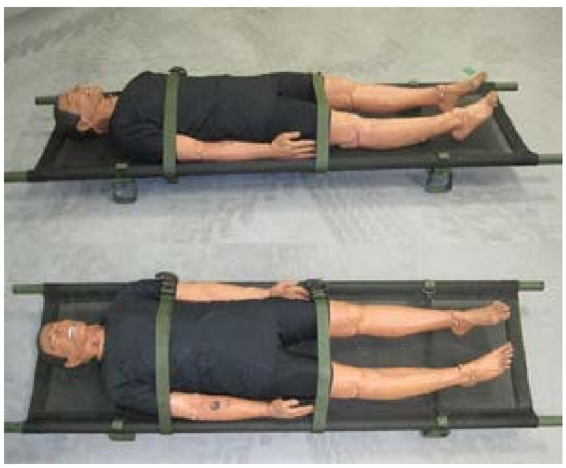

Figure 2. Litter straps test setup.

Figure 3 is the BTX-50-1 Digital Strap Tension Meter that was used for all three phases to measure the strapping tension.

Figure 3. BTX-50-1 Digital Strap Tension Meter.

Acceleration and angular velocity measurements were taken using six degree-of-freedom (DOF) sensors and tri-axial accelerometers attached to the MARS, litter, backboard, and human subject. Data were collected using Crystal Instruments CoCo-90® Dynamic Signal Analyzer and Data Collectors. GoPro HERO3® and HERO4® cameras were used to collect video in the dynamic environment.

A MARS platform was used for testing (Figure 4). The platform is supported by six pneumatically supported rams, which are piston-like devices that each move axially to support motion of the platform. The combination of these six rams allows for the movement of the platform in six degrees of freedom.

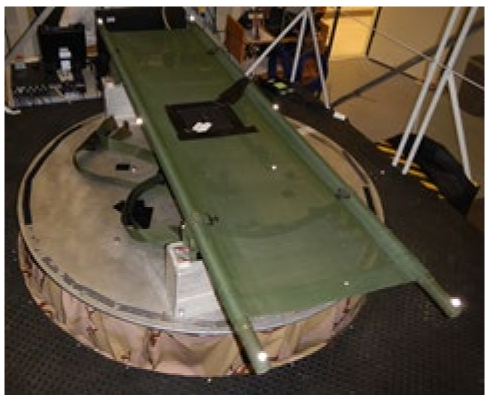

Figure 4. MARS platform.

For the Phase 2 testing the ISMv1.2 was used to collect data (Figure 5). The ISMv1.2 has built in 6DOF sensors in the head, sternum, and pelvis (red squares), and triaxial sensor in the thigh (black square).

Figure 5. ISMv1.2 manikin, and sensor locations.

Methods

The testing was completed over three phases of testing. Phases 1 and 2 were test setup validation from the human subject testing in phase 3.

Phase 1

For this phase, ten 68W Health Care Specialists were asked to secure a manikin to a litter first using whatever method they normally used, then using a method specified by the research team. Eight medics participated at the DUSTOFF Training Complex on Fort Rucker, and two medics participated at the Flatiron medical evacuation detachment on Fort Rucker. They were not given any instructions on strap placement or tension; they were also given an abundance of straps to avoid influencing the amount of straps the medic used. All of the medics either used two or three litter straps to secure the manikin. Depending on how they secured the manikin the first time, they were asked to secure the manikin again using either two or three straps (whichever was not done the first time). For each strapping configuration, the tension was measured, and pictures were taken of the strap locations. This data was used to find an average strapping tension used in the following phases. The tension was measured using the strap tension meter. Figure 6 shows the litter strapping placement for medic 1.

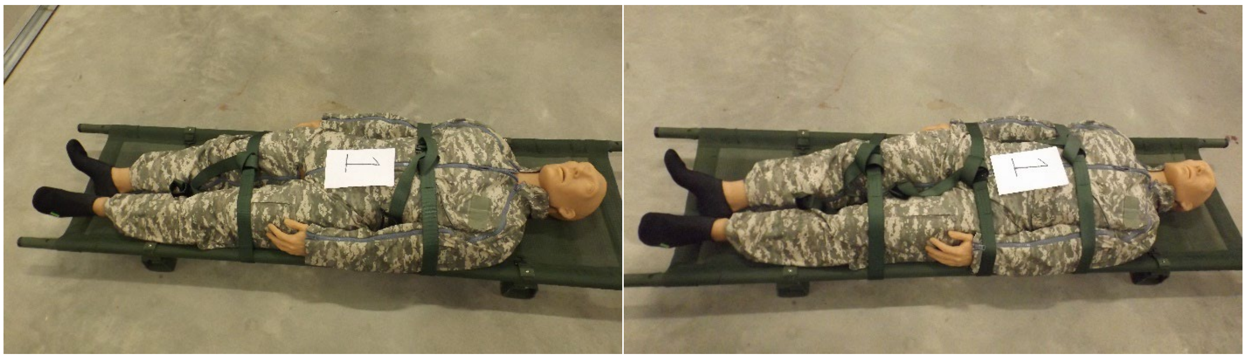

Figure 6. Litter strap placement for Medic #1 during Phase 1 testing.

Table 1 shows the data collected from the medics in phase 1. The red highlighted values are the highest and lowest values. To reduce the wide variance, these minimum and maximum values were dropped and not considered in the average or standard deviation (SD) at the bottom of the table. Medic 8's data was not considered because it was found that they did not meet the study's inclusion criteria.

Table 1. Strapping Tension Measurements for Phase 1

2 Strap Configuration		
Medic	Chest (foot-pound [lbf])	Legs (lbf)
1	10.2	10.8
2	9.8	5.2
3	8.6	10.2
4	3.8	7.2
5	2.4	4.4
6	1.6	7.2
7	4.2	5.6
9	1.2	12
10	6.2	3.2
Average	5.2	7.4
SD	3.1	2.8

3 Strap Configuration			
Medic	Chest (lbf)	Pelvis (lbf)	Legs (lbf)
1	2.2	5.6	6.6
2	9.6	14.6	3.4
3	4.8	13.2	13
4	1.2	4.6	4.4
5	5.2	1.4	3.2
6	1.6	5.2	5.8
7	8.4	15.4	7.6
9	1	5.2	1.6
10	3.6	5.6	5.2
Average	3.9	7.7	5.9
SD	2.5	4.3	3.3

Phase 2

Phase 2 testing took place on the MARS platform at the U.S. Army Aeromedical Research Laboratory, Fort Rucker, AL. This platform realistically mimics ride vibration profiles for military vehicles. Phase 2 was a test setup validation and safety check for phase 3 on the MARS table using the ISMv1.2. Several strapping placements and tensions were tested in this phase, which are listed in Table 2.

Table 2. Strapping Configurations for Phase 2

Configuration	Strap Placement	Strap Tension
1	2 Straps (chest, and legs)	Standard Tension
2	2 Straps (chest, and legs)	Low Tension
3	3 Straps (chest, hips, and legs)	Standard Tension
4	3 Straps (chest, hips, and legs)	Low Tension
5	No Straps	Not Applicable (N/A)

Three ride vibration profiles were used during the testing: Ground, air, and white noise. Each profile was approximately 60 seconds in duration. The ground vehicle profile was a ride signature collected from a military ground ambulance that was driven over a rough road with bumps. This profile contained a predominant low frequency vibration of 2 Hertz (Hz) associated with the vehicle suspension and some higher frequency elements associated with engine operation and jolts from bumps in the road. The air vehicle profile was a compilation of collected signatures from an HH-60M series MEDEVAC helicopter that was performing standard flight maneuvers. This profile contained vibrational energy with a predominant frequency of approximately 17 Hz that is associated with the operation of the main rotor. There were also some minor jolts in the profile from landing maneuvers. The white noise profile is a laboratory-created profile to cover a large range of vibrations. The maximum amplitudes in each ride profile fell within the safety standards described in the ISO 2631 series.

The standard and low strapping tensions for the 2 Strap and 3 Strap configurations were determined from phase 1. The standard tension is the average determined from the testing of the medics; the low tension is half of the average value. For the first day of testing, the straps were kept in place on both the manikin and the litter using tape (Figure 7) to prevent slippage, and the manikin wore a uniform made to replicate the motion of skin in contact with the supporting surfaces. For the second day of testing, the manikin was re-dressed in clothing that would be provided to the subjects in phase 3 and the straps were not secured with tape (Figure 8). Each day the configurations listed in Table 2 were tested. A researcher from ActiBioMotion (ABM) was present for the duration of phase 2 to help collect the data and start the analysis. ABM completed the data analysis for phase 2 and phase 3 of the project and has extensive experience in vibrational data analysis.

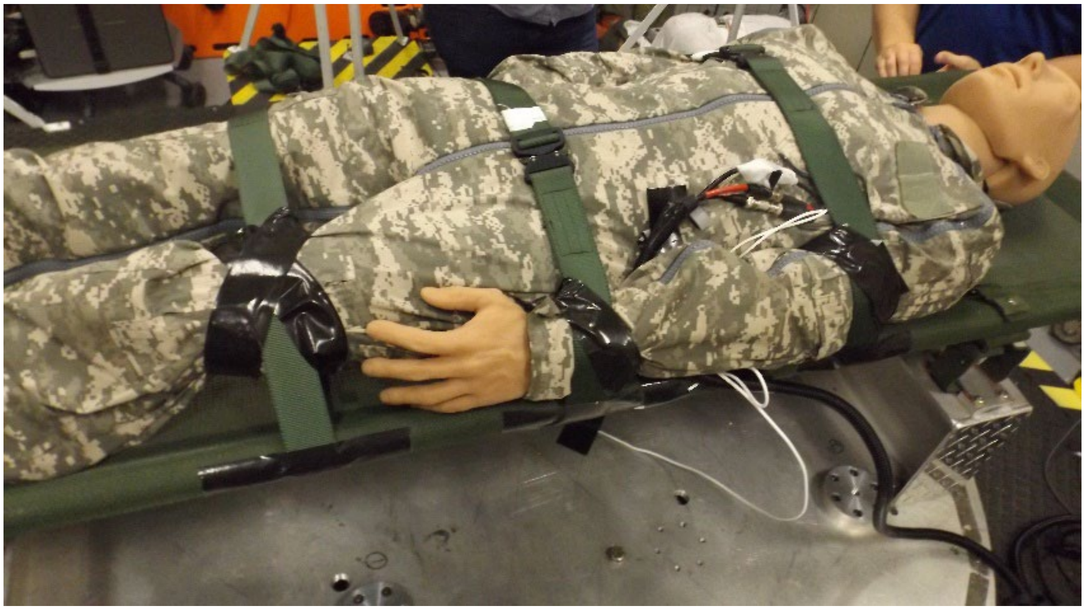

Figure 7. Day 1 litter strap securing method for Phase 2.

Figure 8. Day 2 litter strap securing method for Phase 2.

Phase 3

Phase 3 testing implemented human subject testing on the MARS. The required sample size estimation was calculated using the WebPower software repeated measures analysis of variance (ANOVA) test assuming a confidence interval of 95% and an acceptable power of 80%. A minimum of 22 subjects was found to allow sufficient power in this study to either reject or accept the null hypotheses.

Subjects 19 years of age or older who were in general good health, with no medical conditions that might be adversely affected by exposure to moderate low-frequency vibration, and with no difficulties with the application of immobilization technologies, were recruited for the study. Individuals were denied participation if they had orthopedic injuries (especially back, neck, or head injuries), poor circulation, motion sickness, diabetes, known severe skin sensitivities or allergies to adhesives, or who were pregnant. Refer to the Medical History Questionnaire for all excluding medical criteria (Appendix B). Subjects who did not fall within the target weight ranges were also excluded. Table 3 summarizes the gender and weights for each subject. A total of 25 subjects were tested during Phase 3 of the testing.

Table 3. Subjects Demographics

SUBJECT	GENDER	WEIGHT (kG)
01	Male	105.6
02	Male	82.3
03	Male	86.5
04	Male	85.4
05	Female	64.4
06	Female	74.5
07	Male	81.3
08	Male	87.6
09	Female	71.6
10	Female	52.2
11	Female	48.2
12	Male	92.5
13	Male	72.2
14	Male	69.8
15	Male	97.7
16	Female	72.4
17	Female	79.3
18	Female	71.5
19	Male	85.8
20	Female	89.3
21	Female	103.7
22	Male	80.1
23	Male	86.6
24	Female	74.9
25	Male	64.5

Possible subjects were screened on the phone for inclusion criteria and given a brief overview of the study. Subjects who were still eligible and interested were scheduled for testing. On the day of testing, subjects were first briefed on the informed consent document and any questions they had were answered. A study physician evaluated subjects before testing to make sure they were in good health and met the inclusion criteria. This information was documented on the Medical History Questionnaire. All subjects who passed the medical questionnaire were shown a MARS safety video. If subjects were interested, they were given a tour of the facility after the video. The subjects were asked to a wear long sleeve shirt and long pants for testing; if they did not wear appropriate clothing then they were given clothing and asked to change. This was to try to prevent any irritation due to the skin rubbing on the litter surface.

Before fitting subjects with sensors, anthropometric measurements were taken to help determine how the subject fit on the litter. Measurements were also used in the data analysis if a subject had outlying results. The measurements taken were:

1. Weight
2. Stature with Shoes
3. Stature without Shoes
4. Iliac Crest Height
5. Anterior Superior Iliac Crest Height
6. Bi-deltoid Breadth
7. Hip Breadth
8. Chest Depth
9. Pelvis Depth
10. Buttock Depth

Subjects were fitted with four 6DOF sensors that were placed in the center of the subject's forehead (Figure 9), on the upper sternum (Figure 10), and at the forward-most point of the left anterior superior iliac spine (Figure 11). A tri-axial accelerometer was placed two inches above the top of the patella (Figure 12). Double sided tape, 3-dimensional (3D) printed sensor mounting plates, and athletic wrap were used to secure the sensors. Details of the sensors used are described in Appendix C. A 6DOF sensor was also placed on the MARS surface (Figure 13) and a tri-axial sensor was placed underneath the litter mesh (Figure 14).

Figure 9. Forehead sensor.

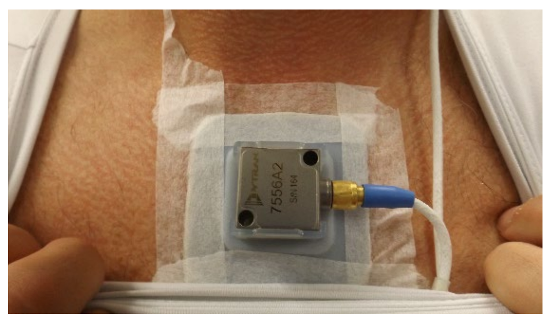

Figure 11. Sternum sensor.

Figure 10. Hip sensor.

Figure 12. Knee sensor.

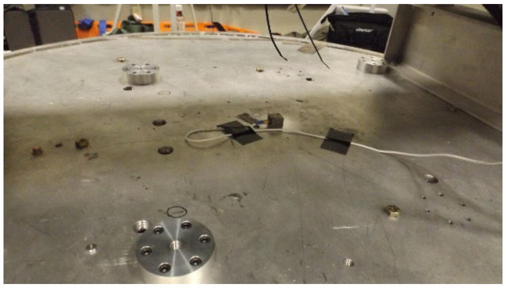

Figure 13. MARS surface sensor.

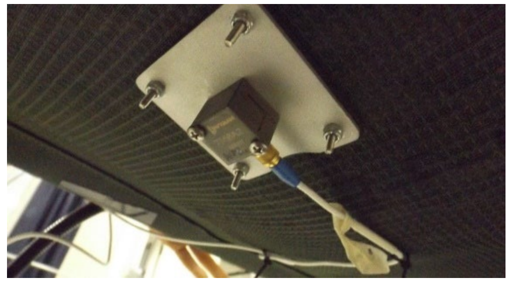

Figure 14. Litter mesh sensor.

After placing the sensors on the subjects, more anthropometric measurements were taken to record the sensor locations on the body. Then the subjects were taken to the MARS platform and secured in the first testing configuration. The order of the configurations and ride profiles were randomized between subjects.

The same three ride profiles were used in phases 2 and 3. In between each ride profile, strap tension was measured and adjusted if necessary. The subjects were also given a short verbal comfort survey to make sure that they were not in any distress after each ride profile. If subjects reported a maximum discomfort rating of seven or above, or a pain rating of three or above, the testing was stopped so the subject could be evaluated by the study physician. The study physician also evaluated participants at the conclusion of testing to ensure there were no medical concerns. To avoid slipping of the litter strap, the strap was taped to pole of the litter (Figure 15).

Figure 15. Tape to secure litter strap to litter for Phase 3.

The primary data collected under this protocol were acceleration data, angular velocity data, anthropometric measures, verbal survey data, videos, and photographs (Table 4). Medical history was collected for determination of subject suitability against inclusion and exclusion criteria but was not included in the data analyses. The videos and photographs were collected for reference and qualitative viewing of the subjects' experience. Verbal survey data was used to determine subject discomfort and/or pain during the course of testing. These ratings were an indicator of whether testing needed to be halted for subject comfort or safety and were also not included in the analysis.

Table 4. Types of Data Collected

Data Element/Variable	Source	Operational Specification
Strap Tension Data	Strap holding human subject to litter surface	0.2 pounds (lb) (1-50 lb) or 1 lb (1-500 lb)
Acceleration data	Human subject (head, sternum, pelvis), MARS platform, and ISMv1.2 manikin	200 millivolts per unit of gravity (mV/g) (+/- 5 unit of gravity (g))
Gyroscope data	Human subject (head, sternum, pelvis), MARS platform, and ISMv1.2 manikin	1 millivolt per degree per second (mV/deg/s) (+/- 1000 degree per second [deg/s])
Acceleration data	Litter surface, and human subject (knee)	174 mV/g (+/- 5 g)
Discomfort/pain ratings	Human subject	Scale 1 to 10
Anthropometric data	Human subject	Weight, height, anthropometric measurements (kg/centimeters [cm])
Video	Testing of subject on MARS	60 frames per second
Medical history	Human subject	N/A

Results

The data analysis was completed by ABM. The full report from ABM can be found in Appendix D at the end of the report.

Data Reduction and Preparation

There were two sets of vibration data analyzed for this project, the manikin data and the human subject data. The manikin data was fully synced and calibrated by its internal data acquisition (DAQ) system, but the human subject data was collected on two separate DAQ units. To sync the data, a square wave signal was input to the 16th channel on both DAQs from one source. Once the data was synced, the raw voltage data was converted to accelerations and angular velocities based on the calibration values of the individual sensors.

After all of the data had been synchronized and calibrated, the next step was to convert the local coordinates of each sensor into one global coordinate system. The global coordinate system was determined by aligning the z-axis of the multi-axis sensors with the direction of gravity.

Input Vibration Profiles

There were three vibration profiles used in the study in phases 2 and 3: air, ground, and white noise. The power spectral density (PSD) was taken of the profiles to better understand the input signals. Figure 16 shows the PSD of the profiles. The left column shows the PSD in logarithmic scale (decibels [dB]) and right column shows the PSD in a linear scale.

The air profile consisted of seven different ten-second maneuvers performed in a H-60 series MEDEVAC helicopter. The PSD analysis shows that higher energy peaks can be seen in the 17 – 23 Hz range, which is due to the passage of the four rotor blades at the main rotors fundamental frequency of approximately 4.3 Hz. The *z*-axis (yellow lines on the graph) contains the majority of the total power, which is shown on the linear scale graph. For the ground profile most of power is concentrated in the 2 Hz range, with some small peaks in the higher frequencies. Similar to the air profile, the *z*-axis contains the majority of the power. Lastly, the white noise profile had increased amplitudes in the middle frequencies. Unlike the air and ground profiles, the *x*- and *y*- axes contained the most power for the white noise profile.

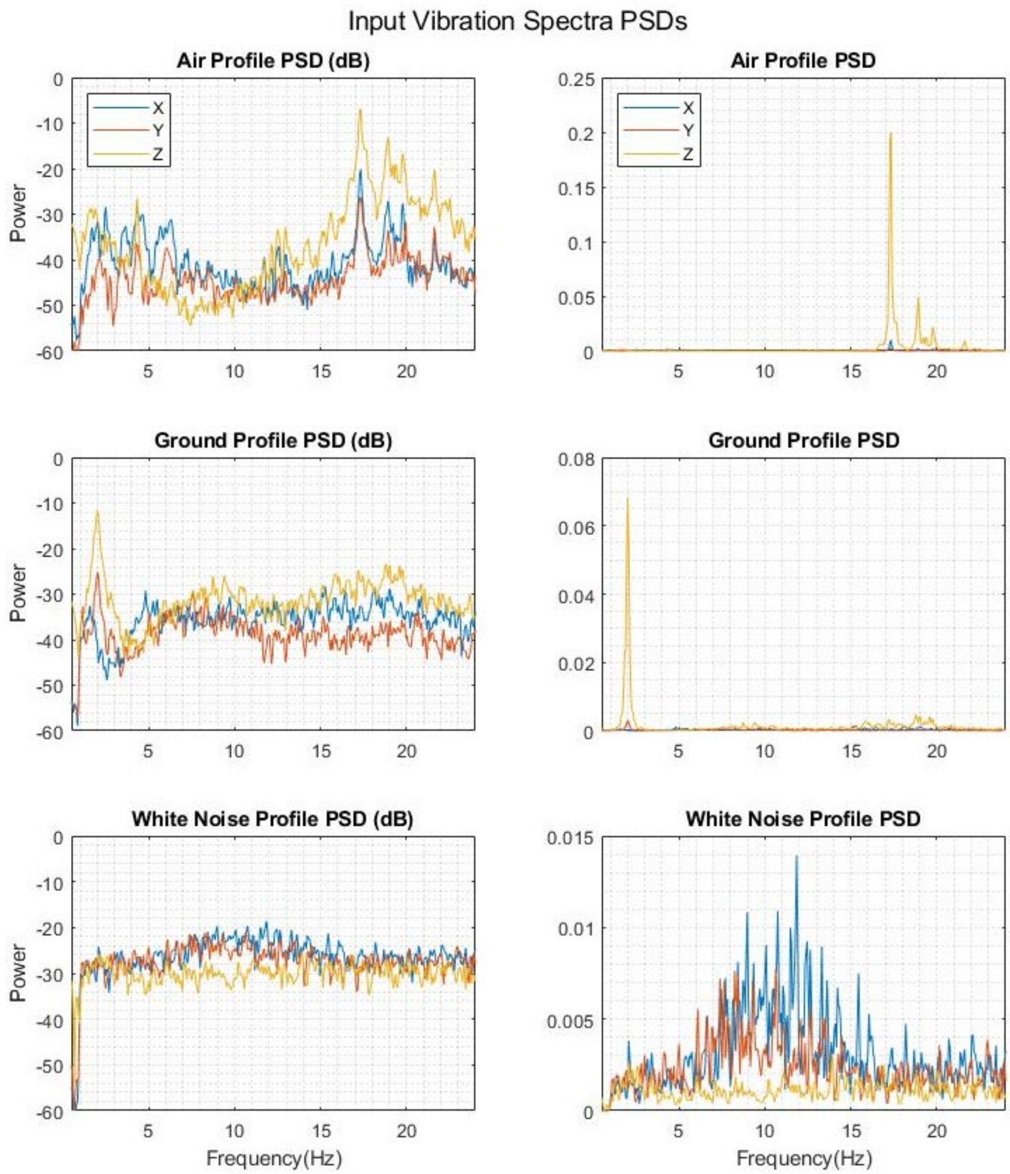

Figure 16. Power spectral densities for the three input vibration spectra expressed on a logarithmic scale as decibels (left column) and on a standard linear scale (right column).

Transmissibility

Transmissibility is the ratio of the output divided by the input. If the ratio is above 1.0 then there is amplification in the system. A transmissibility below 1.0 indicates that the output signal was attenuated, and if the ratio is equal to 1.0 then the output signal is equal to the input. Transmissibility has been used to characterize the human system as a single-output/single-input function or as a multiple-output/multiple-input function (Paddan & Griffin, 1998; DeShaw and Rahmatalla, 2014b; Hinz et al., 2010).

The transmissibility was analyzed in three different ways: (1) area under the transmissibility curve, (2) maximum transmissibility, and (3) resonant frequency. The area under the transmissibility curve is the integral of the area under the transmissibility curve from 1.1 to 22 Hz. The maximum transmissibility is the maximum amplitude of transmissibility between the ranges of 1.1 to 22 Hz. The resonant frequency is the frequency at which the maximum transmissibility is located.

Phase 2 – Manikin Results

There were five configurations tested for the manikin. These included the no straps, two straps (standard and low tensions), and three straps (standard and low tensions).

Figure 17 shows the transmissibility curves for the head segment of the manikin. The head exhibited similar transmissibility curve shapes for all three profiles. The resonant frequency for the air profiles was 8 Hz, but closer to 6.5 Hz for the ground and white noise profiles. When comparing the strapping configurations, the no strap configuration had the highest transmissibility (3.4 to 3.7), while the two strap – standard tension configuration had the lowest transmissibility (~2.4).

This space is intentionally blank.

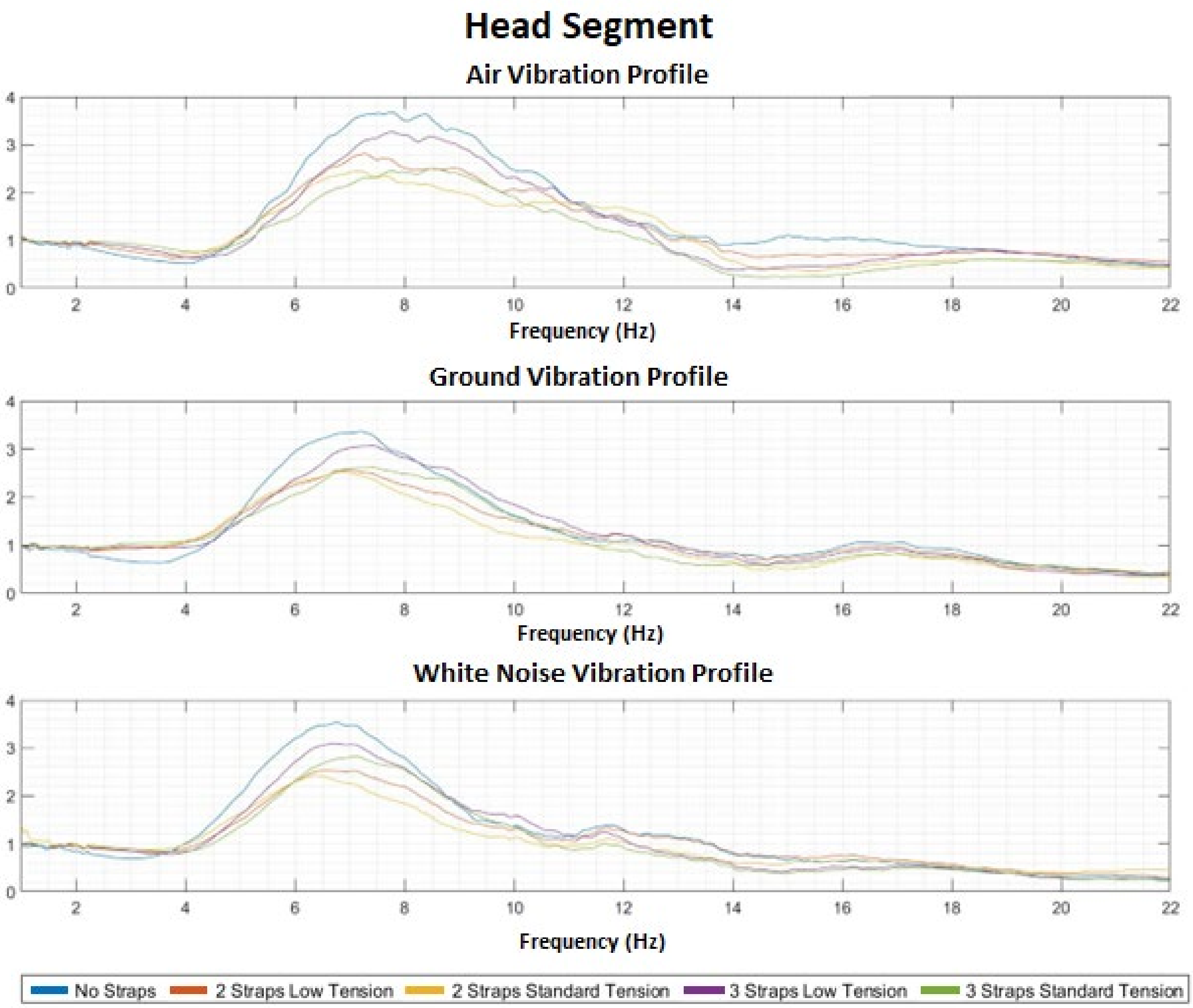

Figure 17. Transmissibility plots for the manikin's head segment.

Figures 18 through 20 show the bar plots comparing the transmissibility metrics calculated from the manikin's body segments.

This space is intentionally blank.

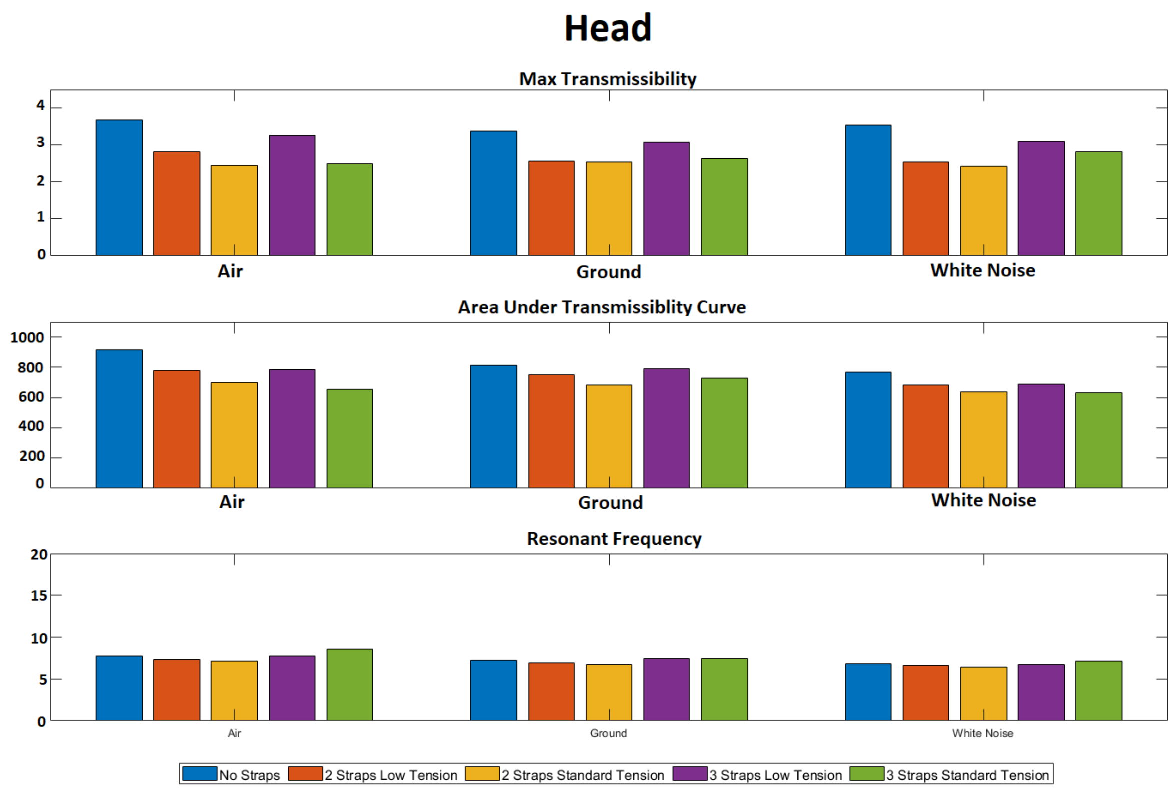

Figure 18. Bar plots comparing metrics calculated from the manikin's head transmissibility plots.

Figure 19. Bar plots comparing metrics calculated from the manikin's chest transmissibility plots.

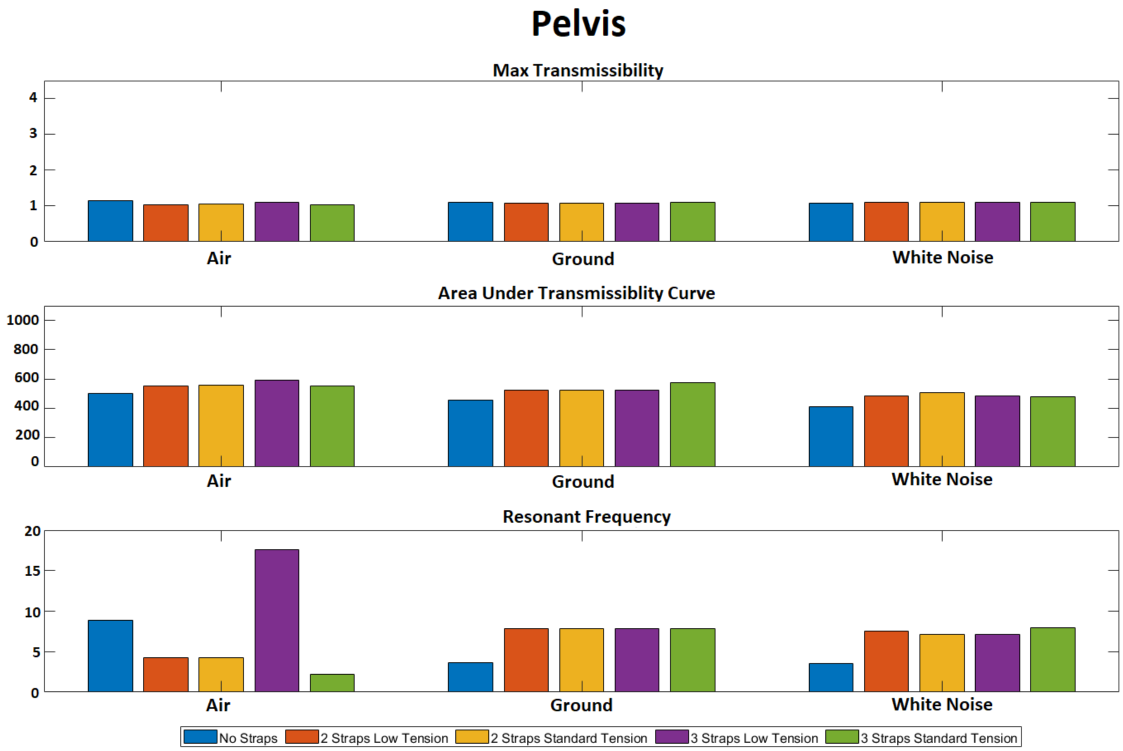

Figure 20. Bar plots comparing metrics calculated from the manikin's pelvis transmissibility plots.

Phase 3 – Human Subject Results

The human subjects were only tested in two configurations: two straps – standard tension, and two straps – low tension. Tables 5 through 7 show the transmissibility results from the data analysis. Table 5 shows the mean maximum transmissibility and the standard deviation for the body segments separated by the vibration profile and strap tension. The head segment had the highest mean maximum transmissibility and standard deviation for all of the vibration profiles and strap tensions. The pelvis had the lowest mean maximum transmissibility and standard deviation for each configuration.

Table 5. Maximum Transmissibility Mean and Standard Deviation for Phase 3

Vibration Profile	**Air**		**Ground**		**White Noise**	
Strap Tension	Low	Standard	Low	Standard	Low	Standard
Head	2.28 ± 0.64	2.43 ± 0.74	2.56 ± 0.51	2.22 ± 0.44	2.64 ± 0.59	2.35 ± 0.52
Chest	1.34 ± 0.21	1.39 ± 0.26	1.32 ± 0.15	1.33 ± 0.17	1.31 ± 0.22	1.29 ± 0.20
Pelvis	1.08 ± 0.11	1.10 ± 0.12	1.15 ± 0.13	1.19 ± 0.14	1.19 ± 0.13	1.22 ± 0.16

Table 6 shows the mean area under the curve and standard deviation. Similar to the maximum transmissibility, the head had the highest mean area under the transmissibility curve and the pelvis had the lowest.

Table 6. Area Under the Transmissibility Curve Mean and Standard Deviation for Phase 3

Vibration Profile	**Air**		**Ground**		**White Noise**	
Strap Tension	Low	Standard	Low	Standard	Low	Standard
Head	446.65 ± 80.69	455.64 ± 72.59	505.07 ± 76.84	457.91 ± 60.37	471.62 ± 76.51	443.52 ± 71.71
Chest	433.44 ± 107.84	479.42 ± 118.72	434.88 ± 88.39	476.12 ± 114.32	391.29 ± 88.77	428.60 ± 114.11
Pelvis	380.63 ± 70.60	404.54 ± 78.13	371.09 ± 78.85	391.04 ± 75.49	365.51 ± 64.70	382.94 ± 66.20

Table 7 shows the mean resonant frequency and standard deviations for the different configuration for the body segments. The chest had the highest mean resonant frequency, and the pelvis had the lowest mean resonant frequency.

Table 7. Resonant Frequency Mean and Standard Deviation for Phase 3

Vibration Profile	**Air**		**Ground**		**White Noise**	
Strap Tension	Low	Standard	Low	Standard	Low	Standard
Head	6.88 ± 0.41	7.15 ± 0.60	6.68 ± 0.47	6.57 ± 0.62	6.38 ± 0.42	6.41 ± 0.60
Chest	7.86 ± 2.65	7.52 ± 2.51	7.11 ± 2.21	6.84 ± 2.25	6.39 ± 1.59	7.03 ± 2.71
Pelvis	5.35 ± 3.54	5.64 ± 3.80	5.91 ± 2.22	6.26 ± 1.97	5.92 ± 1.55	6.35 ± 1.56

The results for each segment for phase 3 testing are as follows:

Head

- High Frequency Input (air vibration profile)
    - Maximum transmissibility showed no significant differences between the low and standard tension strap configurations.
    - Relative segment motion of the head with respect to the chest increased (up to ~5%) for the low-tension configuration.
- Low Frequency Input (ground and white noise profile)
    - Maximum transmissibility was increased (up to ~17%) in the low-tension configuration.

    - Relative segment motion of the head with respect to the chest showed that the vertical acceleration increased, but that the lateral acceleration, lateral rotational velocity, and vertical rotational velocity all slightly decreased for the low-tension configuration.

Chest

- High Frequency Input (air vibration profile)
    - Maximum transmissibility increased (up to ~9%) for the low-tension configuration.
- Low Frequency Input (Ground and White Noise Profile)
    - Maximum transmissibility and area under the transmissibility curve both increased (up to 8% and 2.4% respectively) in the low-tension configuration.

Pelvis

- High Frequency Input (air vibration profile)
    - Area under the transmissibility curve decreased (up to ~5%) for the low-tension configuration.
    - Relative segment motion of the pelvis with respect to the chest showed that acceleration and rotational velocity increased in both the lateral and vertical directions for the low-tension configuration.
- Low Frequency Input (ground and white noise profile)
    - Maximum transmissibility and area under the transmissibility curve decreased (up to ~5%) in the low-tension configuration.
    - Relative segment motion of the pelvis with respect to the chest showed that lateral acceleration increased but lateral rotational velocity decreased for the low-tension configuration.

Discussion

The study found that strap tension impacts how input vibration energy is distributed, amplified, reduced, and focused throughout a subject's body. Also, the results show that the manner of this distribution is dependent on the type of input vibration.

Phase 1 testing produced the average standard tensions that were used for the phase 2 and 3 testing. Phase 1 was also used to determine the low-tension measurement by halving the standard tension. Data from only nine medics were used to find this average, and outliers were excluded from the dataset (n = 7).

The phase 2 testing included three extra testing configurations compared to phase 3, which included no strap and three strap (standard and low-tension). When testing the manikin with the two strap configurations, the results generally trended similarly to the human subject testing. The standard tension condition reduced the maximum transmissibility and area under the transmissibility curve, especially in the head; this was also seen in phase 3 data. This suggests that the three strap and no strap configurations for the manikin are indicative of how a human would respond. When comparing three straps to two straps, adding the third strap in general tended to increase the transmissibility. The third strap also increased the relative segment motion, especially in the head. The manikin results suggest that the two-strap configuration produced less gross motion than the three-strap configuration for the strap locations tested in this study.

For phase 3 testing, if the input signal had higher frequency content, like the air profile, then the low-tension configuration exhibited a slightly lower maximum transmissibility and area under the transmissibility curve when compared to the standard tension configuration. However, it did allow more relative segment motion. If the input signal had lower frequencies like the ground and white noise configurations, then the standard tension configuration showed less motion in the body segments. The low-tension configuration for these profiles allowed transmission of more vibrational energy to the head, which increased the maximum transmissibility by up to 19% in some cases.

Conclusion

This study had a few limitations that could have affected the data. Large differences in subject anthropometry resulted in highly variable biodynamic responses between subjects, even for the same strap tension and vibration profile. The subjects' weights ranged from 48.2 – 105.7 kg, and height ranged from 154.2 – 181.2 cm. To attempt to reduce the effects of the variability in the data, intra-subject normalization was implemented. There was also a lack of repetition for the configurations on the MARS. Each strapping configuration was only tested once for each ride profile. More repetitions of the ride profiles could have altered the results since subjects may have gotten more relaxed as testing went on leading to muscle thixotropy.

Results from this project will provide significant information and strategies that can be used to increase patient safety, reduce patient discomfort, and develop vibration mitigation systems. The relative segment motion increased in the vertical direction for the low tension but decreased in the lateral directions. When transporting a trauma patient with injuries to the head or spinal column, reducing the patient's vibration in terms of both body segment acceleration and relative body segment motion is desirable. When taking the results into consideration, in general, the standard tension configuration tended to produce a more clinically favorable biodynamic response than the low-tension configuration.

References

Conti, C., Kroening, L., Lloyd, A., Kinsler, R., & Molles, J. (2019). *Effect of patient weight as a factor during use of an immobilization system versus no immobilization system* (USAARL Technical Report No. 2020-04). U.S. Army Aeromedical Research Laboratory.

DeShaw, J., & Rahmatalla, S. (2014a). Predictive discomfort in single-and combined-axis whole-body vibration considering different seated postures. *Human Factors, 56*(5), 850–863.

DeShaw, J., & Rahmatalla, S. (2014b). Effective seat-to-head transmissibility under combined-axis vibration and multiple postures. *International Journal of Vehicle Performance, 1*(3-4), 235–253.

DeShaw, J., & Rahmatalla, S. (2016). Predictive discomfort of supine humans in whole-body vibration and shock environments. *Ergonomics, 59*(4), 568–581.

Deshaw, J, Frick, E., Rahmatalla, S., Kinsler, R., & Barazanji, K. (2019). *Biodynamically validated instrumented supine manikin for evaluation of patient systems* [Abstract]. Military Health System Research Symposium, Kissimmee, FL.

Griffin, M. J. (1990). *Handbook of human vibration*. Elsevier Science.

Griffin, M. J. (1998). Predicting the hazards of WBV - considerations of a standard. *Industrial Health, 36*(2), 83–91.

Hinz, B., Menzel, G., Bluthner, R., & Seidel, H. (2010). Seat-to-head transfer function of seated men--determination with single and three axis excitations at different magnitudes. *Industrial Health. 48*(5), 565–583.

International Standards Organization (ISO). (1998). 13090-1. *Mechanical vibration and shock - Guidance on safety aspects of tests and experiments with people - Part 1: Exposure to whole-body mechanical vibration and repeated shock.* International Standards Organization.

ISO. (1997). 2631-1. *Mechanical vibration and shock - evaluation of human exposure to WBV - part 1: General requirements*. International Standards Organization.

ISO. (1989). 2631-2. *Evaluation of human exposure to WBV - part 2: Continuous and shock-induced vibration in buildings (1 to 80 hz).* International Standards Organization.

ISO. (1985). 2631-3. *Evaluation of human exposure to WBV - part 3: Evaluation of exposure to whole-body z-axis vertical vibration in the frequency range 0,1 to 0,63 hz*. International Standards Organization.

ISO. (2001). 2631-4. *Mechanical vibration and shock - evaluation of human exposure to WBV - part 4: Guidelines for the evaluation of the effects of vibration and rotational motion on passenger and crew comfort in fixed-guideway transport systems.* International Standards Organization.

ISO. (2001). 2631-5. *Mechanical vibration and shock - evaluation of human exposure to WBV - part 5: Method for evaluation of vibration containing multiple shocks.* International Standards Organization.

Kinsler, R., Barazanji, K., Lee, J., Fulton, L., & Hatzfeld, J. (2015). *Analysis of two surveys examining enroute care technologies, platforms, and space requirements* [Poster presentation]. Military Health System Research Symposium, August 2015.

Meusch, J., & Rahmatalla, S. (2014a). 3D transmissibility and relative transmissibility of immobilized supine humans during transportation. *Journal of Low Frequency Noise, Vibration and Active Control, 33*(2), 125–138.

Meusch, J., & Rahmatalla, S. (2014b). Whole-body vibration transmissibility in supine humans: effects of board litter and neck collar. *Applied Ergonomics,* 45 (3), 677–685.

Paddan, G. S., & Griffin, M. J. (1998). A review of the transmission of translational seat vibration to the head. *Journal of Sound and Vibration*, *215*, 863–882.

Ratanalert, S., Phuenpathom, N., Saeheng, S., Oearsakul, T., Sripairojkul, B., & Hirunpat, S. (2004). ICP threshold in CPP management of severe head injury patients. *Surgical Neurology*, *61*(5), 429–434.

Reno, J. (2010). Military aeromedical evacuation, with special emphasis on craniospinal trauma. *Neurosurgical Focus*, 28(5), E12.

Appendix A. Acronyms and Abbreviations

3D	3-dimensional
ABM	ActiBioMotion
ANOVA	Analysis of Variance
CASEVAC	Casualty Evacuation
cm	Centimeter
DAQ	Data Acquisition
dB	Decibels
decon	Decontaminable
deg	Degree
DOF	Degree-of-Freedom
DoD	Department of Defense
DTIC	Defense Technical Information Center
g	Unit of Gravity
Hz	Hertz
ISMv1.2	Instrumented Supine Manikin
ISO	International Standards Organization
lb	pounds
lbf	Foot-pound
kg	Kilogram
MARS	Multi-axis Ride Simulator
MEDEVAC	Medical Evacuation
mV	Millivolt
PSD	Power Spectral Density
RMS	Root Mean Square
s	Second
SCI	Spinal Cord Injury
TBI	Traumatic Brain Injury
UAS	Unmanned Aerial Systems
USAARL	United States Army Aeromedical Research Laboratory

Appendix B. Medical History Questionnaire

This space is intentionally blank.

<u>Medical History Questionnaire</u>

GENERAL HEALTH:

Date of last physical examination: ____________________

Date last consulted a doctor: ____________________

Nature of consult:

____
____
____

Are you in good health currently? YES NO - If no, why not?

____
____
____

Do you have any medical waivers (military only)? N/A NO YES – If yes, please describe

____
____
____

Do you have any profiles (military only)? N/A NO YES – If yes, please describe

____
____
____

Have you taken any medication within the past 7 days? NO YES - If yes, please describe

____
____
____

Have you ever had any neck pain or injuries? (whiplash, compression injuries, etc.) NO YES - If yes, please describe

____
____
____

Have you ever had any back pain or injuries? NO YES - If yes, please describe

____
____
____

Have you ever had any head injuries? (TBI, concussion, etc.) NO YES - If yes, please describe

____
____
____

Have you ever had unusual pain or injuries in your upper or lower limbs? NO YES - If yes, please describe

____
____
____

Have you ever had circulatory problems, including deep vein thrombosis? NO YES - If yes, please describe

____
____
____

Have you been diagnosed with diabetes?	NO	YES – If yes, please describe ______
Do you have any known severe skin sensitivities or allergies to adhesives? (glues, surgical tape, etc.)	NO	YES – If yes, please describe ______
Are you prone to motion sickness?	NO	YES – If yes, please describe ______
Are you prone to claustrophobia?	NO	YES – If yes, please describe ______

Are you currently pregnant or trying to get pregnant? N/A NO YES

Pregnancy Test Result: Negative Positive

Date of Test ______

Signature of Verifying Physician ______

Qualified for study? **NO** **YES** Reason for disqualification: ______

______
Principal Investigator's Signature & Date

______
Study Physician's Signature & Date

______
Volunteer's Signature & Date

STUDY PHYSICIAN POST-TEST ASSESSMENT

Is the subject suffering any ill effects from participation in the study? NO YES – If yes, please describe

____

____

____

If answer to first question is YES, is medical intervention recommended? N/A NO YES – If yes, please describe

____

____

____

____

Study Physician's Signature & Date

Appendix C. Sensor Information

Table C1. Sensor Placement and Channel Utilization

Data Acquisition System	Channel	Axis	Sensor Type	Sensitivity	Range	Sensor Location
1	1	AX	6 DOF (combined accelerometers and gyroscopes)	1000 millivolt per unit of volt (mV/V)	±6 unit of gravity (g)	Subject's head
	2	AY		1000 mV/V	±6 g	
	3	AZ		1000 mV/V	±6 g	
	4	GX		1 mV/deg/s	±1000 deg/s	
	5	GY		1 mV/deg/s	±1000 deg/s	
	6	GZ		1 mV/deg/s	±1000 deg/s	
	7	AX	6 DOF (combined accelerometers and gyroscopes)	1000 mV/V	±6 g	Subject's sternum
	8	AY		1000 mV/V	±6 g	
	9	AZ		1000 mV/V	±6 g	
	10	GX		1 mV/deg/s	±1000 deg/s	
	11	GY		1 mV/deg/s	±1000 deg/s	
	12	GZ		1 mV/deg/s	±1000 deg/s	
	13	X	Triaxial accelerometers	1000 mV/V	±5 g	Litter surface
	14	Y		1000 mV/V	±5 g	
	15	Z		1000 mV/V	±5 g	
	16	N/A	N/A	1000 mV/V	±5 volt (V)	Synchronization pulse (square wave CoCo-90 output)
2	1	X	6 DOF (combined accelerometers and gyroscopes)	1000 mV/V	±5 g	MARS platform surface
	2	Y		1000 mV/V	±5 g	
	3	Z		1000 mV/V	±5 g	
	4	X		1 mV/deg/s	±5 g	
	5	Y		1 mV/deg/s	±5 g	
	6	Z		1 mV/deg/s	±5 g	
	7	X	Triaxial accelerometers	1000 mV/V	±5 g	Subject's knee
	8	Y		1000 mV/V	±5 g	
	9	Z		1000 mV/V	±5 g	
	10	AX	6 DOF (combined accelerometers and gyroscopes)	1000 mV/V	±6 g	Subject's pelvis
	11	AY		1000 mV/V	±6 g	
	12	AZ		1000 mV/V	±6 g	
	13	GX		1 mV/deg/s	±1000 deg/s	
	14	GY		1 mV/deg/s	±1000 deg/s	
	15	GZ		1 mV/deg/s	±1000 deg/s	
	16	N/A	N/A	1000 mV/V	±5 V	Synchronization pulse (square wave CoCo-90 output)

Appendix D. ActiBioMotion Data Analysis Report

This space is intentionally blank.

Impact of Transport Forces and Immobilization Practices on Patient Physiology: Evaluate Effect of Strapping Tension

By ActiBioMotion LLC

January 14, 2022

Table of Contents

This page is intentionally blank

Abstract

Overview

Varying strap tension was found to have statistically significant effects on vibration response metrics of human subjects. Low strap tension, when compared against standard strap tension, increased relative motion of adjacent body segments for high frequency inputs and increased head transmissibility for low frequency inputs.

Methodology

The effect of strap tension on biodynamic response was evaluated using a manikin and healthy human subjects. The manikin was tested under both two and three strap conditions, while the human subjects were tested under only the two strap condition. Both the manikin and human subjects were tested with low and standard tension strap conditions.

The calculated vibration-based metrics (transmissibility and relative segment motion determined by the root mean squared values of translational acceleration and rotational velocity) differed greatly between human subjects. This is assumed to be due primarily to the wide range of anthropometries. To address this inter-subject variability, each subject acted as his/her own control by reporting the ratio of the low tension results divided by the standard tension results. For example, if the max transmissibility for Subject 3 was 2.5 under low tension straps and 2.1 under standard tension straps, the resulting ratio was reported as 2.5/2.1 = 1.19. This indicates that the max transmissibility was 19% greater for subject 3 for low tension strap condition when compared with the standard tension results.

The transmissibility analysis was calculated over a large frequency range (1.1 – 22 Hz). This wide frequency band ensured a comprehensive and robust analysis of the differences between strap conditions. However, while the use of such a wide frequency range preserved statistically significant differences between the conditions, it tended to minimize the magnitude of the differences. Therefore, the analysis was repeated over a smaller frequency range (5-9 Hz) via a bandpass filter, both to verify the previous results and to mitigate the minimization of magnitude differences. The bandpass results corroborated the original results, and provided what can be considered a more accurate assessment of the magnitude differences. For this reason, numerical differences listed in the results section of this abstract are primarily drawn from the bandpass results.

Results

<u>High Frequency Input</u>: Under the low tension condition, high frequency input vibration (Air Vibration Profile) slightly decreased overall energy transfer (area under the transmissibility curve was ~3% lower overall) but tended to increase relative segment motions and chest max transmissibility, while decreasing pelvis max transmissibility.

<u>Low Frequency Input</u>: Under low tension conditions, low frequency input vibration (Ground and White Noise vibration profiles) shifted energy from the chest and pelvis segment into the head segment. This resulted in a significant increase in the head transmissibility (up to a 19% increase) but a slight decrease and in the chest and pelvis transmissibilities. Relative segment

motion was increased in the vertical direction, but decreased in the lateral directions. This was true of both the head and pelvis segments with respect to the chest, though the effects were more pronounced in the head's relative motion.

Response by Segment:

Head

- High Frequency Input (Air Vibration Profile)
  - Max Transmissibility showed no significant differences between strap conditions
  - Relative segment motion of the head with respect to the chest increased (up to ~5%) in the low tension configuration.
- Low Frequency Input (Ground and White Noise Profile)
  - Max Transmissibility was increased (up to ~17%) in the low tension configuration
  - Relative segment motion of the head with respect to the chest showed that the vertical acceleration increased, but that the lateral acceleration, lateral rotational velocity, and vertical rotational velocity all slightly decreased.

Chest

- High Frequency Input (Air Vibration Profile)
  - Max transmissibility increased (up to ~9%) for low tension condition.
- Low Frequency Input (Ground and White Noise Profile)
  - Max Transmissibility and Area under the transmissibility curve both increased (up to 8% and 2.4% respectively) in the low tension case.

Pelvis

- High Frequency Input (Air Vibration Profile)
  - Area under the transmissibility curve decreased (up to ~5%) for the low tension case.
  - Relative segment motion of the pelvis with respect to the chest showed that acceleration in the and rotational velocity increased in both the lateral and vertical directions
- Low Frequency Input (Ground and White Noise Profile)
  - Max Transmissibility and Area under the transmissibility curve decreased (up to ~5%) in the low tension case.
  - Relative segment motion of the pelvis with respect to the chest showed that lateral acceleration increased but lateral rotational velocity decreased.

Discussion

The human results corroborated the manikin results (in terms of the two strap condition), lending credence to the manikin's three strap results, which suggested that two straps resulted in a lower maximum transmissibility response than the three straps configuration, which is in general more desirable for patient transport. Note that these results may be limited to this experiment, and results may change if the strap placement is different.

It is outside the scope of this work to draw or infer causal relationships between vibration-induced subject motion and injury severity or incidence. However, it is reasonable to assume that reducing patient motion (in the form of max transmissibility and relative segment motion) may provide better patient outcome. The analysis and discussion of this work will be presented with this assumption in mind.

Overall, the results suggest the use of standard tension straps is generally preferrable to low tension straps, since the standard tension produced less absolute and relative body motions. Clinically, this is desirable to stabilize trauma patients with severe injuries including spinal and head injuries. When considering a large frequency band, many of observed differences were statistically significant, though the actual difference between the strapping conditions was small. However, when examination was completed with more narrow frequency bands, the benefits of the standard tension straps became more pronounced – standard tension straps generally, though not always, resulted in lower max transmissibilities than low tension straps. Max transmissibility determines the greatest magnification of input vibration that will occur in a subjects body segments. Therefore, reduction of max transmissibility, in general, will reduce discomfort and pain in supine patients (Kinsler et al, 2015; Rahmattala and DeShaw, 2015).

That standard tension straps did not universally reduce vibration and relative segment motion better than low tension straps should not be seen as an endorsement of low tension strap use. Rather, it should be taken as a reflection of the large number of variables (and their interplay) tested and the complexity of the human biodynamic response, not an endorsement of low tension straps.

Two potential limitations of this study were the large variation in subject anthropometry and the lack of trial repetition. The anthropometric variations were largely mitigated by use of intra-subject comparison and normalizing each subject's low tension results to his/her standard tension results. The lack of trial repetition refers to the fact that each subject was exposed to each condition only once. Repeating the same trial multiple times could have altered the results. This would be especially true if the subjects became accustomed to vibration with each trial and relaxed their muscles more as the trials progressed. If such a relaxation effect was present, it could mitigate the randomization of the trial order.

Introduction

Recent surveys on health care providers in the field have reported severe discomfort and pain experienced by casualties during military ground and air transport and attributed the pain to vibration and repeated shock associated with the transport (Kinsler, Barazanji, Lee, Fulton, and Hatzfeld, 2015). The transmitted forces and vibrations to the patient's body through the transport system can have severe consequences, especially for neurotrauma patients sensitive to increased intracranial pressure (Ratanalert, 2004; Reno, 2010). Prior to transport, casualties with serious injuries such as head and back injuries are required to be immobilized to prevent movement that may lead to further complications. In some circumstances, patients may get transported using only litters with no backboard.

Subjective observations during field evacuation of patients have indicated cases where patients undergo unexpected mechanical shocks and motions during loading/unloading that may include situations with litter dropping. The transmitted severe forces/motions may have dramatic consequences on the patient health outcome and well-being. While motion transmitted to the human body is the main focus in most transmitted-vibration analysis studies (Meusch and Rahmatalla, 2014a, 2014b; DeShaw and Rahmatalla, 2016), the measurement of the forces transmitted to the different body segments of the supine patient during transport has not been reported in the literature.

Besides the transmitted forces to the human body, patients may also suffer from discomfort/pain resulting from the formation of pressure sores at the contact points between the patient's body and the transport system. Strapping the patient and the degree of strapping tension varies dependent on patient condition and injuries, and may play an effective role in the formation of pressure sores. It may also affect the severity of the motion transmitted to the patient's neck and lower back areas. Due to the inertial effect, it is expected that the severity of the resulting motion will be proportional to the patient's body mass.

The complexity of the biodynamic response of different body segments presents a challenging task for analysis. Unexpected large body motion can dramatically change the directions of the sensors attached on the body and the transport system, which can generate significant assessment and conclusion errors. However, with the current advances in new motion measurement technologies, recent publications have outlined effective methodologies to deal with such complicated environments (DeShaw and Rahmatalla, 2012). Little work have been reported in the literature in the area of effects of whole body vibration on supine humans (DeShaw and Rahmatalla, 2015) compared to seated transport.

A recent study was completed by USAARL to evaluate the effect of patient weight as a factor when using an immobilization system versus no immobilization system (litter only) during patient transport. Significant differences were found between weight groups and immobilization configurations within weight groups, in regards to vertical transmissibility, area under the vertical transmissibility curve, vertical transmissibility resonance frequency, root mean square (RMS) z-axis acceleration, and RMS rotational velocity (Conti, Lloyd, Kinsler, Kroening, and Molles, 2020).

In this study, the effect of the strap tension with which subjects were fixed to the litter (without a spine board) on the subject's biodynamics response was explored. The strap tension applied by medics during transport is often determined by the acting medic's training and experience. The purpose of this study was to identify and characterize the effects of different strap tensions. This characterization was carried out via metrics based on transmissibility (primarily max transmissibility) and relative segment motion.

Methods

This study had two phases of data collection. One made use of the Instrumented Supine Manikin for Vibration (ISMV, developed by ActiBioMotion LLC), and the other included 25 human subjects of varying anthropometry. In both phases, the data collection process was the same – the manikin or subject was exposed to three different vibration spectra (termed Air, Ground, and White Noise) while secured to the litter with two straps under standard tension or low tension. The manikin was also tested with no straps as well as three straps at both standard and low tension. Overall, this led to 15 trials for the manikin (five strap conditions at each of the three vibration profiles) and 150 trials for the human subjects (25 subjects tested at two strap conditions for each of the three vibration profiles).

The images below (Figure 1, Figure 2, Figure 3, and Figure 4) provide detail and context for the aforementioned strap conditions, ISMV, and overall setup. Figure 1 shows the three strap conditions as applied to the manikin. The same approach/strap locations were used on the human subjects, with the exception of the no strap and three strap conditions, which were not tested on human subjects. The rigid platform of the vibration (shaker) table can be seen in the bottom two images; it is the silver-colored circular plate. Figure 2 shows the locations of the body segment sensors in the manikin (internal) and the human subjects (external). Figure 3 and Figure 4 show the locations of the auxiliary sensor (measured the input vibration) and the vibration table sensor respectively.

Figure 1: Images of the three utilized strap conditions. At top is the no strap condition, left is the two-strap condition, and right is the three-strap condition.

Figure 2: Instrumented Supine Manikin for Vibration (ISMV) in the two-strap condition with the body segment sensors identified by red squares. From left to right, the identified segments are the thigh, pelvis, chest, and head. The sensors are internally located for the ISMV, and externally located for the human subjects.

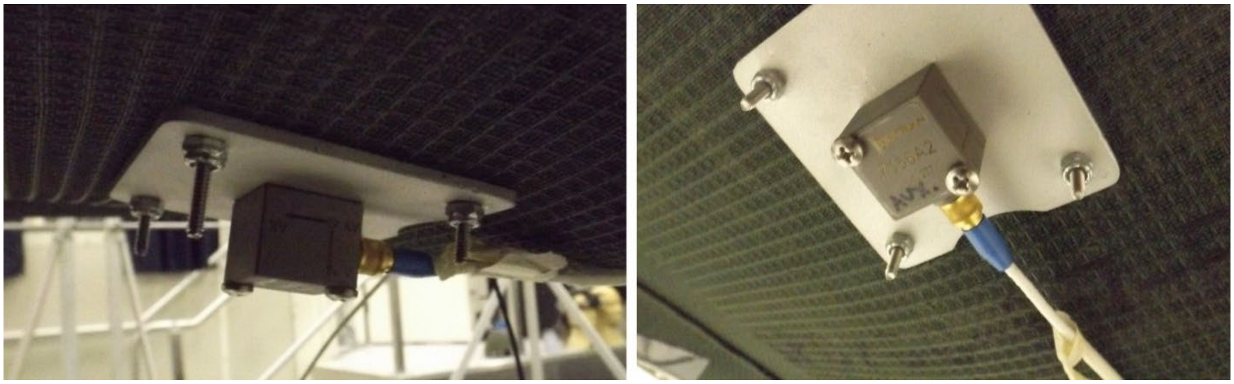

Figure 3: Location of the auxiliary sensor, and how it was mounted. This sensor was placed on the bottom of the litter mesh, and provided the measurements of the input vibration. As seen on the left, the wire was taped to the mesh to prevent wire motion from interfering with the sensor readings.

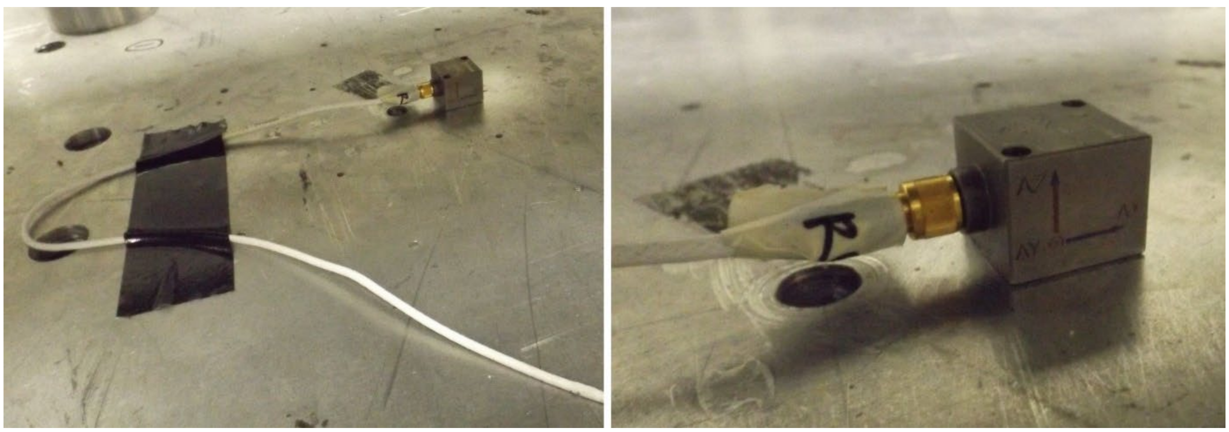

Figure 4: Location of the vibration table sensor, and how it was mounted. The wire was taped to the table to prevent wire motion from interfering with the sensor readings.

Strap tension was measured via digital strap tension meter (Tensitron BTX-500-1 or BTX-50-1), and the value for standard tension had been previously determined by measuring the tensions at which several field medics secured the straps. Low tension was defined as half the value of standard tension.

Input Vibration Profiles

The vibration profiles were termed Air, Ground, and White Noise, with the terms reflecting the content used to generate each profile. Figure 5 shows the power spectral densities (PSD) of these three profiles. The left columns of the figure express the PSD on a logarithmic scale (decibels) and the right columns express it on a linear scale. *Note that while the y-axis limits are the same for the left column, they vary significantly in the right column*. For example, the max power of the air profile is nearly 15 times greater than the max power of the white noise profile.

The air profile was ~70 seconds long, and consisted of seven different ten-second vibration signatures collected from an H-60 series MEDEVAC helicopter performing standard maneuvers. The PSD shows the majority of the power is concentrated at 17 – 23 Hz (due to the blade rotor).

Furthermore, the Z axis (vertical gravity direction) contains the vast majority of the total power. The ground profile has most of its power concentrated at 2 Hz, but there is some power at the higher frequencies as well. As with the air profile, the Z axis contains the vast majority of the overall power. Finally, the white noise profile exhibits power from 1 – 24 Hz, with increased power at the middle frequencies in the lateral directions. Unlike the other profiles, the fore-aft axis (X axis) and side-to-side lateral axis (Y axis) of the White Noise profile contained more power than the Z axis.

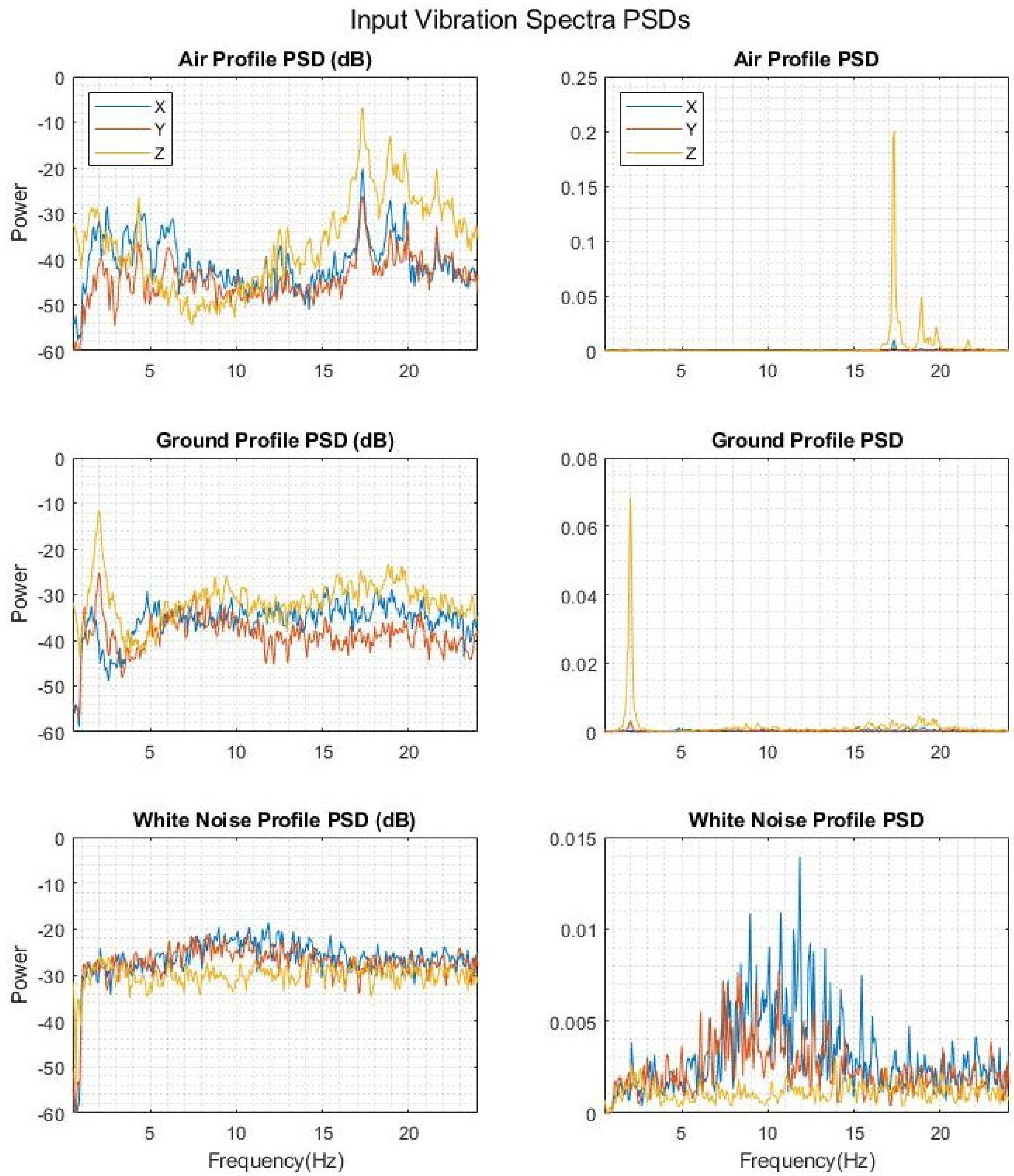

Figure 5: Power spectral densities for the three input vibration spectra expressed on a logarithmic axis as decibels (left column) and on a standard linear axis (right column).

Data Reduction

The data collected by the manikin was exported fully synced and calibrated, but the data from the subjects was exported as voltages from two un-synced Data Acquisition (DAQ) systems, called Cocos. To allow for time-syncing, the 16th channel of each Coco DAQ produced and recorded a square wave. As the voltages from these channels were known to be equivalent with the exception of a time delay, cross-correlation algorithms were used to determine and remove the time delay. Once the DAQs were synced, the voltages were converted to accelerations and angular velocities based on the calibration data provided by USAARL. After the calibration was applied, the resulting values were checked and another set of calibration values was requested from USAARL if the values were demonstrably off (such as if the norm of the accelerometer values at rest were not close to that of gravity).

Data Preparation

Once all the data had been synced and calibrated, the next step was to make the measurements from different segment locations comparable by converting the measurements of all the sensors made in multiple local coordinate systems (LCS) to a single, shared, global coordinate system (GCS). Said GCS is determined by aligning the Z axis with the direction of gravity – further details can be seen in Figure 6 below.

Figure 6: Definition of the global coordinate system used for data processing. The global X axis passes through the manikin, entering through the soles of the feet and exiting the top of the head. The global Y axis was mutually perpendicular to the global X and Z axes.

The process of converting the measurements made in the multiple LCSs to a shared GCS was accomplished via a process called sensor fusion. Sensor fusion is the process of combining the measurements of two or more sensors to compensate for each sensor type's weakness. Typically, the sensor measurements are propagated through a model such that each sensor generates its own prediction of some underlying state (the state estimation). The state estimations are combined with knowledge of each sensor's error characteristics to generate a single, more accurate state estimation. Here, the accelerometer can be used to identify the vertical gravity vector, but only if there is little free acceleration (free acceleration is acceleration other that caused by gravity). Conversely, the gyroscope data can be integrated (the initial conditions are provided by the accelerometer's orientation estimate) to obtain very accurate orientation estimates, but the accuracy degrades over time. Applying sensor fusion allows the orientation estimates of the accelerometer and gyroscope to be combined such that the gyroscope stabilizes the estimates of the accelerometer during periods of free acceleration, and the accelerometer estimates stabilize the gyroscope's drift over time (Madgwick et al., 2011). The end result is a robust estimation of sensor orientation over time.

Two issues of import are horizontal orientation drift, and the orientation estimates of the locations that only have accelerometric measurements. Horizontal orientation drift occurs because the accelerometer cannot provide a stabilizing measurement of a horizontal vector, subjecting the yaw measurement to a time-based drift. This is mitigated through a series of techniques designed to reduce integration drift by minimizing gyroscope bias (the cause of the drift). As for the locations where only accelerometric data is available (i.e. the litter and thigh), frequency filtering is used to remove free acceleration and an optimization protocol (gradient descent) is implemented to maximize the accuracy of the orientation estimates.

After completion of the sensor fusion process, the data consisted of three parts: (1) LCS measurements, (2) GCS measurements, and (3) the sets of quaternions/rotation matrices used to project measurements from the LCS to the GCS. The orthogonality of rotation matrices guarantees that their inverse is equal to their transpose, therefore the rotation matrices needed to convert from the GCS to the LCS were also readily available (as no further calculation was required).

General Transmissibility Calculations

Transmissibility is a metric that describes how energy propagates through a system. Specifically, it is a transfer function that provides the ratio of an output metric to the input metric as a function of frequency. This built-in normalization property makes transmissibility attractive as a method for comparing vibration output. However, as with other digitally applied frequency-based metrics, such as the Discrete Fourier Transform, rigorous attention must be paid to the input parameters to ensure that the results are not contaminated by mathematical artifacts. In this study the most relevant transmissibility parameters was the window size. Window size has an effect analogous to that of the span of a moving average filter, though the effects of window size are reversed. Too large a window will leave the data noisy and discontinuous, but too small a span will remove much of the information from the data. To illustrate this, consider the well-known Welch's method for estimating spectral density, which applies windowing and averaging to generate a modified periodogram that is often more useful than the original periodogram. Specifically, the Welch method reduces the noise content of a periodogram by reducing the frequency resolution.

It should be noted that transmissibility can be calculated from any link set of input and output metrics. For example, the transmissibility relating the input vibration in the X axis with the output vibration in the Y axis could be calculated. In this report, transmissibility refers specifically to the transfer function obtained by relating the input vibration (as measured by the litter-mounted auxiliary sensor) in the vertical Z axis (Figure 6) to the output vibration in the same axis (mounted on the various body segments. This is sometimes referred to as the ZZ transmissibility in the literature.

Returning to the methodology of the transmissibility calculations in this project, the useful window size, that is the window size that reduces noise whilst retaining the necessary frequency resolution, varies based on both input and output frequency content. In this study, the frequency content of the input varied greatly (see Figure 5), and the frequency content of the output also varied greatly due to the large variation in anthropometry of the human subjects. This led to scenarios where a particular window size was ideal for one subject but produced noisy and discontinuous results for another.

To overcome this dilemma in processing data from human subjects, it was decided that the same, very large window would be used for all trials, subjects, and vibration profiles (analogous to a very small span in a moving average filter). This generated results with a very high frequency resolution but a large amount of noise. Therefore, a moving average filter was applied directly to the calculated transmissibility to denoise it. The span of the moving average filter applied was 75 samples, roughly one tenth of the overall sample length of 720.

Three different metrics were calculated from the transmissibility curves: (1) Max Transmissibility (MT), (2) Area under the transmissibility curve (AuT), and (3) Resonant Frequency (Wn). The MT is maximum transmissibility value over the frequency range of 1.1 – 22 Hz. The range starts at 1.1 Hz because below that frequency the transmissibility calculation can become noisy, leading to incorrect maximum identification. The 1.1 Hz value will be the starting frequency for all three of the metrics for that same reason. AuT is the integral of the transmissibility plot from 1.1 – 22 Hz. Wn is the frequency at which the MT is located.

In order to statistically assess the significance of the differences between the aforementioned metrics, a t-test with significance level of $\alpha = 0.05$ was used, and p-values less than 0.10 were considered marginally significant. These standards for significance were used for all statistical testing in this report.

The transmissibility metric is useful as it normalizes the results based on the input. However, it does not contain any form of normalization with respect to inter-subject variability. Variations in transmissibility can be substantial due to varying subject anthropometries. To normalize for inter-subject variability, intra-subject normalization was applied in which intra-subject ratios were calculated and then subjected to the t-test. That is, instead of comparing the MTs for all subjects in the low tension case with the MTs of the standard tension case, an MT ratio was calculated for each subject. For each subject the MT of the low tension case was divided by the MT of the standard tension case, resulting in a ratio. If the corresponding MTs were equal, the ratio would be equal to one. Therefore, the ratios for all 25 subjects were subjected to a t-test to determine if the set of ratios varied significantly from the null hypothesis case of 1. This ratio-based approach was applied for all transmissibility and relative segment metric comparisons that involved human subjects. This process will henceforth be referred to as intra-subject normalization. Finally, to provide context, the calculations and t-test results calculated from the data without intra-subject normalization was also calculated and presented.

Bandpass Transmissibility Calculations
As discussed above, the transmissibility calculations covered a broad frequency range (1.1 – 22 Hz) and a moving average filter was applied the results. This approach was taken to provide the most complete and robust analysis possible. However, examining such a broad frequency range and applying a filter are likely to have an "averaging" effect on the results. This "averaging" is intended to minimize the effects of things like numerical artefacts from impacting the results, especially as much of the considered frequency range has either little input energy or produces little output energy. This is important to ensure that overall trends can be robustly detected. However, this "averaging" will also likely have a mitigating effect on the magnitude of difference between the conditions being compared.

In order to address this mitigation of magnitude difference, a second set of transmissibility calculations were carried out, in which a bandpass filter is used to isolate the frequency band of 5 – 9 Hz, and no moving average filter is applied. The 5 – 9 Hz range was chosen as it exhibited both sufficient input energy and biodynamic response across the majority of vibration profiles that the transmissibility calculations would not be overly impacted by contaminating factors such as numerical artefacts, and would not need to subjected to the moving average filter. Therefore, the overall trends in this range should still be robustly detectable, but the magnitude of difference will not be minimized.

Other than application of a 5 – 9 Hz bandpass filter and lack of moving average filter application, these transmissibility calculations and analysis were carried out the same as the previous transmissibility calculations. These results will be presented in the Appendix as supporting evidence (Figure 33, Figure 34, and Figure 35).

Segmented Air Profile Transmissibility

As previously mentioned, the Air vibration profile is not single, continuous signal but is rather a combination of seven different ten second segments of varying frequency spectra. The flight maneuvers associated with each of the seven segments are listed below in the temporal order they occurred in:

1. Ground with Rotors Turning
2. In Ground Effect Hover (10 ft above ground hover performance)
3. Out Ground Effect Hover (70 ft above ground hover performance)
4. Approach to Hover (SHUDDER) (high vibration visual approach)
5. Roll-on Landing (high-speed rolling landing)
6. Rolling Take Off (high-speed rolling take-off)
7. Flight at Vh (maximum speed for level flight)

The list above shows that the seven segments vary widely in content. Therefore, in addition to assessing the profile as a whole (as was discussed in the previous section), it was decided that the transmissibility of each segment should be examined individually to assess the impact of varying the strap tension. The purpose of examining the Air profile when broken into time segments is intended to provide insight into the complex vibration environment exhibited by aircraft. In order to determine statistical significance, and to graphically present the data in a meaningful way, the data for these calculated was subject to intra-subject normalization as in the previous section. Significance values were calculated via t-test and presented. Plots showing the means and standard deviations corresponding to said significance values are also presented.

Relative Segment Motion

Another set of metrics investigated centered around the analysis of how the head and pelvis segments moved with respect to the chest segment. The first set of metrics were inertial-based, that is the triaxial acceleration and angular velocity of head relative to the chest. From the sensor fusion process, all sensor data could be expressed in the global CS as well as the local CS. Furthermore, the time-varying quaternions/rotation matrices describing the orientation of each sensor/segment was also known. These calculations were applied to both the manikin and human subject results. Relative motion between the head and chest, as well as between the pelvis and chest were considered. All results are expressed in the local CS of the chest segment's sensor.

In order to calculate relative segment motion, local segment measurements and the corresponding orientations (in the form of quaternions/rotation matrices) are leveraged. Relative segment motion is found by simply subtracting the measurements of one segment from the other. The complexity lies in ensuring that the measurements are expressed in the same CS, and that the difference is expressed in the correct CS. The process for obtaining the acceleration of the head segment with respect to the chest is explained below, but it can be readily adapted to accommodate the pelvis in lieu of the head.

$$R_{Chest} = R * R_{Head}$$

Equation 1

$$R = R_{Chest} * R_{Head}^{T}$$

Equation 2

$$a_{Head}^{Chest} = R * {a_{Head}^{Head}}^{T}$$

Equation 3

In Equation 1, $\mathrm{R}_{\mathrm{Chest}}$ is the orientation matrix defining the chest segment frame, $\mathrm{R}_{\mathrm{Head}}$ is the orientation matrix defining the head segment frame, and R is defined as the rotation matrix that transforms $\mathrm{R}_{\mathrm{Head}}$ into $\mathrm{R}_{\mathrm{Chest}}$. In Equation 2 and Equation 3 the superscript T denotes the matrix and vector transpose respectively. In Equation 3, a_{Head}^{Chest} denotes the acceleration measured at the head segment expressed in the chest segment frame (expressed as a 3x1 column vector), and a_{Head}^{Head} denotes the acceleration measured at the head segment expressed in the head segment frame.

$$a_{Head/Chest}^{Chest} = a_{Head}^{Chest} - a_{Chest}^{Chest}$$

Equation 4

The formatting of **Error! Reference source not found.** is the same as previously, with the addition that $a_{Head/Chest}^{Chest}$ denotes the acceleration of the head segment relative to the chest segment expressed in the chest segment frame.

The root mean square was applied to the relative segment motion calculation to allow for straightforward comparison. As was done with the transmissibility results, intra-subject normalization was also applied to the calculated relative segment motion metrics, and the results subjected to t-tests. Also as was done for the transmissibility data, the calculations and t-test results calculated from the relative segment motion data without intra-subject normalization was also calculated and presented.

Results

Manikin Results

To simplify discussion of the strap conditions used on the manikin, the following acronyms will be utilized:

- NS-C for the no strap case
- 2S-LT-C for the two strap low tension case
- 2S-ST-C for the two strap standard tension case
- 3S-LT-C for the three strap low tension case
- 3S-ST-C for the three strap standard tension case

To display the manikin results, first the transmissibility curves will be shown, then bar plots comparing metrics derived from the transmissibility plots will be shown

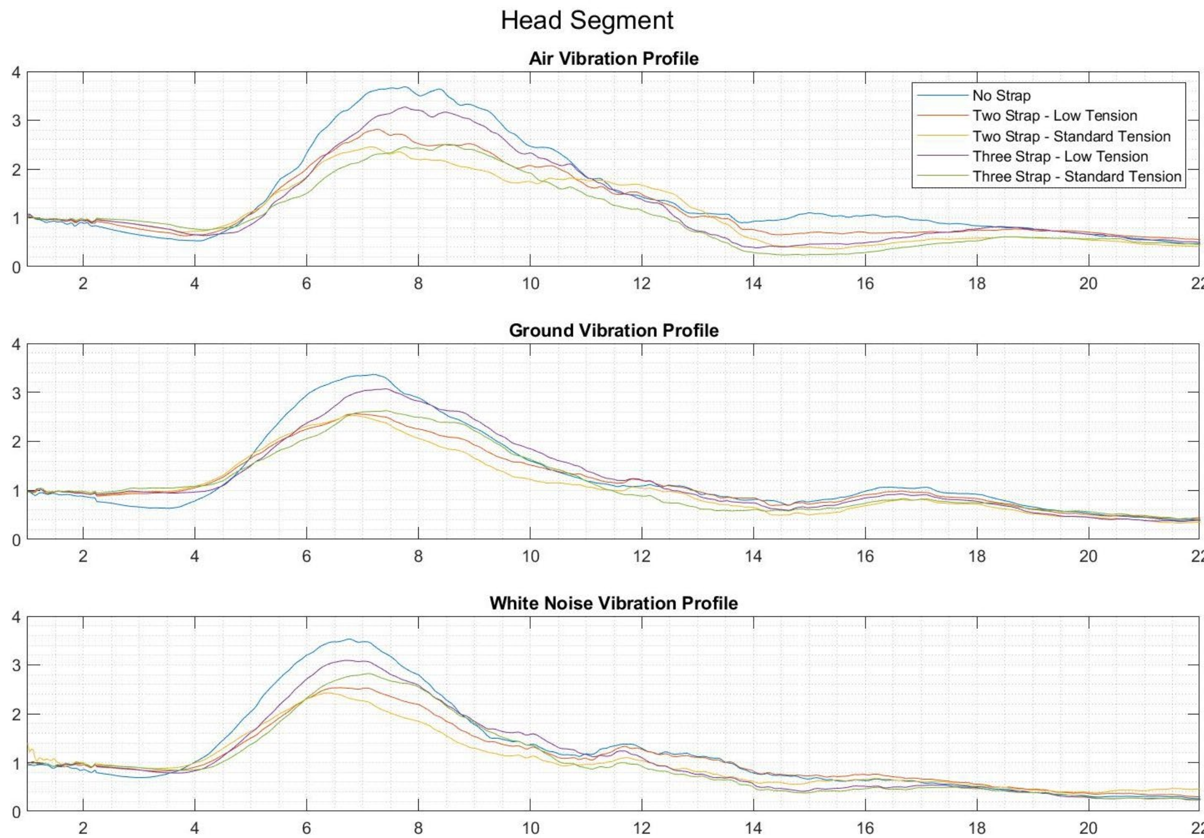

Figure 7: Transmissibility (meaning the frequency response) plots concerning the manikin's head segment. Results for all five strap conditions and all three vibration profiles are shown. The X-axis is frequency (Hz) and the Y-axis is the transmissibility ratio.

The manikin head segment exhibited transmissibility curves of similar shape for all five strap tensions and all three vibration profiles. The resonant frequency was around 8 Hz for the Air profile, but closer to 6.5 Hz for both the Ground and White Noise profiles. As a general pattern, the highest transmissibility (3.4 to 3.7) was achieved in the NS-C and the lowest (~2.4) in the 2S-ST-C. The 3S-LT-C exhibited the second highest transmissibility. See Figure 10 for a quantitative explication of the results.

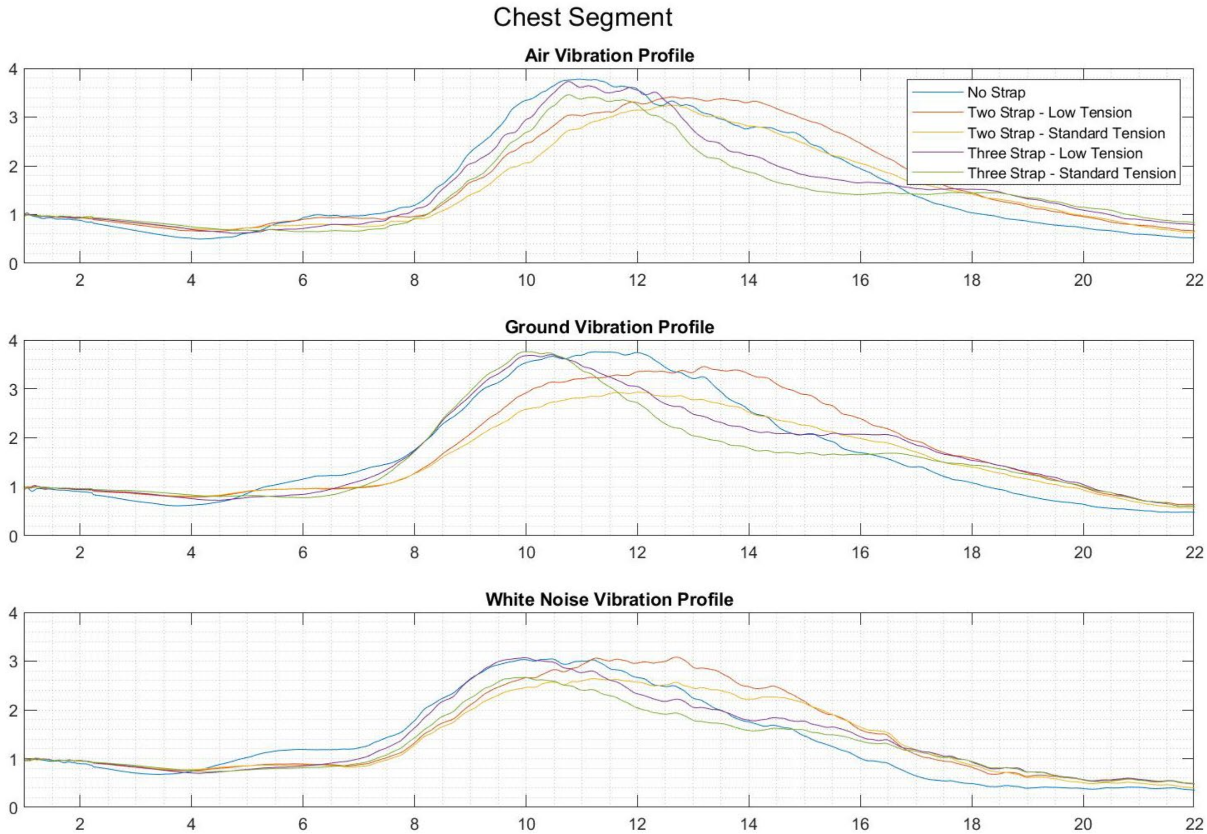

Figure 8: Transmissibility (meaning the frequency response) plots concerning the manikin's chest segment. Results for all five strap conditions and all three vibration profiles are shown. The X-axis is frequency (Hz) and the Y-axis is the transmissibility ratio.

The manikin chest segment exhibited transmissibility curves of similar shape for all five strap tensions and all three vibration profiles. The resonant frequency was around 11 Hz for the Air profile, but closer to 10 Hz for both the Ground and White Noise profiles. Compared with the head segment, the chest segment transmissibility exhibited greater variability with respect to the strap configuration. For example, in the Ground vibration profile, the resonant frequency was around 10 Hz for both three strap configurations but around 13.5 Hz for the 2S-LT-C. As with the head segment, the 2S-LT-C tended to exhibit the lowest max transmissibility. See Figure 11 for a quantitative explication of the results.

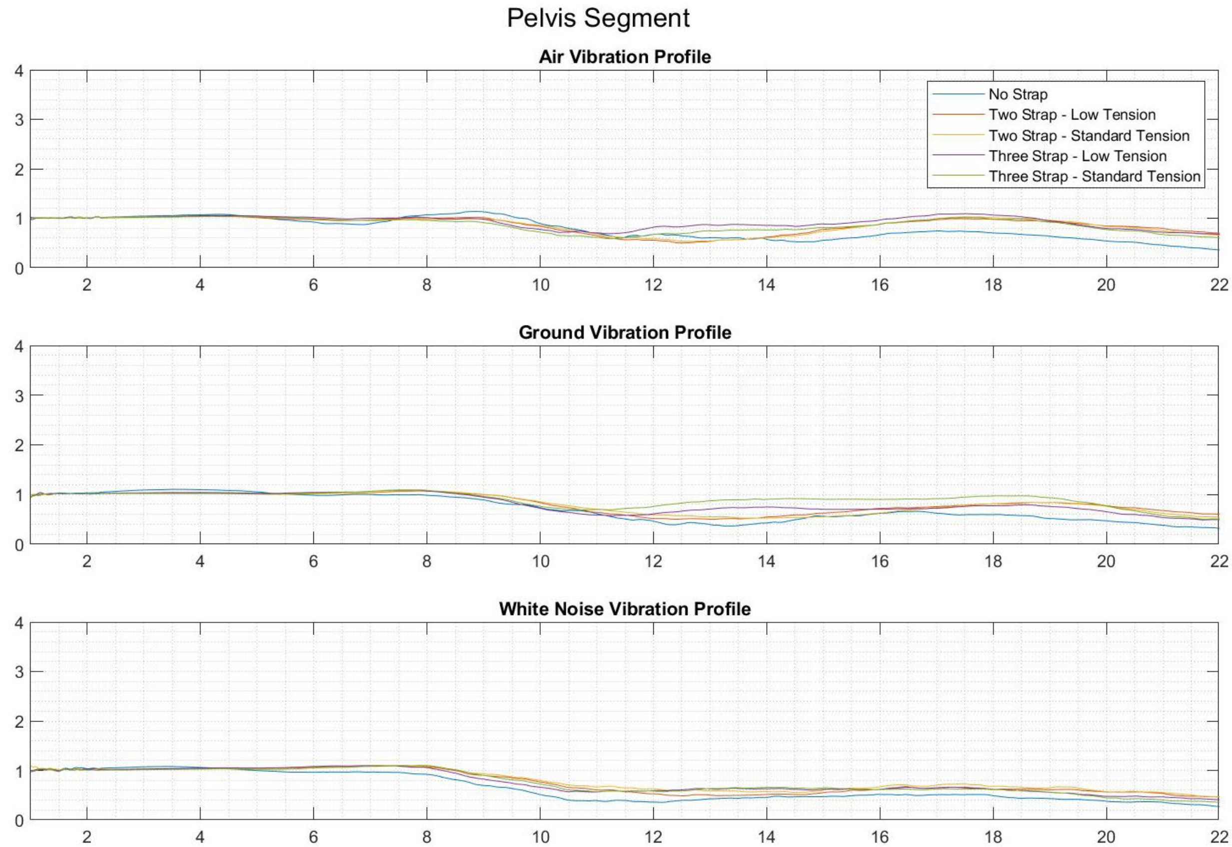

Figure 9: Transmissibility (meaning the frequency response) plots concerning the manikin's pelvis segment. Results for all five strap conditions and all three vibration profiles are shown. The X-axis is frequency (Hz) and the Y-axis is the transmissibility ratio.

The manikin pelvis segment exhibited predominantly flat transmissibility curves for all five strap tensions and all three vibration profiles. The most obvious pattern was that the NS-C tended to exhibit the lowest transmissibility above 12 Hz. See Figure 12 for a quantitative explication of the results.

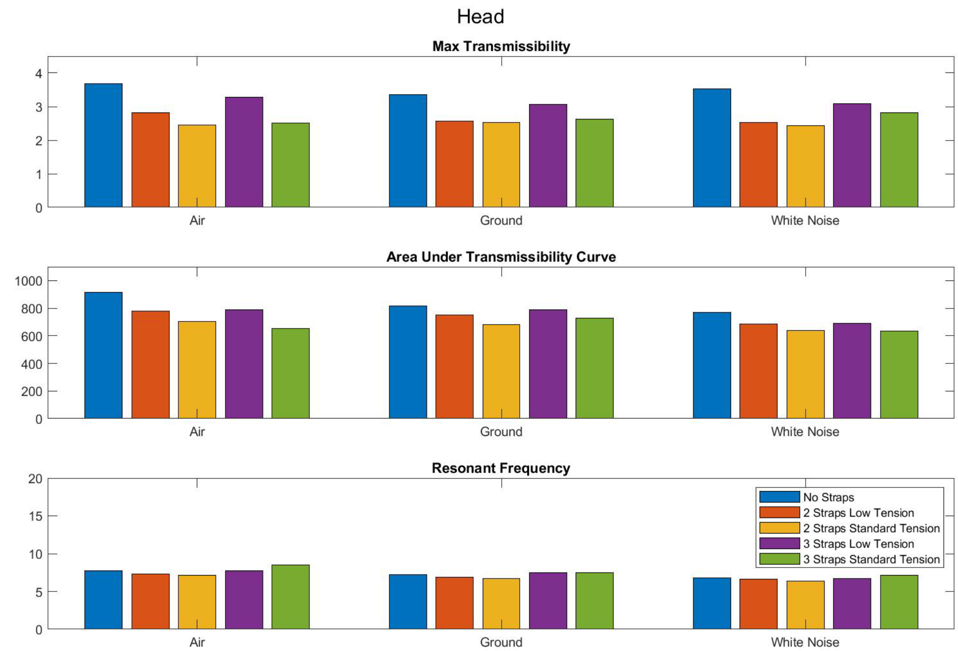

Figure 10: Bar plot comparing metrics calculated from the manikin's head transmissibility plots. Variation in the metrics of max transmissibility, area under the transmissibility curve, and resonant frequency are shown. The results are organized by both strap condition and input vibration profile.

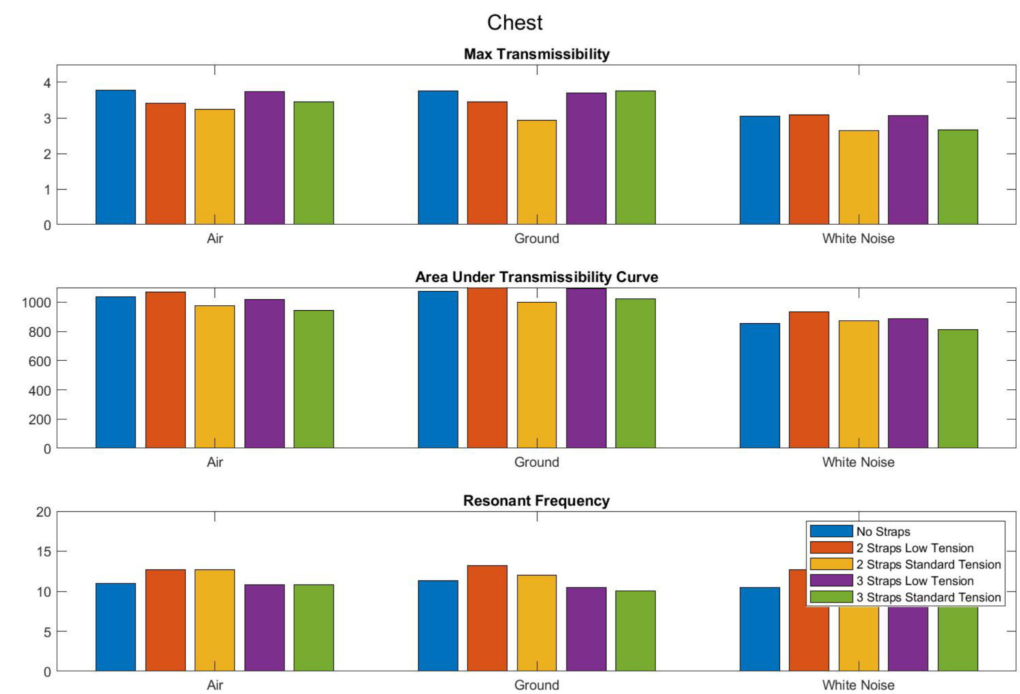

Figure 11: Bar plot comparing metrics calculated from the manikin's chest transmissibility plots. Variation in the metrics of max transmissibility, area under the transmissibility curve, and resonant frequency are shown. The results are organized by both strap condition and input vibration profile.

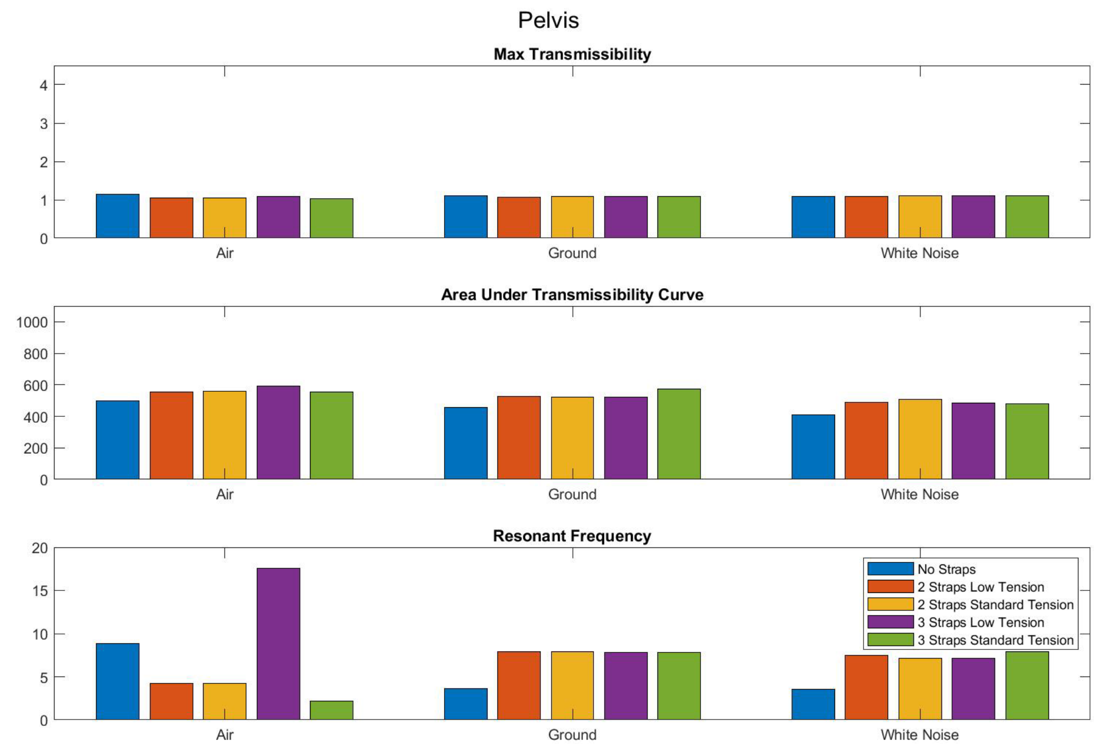

Figure 12: Bar plot comparing metrics calculated from the manikin's pelvis transmissibility plots. Variation in the metrics of max transmissibility, area under the transmissibility curve, and resonant frequency are shown. The results are organized by both strap condition and input vibration profile.

When considering the metrics derived from the transmissibility curves for the manikin head segment, two patterns are clear for the MT and AuT: The NS-C exhibited the highest values, and the standard tension cases exhibited lower values than the low tension cases. In terms of MT, the two strap cases were lower than the three strap cases, but in terms of AuT the number of straps did not make much difference. In terms of resonant frequency, the 3S-ST-C was the highest and the 2S-ST-C was the lowest.

When considering the metrics derived from the transmissibility curves for the manikin chest segment, the only pattern similar to that of the head segment is that the standard tension configuration exhibited lower MTs and AuTs than the low tension configuration. A notable exception is the MT for the Ground profile. In terms of resonant frequency, the two strap conditions were the highest for all three vibration profiles, while the NS-C and three strap configurations were similar to each other.

When considering the metrics derived from the transmissibility curves for the manikin pelvis segment, little variability is expected based on the transmissibility plots. The MT was similar for all cases. With respect to AuT, results varied over the vibration profiles, with the exception that the NS-C case was always the lowest. The resonant frequency results varied greatly depending on the vibration profile. The Ground and White Noise profiles offered similar results – all strapped conditions were similar and the NS-C was distinctively lower (~3.5 Hz vs ~7.5 Hz).

For the Air profile, the strapped conditions were distinctively lower than the NS-C (2.2 – 4.2 vs 8.9) but the 3S-LT-C was by far the highest at 17.6. These variations in resonant frequency should be considered cautiously, however, as the differences in transmissibility they suggest are far greater than the actual transmissibility plots show.

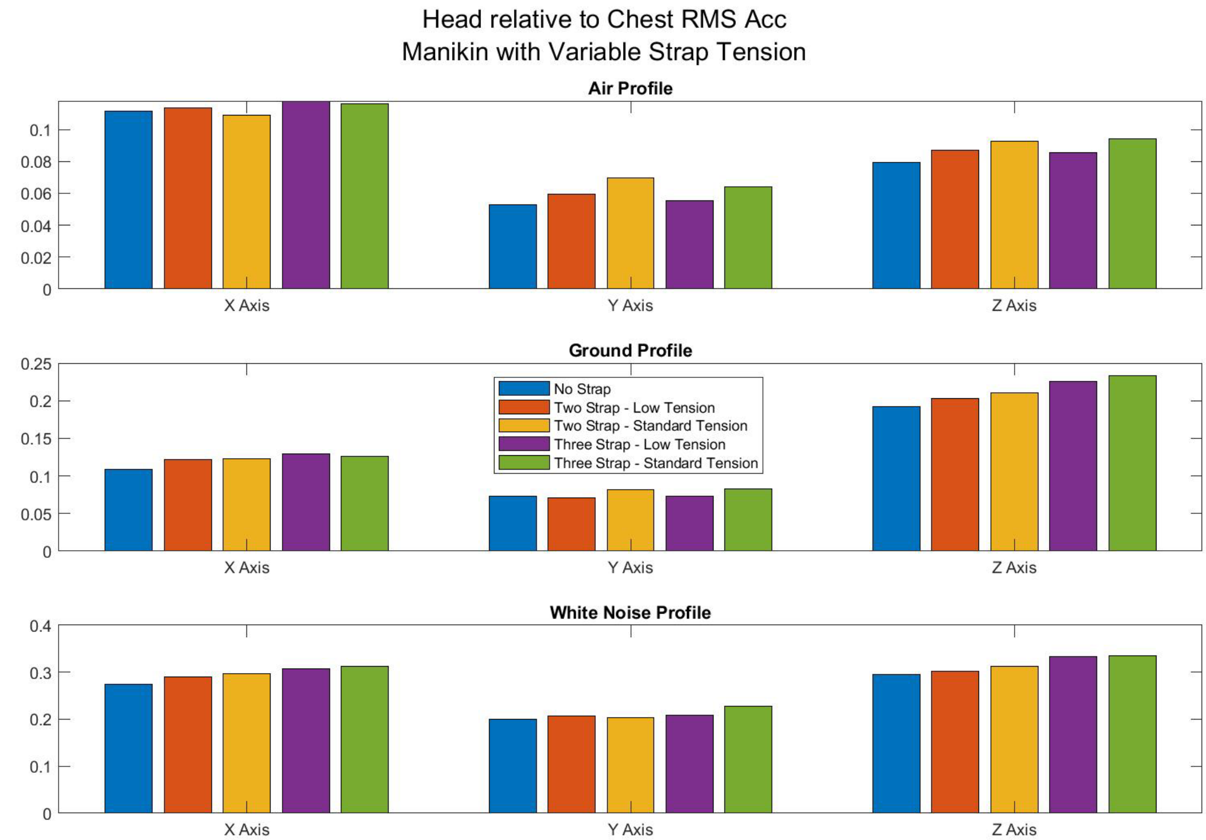

Figure 13: Bar plots showing the RMS accelerations for the relative motion of the manikin head segment with respect to the manikin chest segment. The RMS accelerations are broken out into its three axes, five strap conditions, and three vibration profiles.

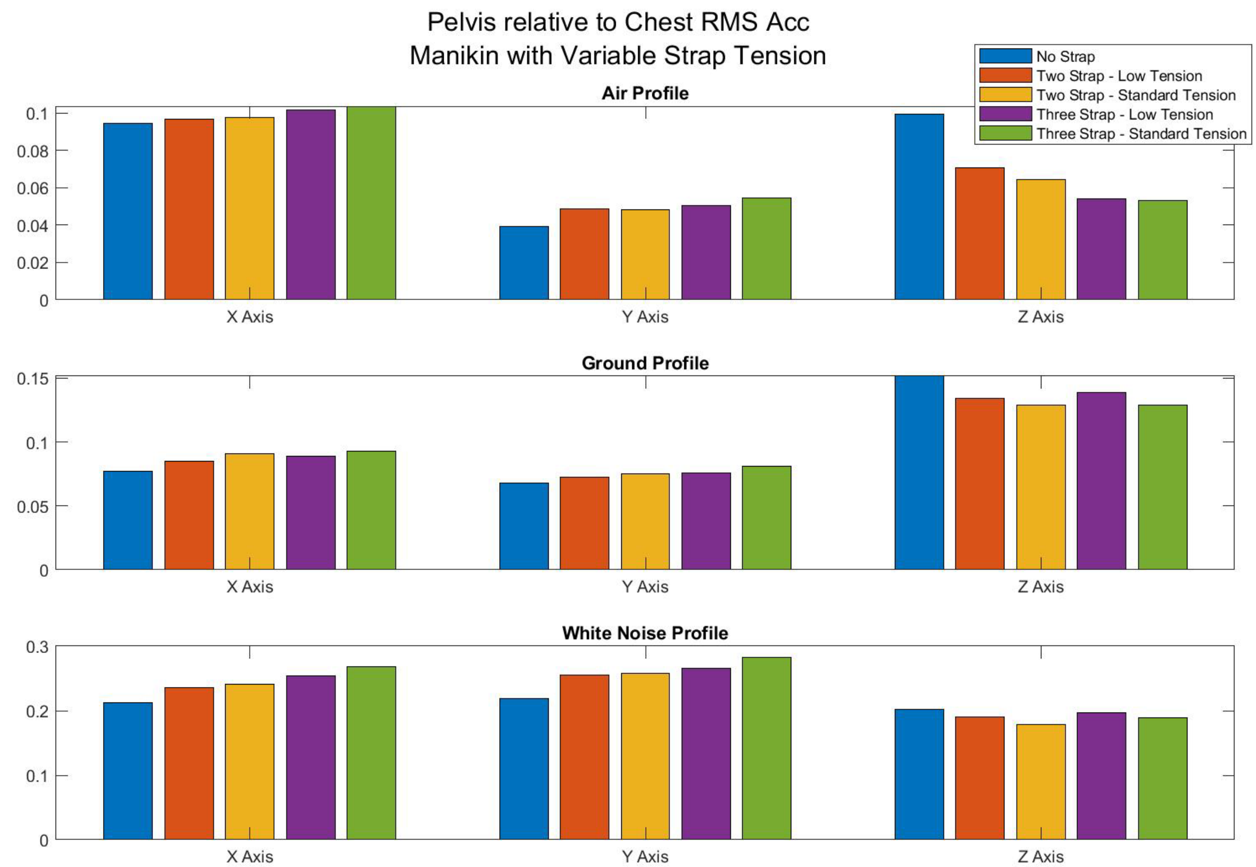

Figure 14: Bar plots showing the RMS accelerations for the relative motion of the manikin head segment with respect to the manikin chest segment. The RMS accelerations are broken out into its three axes, five strap conditions, and three vibration profiles.

Human Subjects Results

Presentation Format of Human Results Plots

Note that the result plots presented for the human subjects will follow a different format than those of the manikin. This is for three reasons. First, the manikin was tested under five strap conditions (NS-C, 2S-LT-C, 2S-ST-C, 3S-LT-C, and 3S-ST-C) where as the human subjects were tested only under two conditions – two strap low tension and two strap standard tension – which are analogous to the manikin's 2S-LT-C and 2S-ST-C cases respectively. Second, the manikin data consisted of a single "subject", whereas the human data consisted of 25 subjects. Statistical analysis can be applied to 25 subjects, and the format of the results plots were altered to accommodate the inclusion of this extra information. Third, the human data was gathered from subjects of varying anthropometries, and results often varied greatly between subjects within the same trial. To accommodate this large inter-subject variability, intra-subject normalization (as discussed in the Methods section) was applied. This intra-subject normalization altered the metrics from direct measurements to a ratio of the low and standard tension results, hence human subject results were calculated as ratios determined from the direct measurements, rather than the direct measurements.

The upshot of this is that the results of human testing are presented as a ratio calculated by dividing the low tension results by the standard tension results. Therefore a ratio value below one indicates that the low tension results were less than the standard tension results, and a ratio value above one indicates that the low tension results were greater than the standard tension results.

Transmissibility Results
To provide general context for interpreting the transmissibility results, the means and corresponding standard deviations (prior to intra-subject normalization) for each transmissibility metric are shown below in Table 1. Next, the results of t-tests applied to the data after intra-subject normalization are presented (Table 2). Following this, the corresponding means and standard deviations are explored via bar plots (Figure 15, Figure 16, and Figure 17). Furthermore, the reader is strongly encouraged to peruse the corresponding transmissibility plots, shown in the Appendix (Figure 24 to Figure 32), as these plots are helpful in understanding the frequency responses for each body segment when exposed to the different vibration inputs.

Table 1: Means and corresponding standard deviations for head, chest, and pelvis segments for each transmissibility metrics. Data is also broken down by vibration profile and strap tension.

Transmissibility Metric		Max Transmissibility					
Vibration Profile		Air		Ground		White Noise	
Strap Tension		Low	Standard	Low	Standard	Low	Standard
Mean and Standard Devations	Head	2.28±0.64	2.43±0.74	2.56±0.51	2.22±0.44	2.64±0.59	2.35±0.52
	Chest	1.34±0.21	1.39±0.26	1.32±0.15	1.33±0.17	1.31±0.22	1.29±0.20
	Pelvis	1.08±0.11	1.10±0.12	1.15±0.13	1.19±0.14	1.19±0.13	1.22±0.16
Transmissibility Metric		Area Under Transmissibility Curve					
Vibration Profile		Air		Ground		White Noise	
Strap Tension		Low	Standard	Low	Standard	Low	Standard
Mean and Standard Devations	Head	446.65±80.69	455.64±72.59	505.07±76.48	457.91±60.37	471.62±76.51	443.52±71.71
	Chest	433.44±107.84	479.42±118.72	435.88±88.39	476.12±114.32	391.29±88.77	428.60±114.11
	Pelvis	380.63±70.60	404.54±78.13	371.09±78.85	391.04±75.49	365.51±64.70	382.94±66.20
Transmissibility Metric		Resonant Frequency					
Vibration Profile		Air		Ground		White Noise	
Strap Tension		Low	Standard	Low	Standard	Low	Standard
Mean and Standard Devations	Head	6.88±0.41	7.15±0.60	6.68±0.47	6.57±0.62	6.38±0.42	6.41±0.60
	Chest	7.86±2.65	7.52±2.54	7.11±2.21	6.84±2.25	6.39±1.59	7.03±2.71
	Pelvis	5.35±3.54	5.94±3.80	5.91±2.22	6.26±1.97	5.92±1.55	6.35±1.56

Table 2 below lists the significance values for the transmissibility metrics that have been subjected to intra-subject normalization. The results were obtained by t-test. Yellow highlights denote statistically significant values ($p < 0.05$) and green highlights denote marginally statistically significant values ($p < 0.10$).

Table 2: Tabulated p-values for the three transmissibility metrics applied to the human subject data that have been subjected to intra-subject normalization. Yellow highlights denote statistically significant values ($p < 0.05$) and green highlights denote marginally statistically significant values ($p < 0.10$).

VIBRATION PROFILE	BODY SEGMENT	MAX TRANSMISSIBILITY	AREA UNDER TRANS. CURVE	RESONANT FREQUENCY
AIR	Head	0.57	0.45	0.01
	Chest	0.15	0.00	0.15
	Pelvis	0.12	0.01	0.73
GROUND	Head	0.00	0.00	0.06
	Chest	0.92	0.00	0.25
	Pelvis	0.03	0.00	0.82
WHITE NOISE	Head	0.00	0.00	0.95
	Chest	0.21	0.00	0.23
	Pelvis	0.19	0.00	0.00

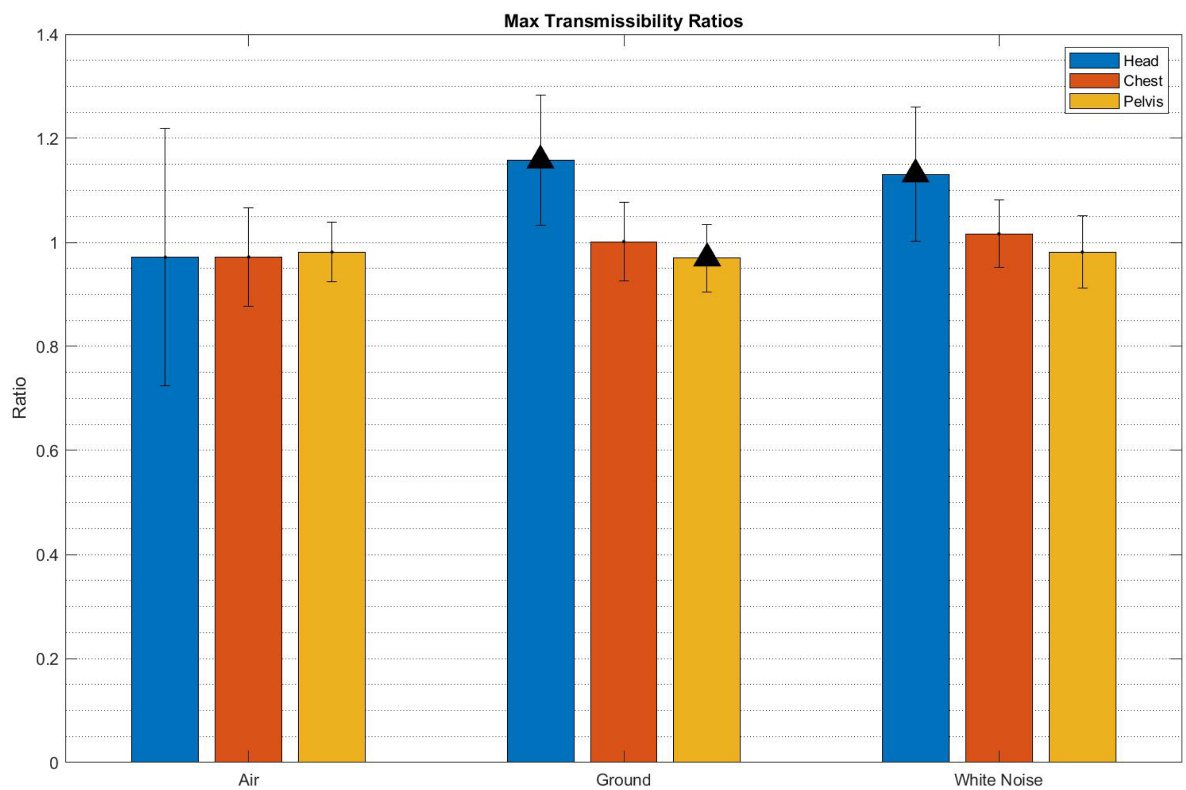

Figure 15: This figure depicts the mean ratio values and corresponding standard deviations of the max transmissibility ratios for the head, chest, and pelvis body segments. The bar shows the mean ratio, the black brackets show the corresponding standard deviation, and the black triangles denote statistically significant results.

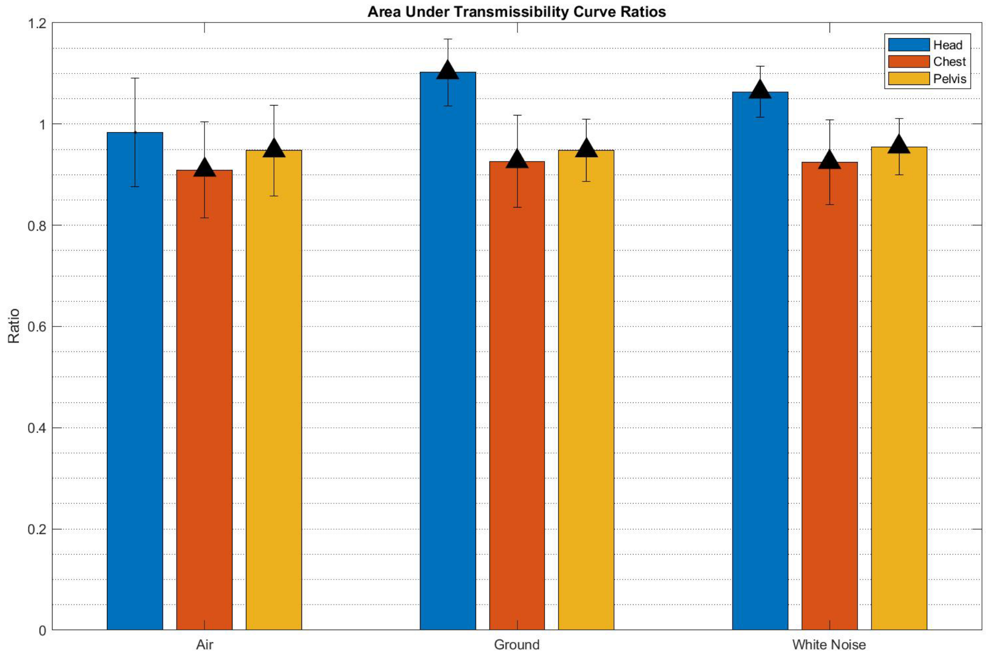

Figure 16: This figure depicts the mean ratio values and corresponding standard deviations of the area under the transmissibility curve ratios for the head, chest, and pelvis body segments. The bar shows the mean ratio, the black brackets show the corresponding standard deviation, and the black triangles denote statistically significant results.

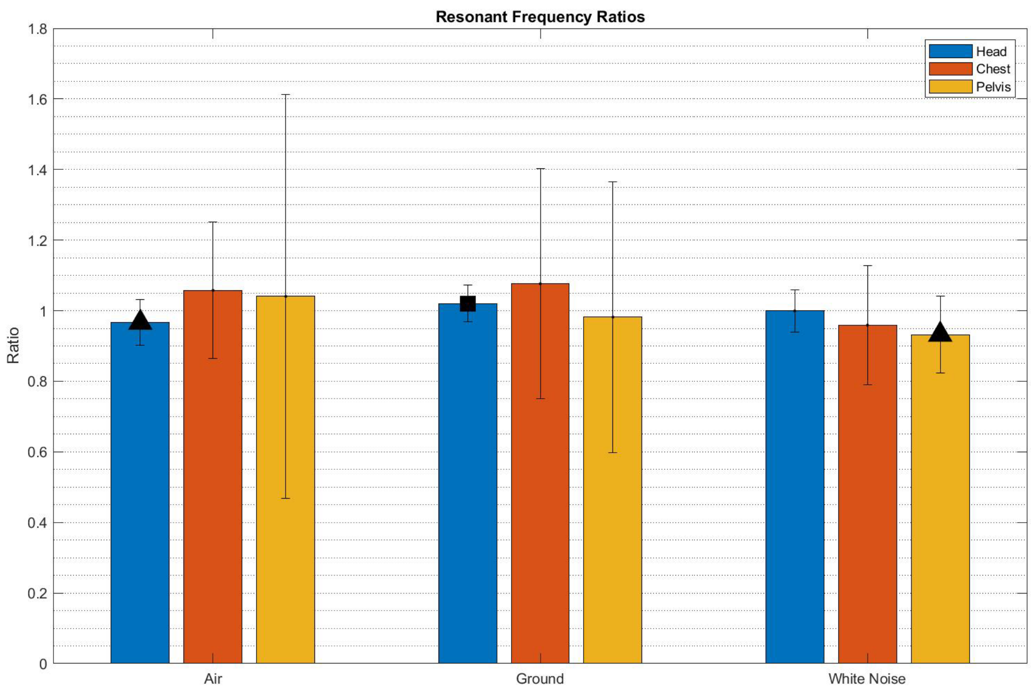

Figure 17: This figure depicts the mean ratio values and corresponding standard deviations of the resonant frequency ratios for the head, chest, and pelvis body segments. The bar shows the mean ratio, the black brackets show the corresponding standard deviation, the black triangles denotes statistically significant results, and black squares denote marginal statistical significance.

Segmented Air Profile Results

Table 3 below contains the p-values associated with the transmissibility metrics for the time-segmented Air vibration profile. The data was subjected to intra-subject normalization before calculating the significance values. Below the table, Figure 18, Figure 19, and Figure 20 exhibit the means and standard deviations associated with the values in Table 3 in terms of MT, AuT, and Wn respectively.

Table 3: Tabulated p-values for the segmented air vibration profile transmissibility metrics applied to the human subject data (with intra-subject normalization applied). Yellow highlights denote statistically significant values ($p < 0.05$) and green highlights denote marginally statistically significant values ($p < 0.10$).

	Segment Number	Segment 1	Segment 2	Segment 3	Segment 4	Segment 5	Segment 6	Segment 7
Max Transmissibility	Head	0.92	0.13	0.90	0.00	0.89	0.50	0.31
	Chest	0.14	0.01	0.30	0.37	0.06	0.16	0.07
	Pelvis	0.64	0.95	0.52	0.14	0.03	0.04	0.53
Area Under Transmissbility Curve	Head	0.35	0.09	0.41	0.16	0.84	0.70	0.53
	Chest	0.00	0.00	0.00	0.01	0.00	0.00	0.00
	Pelvis	0.03	0.22	0.01	0.02	0.48	0.03	0.00
Resonant Frequency	Head	0.03	0.72	0.00	0.31	0.57	0.87	0.15
	Chest	0.95	0.60	0.08	0.00	0.91	0.88	0.06
	Pelvis	0.28	0.47	0.75	0.00	0.31	0.49	0.25

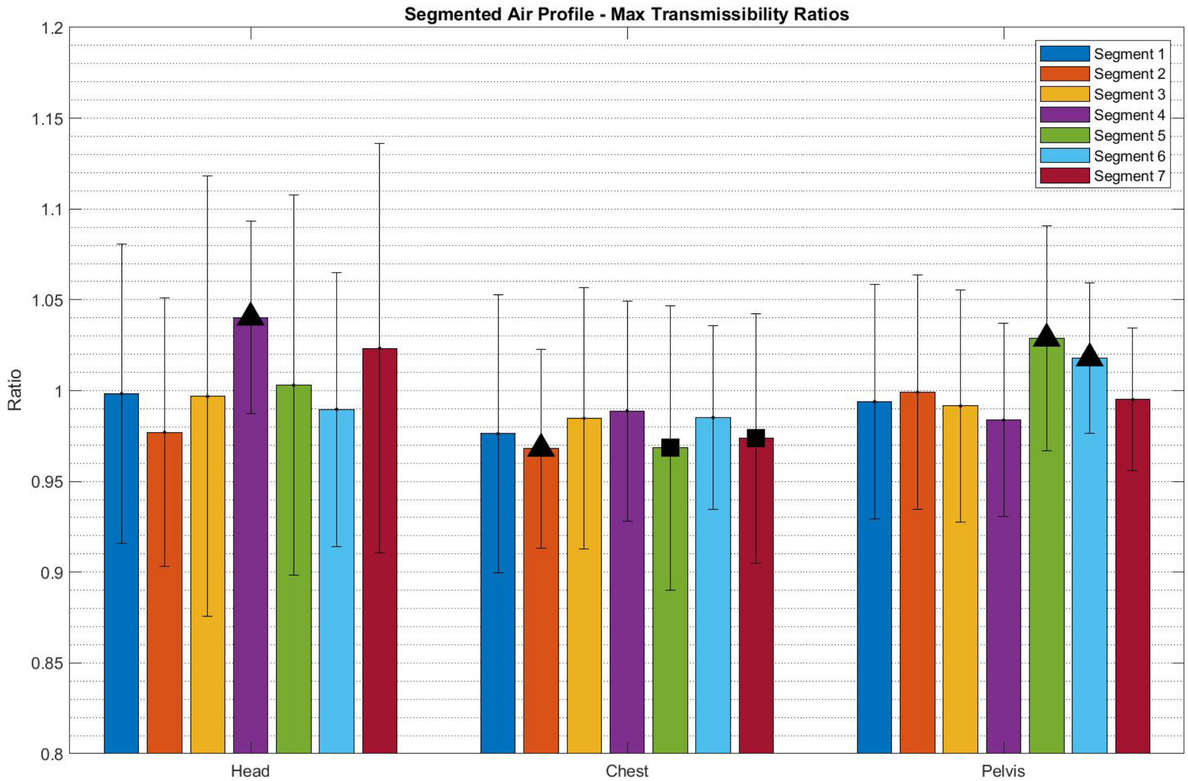

Figure 18: This figure depicts the mean ratio values and corresponding standard deviations of the max transmissibility ratios for the head, chest, and pelvis body segments over the seven time segments of the Air vibration profile. The bar shows the mean ratio, the black brackets show the corresponding standard deviation, the black triangles denotes statistically significant results, and the black squares denote results of marginal statistical significance.

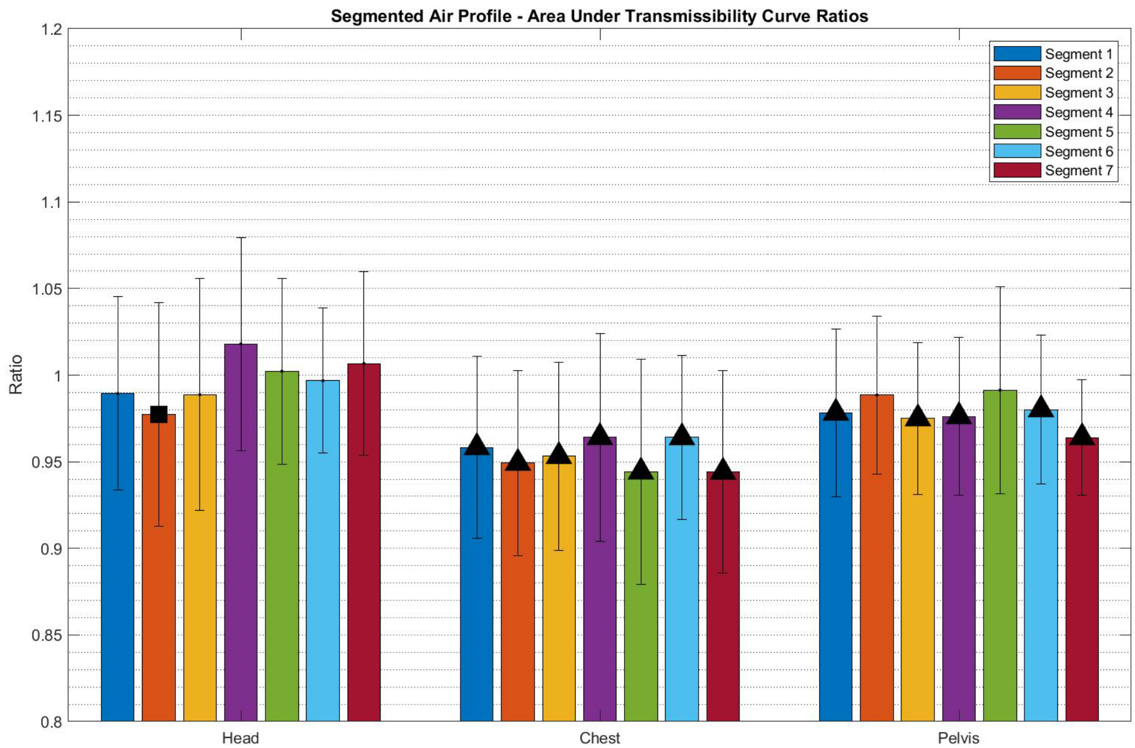

Figure 19: This figure depicts the mean ratio values and corresponding standard deviations of the area under the transmissibility curve ratios for the head, chest, and pelvis body segments over the seven segments of the Air vibration profile. The bar shows the mean ratio, the black brackets show the corresponding standard deviation, the black triangles denotes statistically significant results, and the black squares denote results of marginal statistical significance.

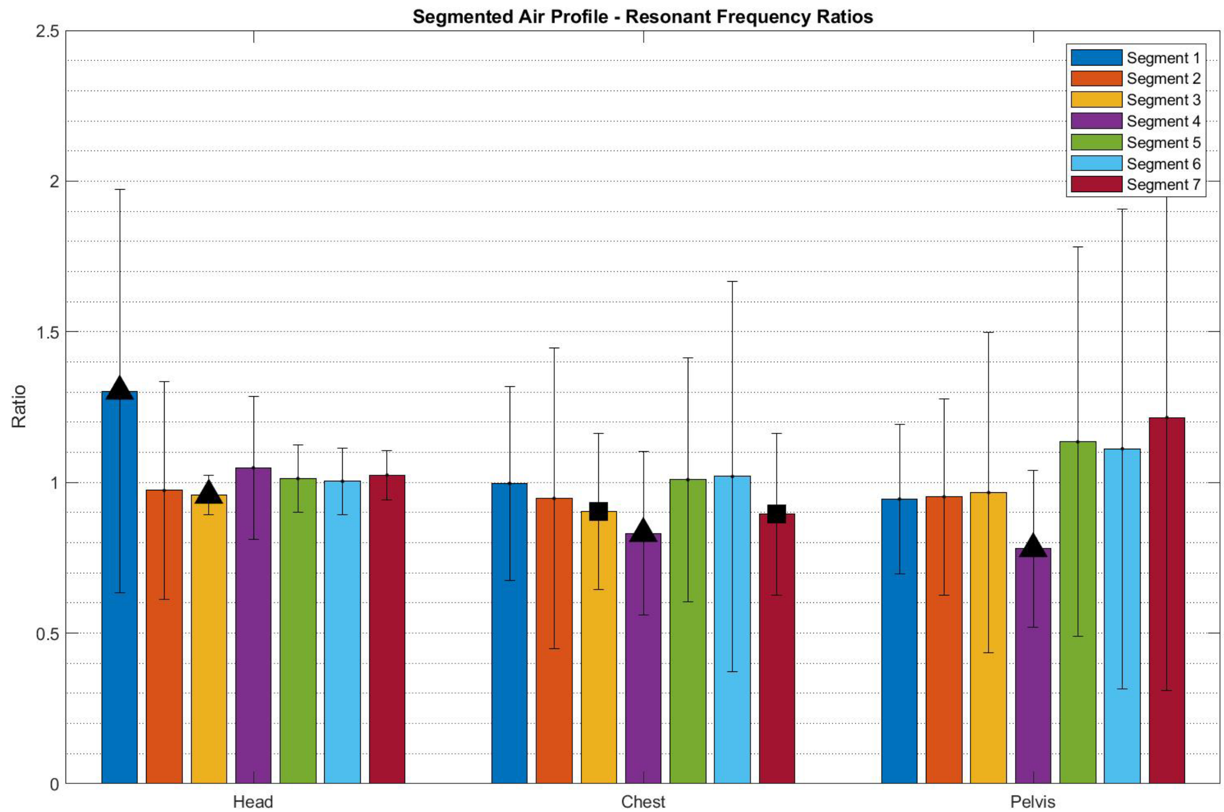

Figure 20: This figure depicts the mean ratio values and corresponding standard deviations of the resonant frequency ratios for the head, chest, and pelvis body segments over the seven segments of the Air vibration profile. The bar shows the mean ratio, the black brackets show the corresponding standard deviation, the black triangles denotes statistically significant results, and the black squares denote results of marginal statistical significance.

Relative Segment Motion Results

The relative segment motion results will be presented in the same format as transmissibility results. First the means and standard deviations of the data (without intra-subject normalization) are presented (Table 4). Next t-testing is applied to the same results after intra-subject normalization has been applied (

Table 5). Finally, the means and standard deviations corresponding to the t-test results shown in are presented in form of bar plots (Figure 21, Figure 22, and Figure 23). Furthermore, the reader is referred to the appendix for the subject specific values used to construct the means and standard deviations presented in Table 4. These results can be seen in Table 9 to Table 14.

Table 4: Means and corresponding standard deviations for the head, chest, and pelvis segments for each of the relative segment motion in terms of the axial RMS components for acceleration and angular velocity (units are gs and deg/s respectively). The tabulated data is further broken down by vibration profile and strap tension.

		RMS Acceleration					
		X Axis		Y Axis		Z Axis	
Strap Tension		Low	Standard	Low	Standard	Low	Standard
Vibration Profile	Segment Relative to Chest						
Air	Head	0.10±0.04	0.09±0.03	0.09±0.01	0.08±0.01	0.06±0.01	0.05±0.01
	Pelvis	0.06±0.02	0.06±0.02	0.07±0.01	0.07±0.01	0.08±0.02	0.07±0.02
Ground	Head	0.07±0.01	0.07±0.01	0.13±0.02	0.13±0.02	0.08±0.02	0.08±0.02
	Pelvis	0.05±0.02	0.06±0.02	0.07±0.01	0.08±0.02	0.08±0.02	0.07±0.02
White Noise	Head	0.19±0.03	0.20±0.04	0.25±0.04	0.25±0.03	0.16±0.03	0.15±0.03
	Pelvis	0.13±0.02	0.14±0.03	0.13±0.02	0.13±0.02	0.15±0.03	0.15±0.03

		RMS Angular Velocity					
		X Axis		Y Axis		Z Axis	
Strap Tension		Low	Standard	Low	Standard	Low	Standard
Vibration Profile	Segment Relative to Chest						
Air	Head	10.65±2.95	10.47±2.59	8.42±1.80	8.44±2.39	6.73±1.32	6.76±1.36
	Pelvis	9.18±3.20	8.47±2.82	9.99±3.44	10.05±2.74	7.12±2.14	7.00±1.85
Ground	Head	10.82±1.51	11.30±1.53	15.37±4.63	14.99±3.40	8.53±1.30	9.05±1.66
	Pelvis	10.00±2.79	10.50±3.03	13.29±3.80	13.87±3.83	8.04±2.01	8.53±2.55
White Noise	Head	25.94±4.47	26.49±4.28	43.14±9.60	42.02±8.33	22.69±3.68	23.41±4.28
	Pelvis	23.60±5.05	23.82±5.12	35.13±9.46	36.25±9.66	19.15±4.93	19.54±5.85

Table 5: Tabulated p-values for the relative segment motion metrics applied to the human subject data (subjected to intra-subject normalization). Yellow highlights denote statistically significant values ($p < 0.05$) and green highlights denote marginally statistically significant values ($p < 0.10$).

Vibration Profile	Segment Relative to Chest	RMS Acceleration			RMS Angular Velocity		
		X Axis	Y Axis	Z Axis	X Axis	Y Axis	Z Axis
Air	Head	0.18	0.33	0.14	0.45	0.56	0.70
	Pelvis	0.13	0.26	0.02	0.01	0.44	0.52
Ground	Head	0.84	0.28	0.37	0.00	0.31	0.02
	Pelvis	0.00	0.56	0.31	0.25	0.06	0.38
White Noise	Head	0.23	0.46	0.06	0.20	0.16	0.51
	Pelvis	0.00	0.47	0.18	0.72	0.06	0.66

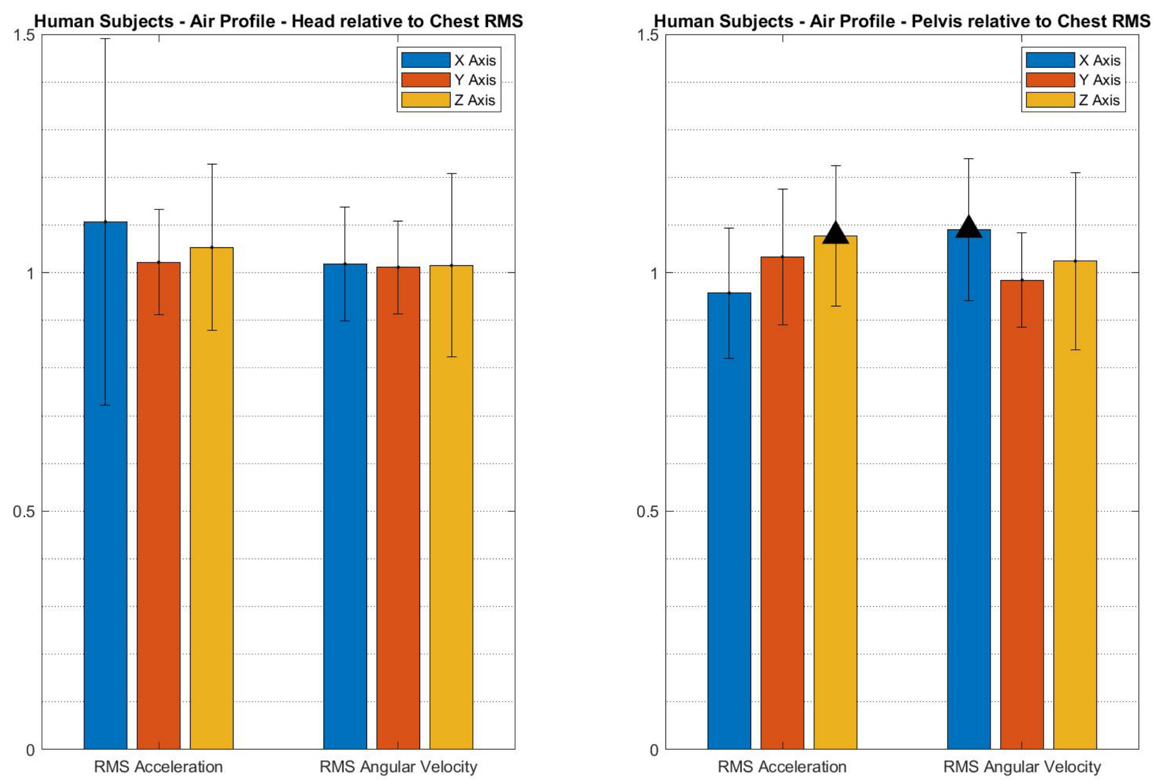

Figure 21: This figure depicts the mean ratio values and corresponding standard deviations of the relative segment motion metrics (RMS Acceleration and RMS Angular Velocity) for Air vibration profile. On the left the metrics concerning the motion of the head relative to the chest are shown, and on the right the pelvis relative to the chest. The bar shows the mean ratio, the black brackets show the corresponding standard deviation, and the black triangles denote statistically significant results.

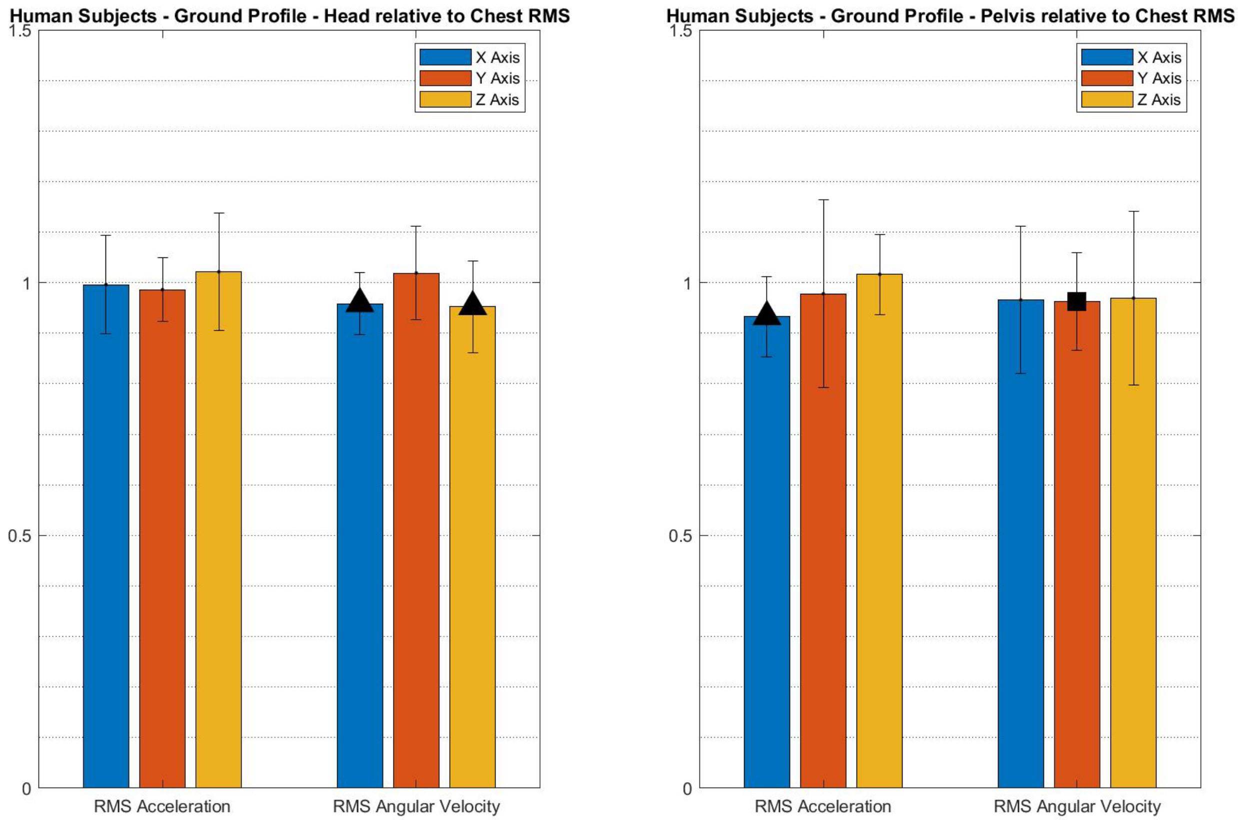

Figure 22: This figure depicts the mean ratio values and corresponding standard deviations of the relative segment motion metrics (RMS Acceleration and RMS Angular Velocity) for Ground vibration profile. On the left the metrics concerning the motion of the head relative to the chest are shown, and on the right the pelvis relative to the chest. The bar shows the mean ratio, the black brackets show the corresponding standard deviation, the black triangles denote statistically significant results, and the black squares denote results of marginal statistical significance.

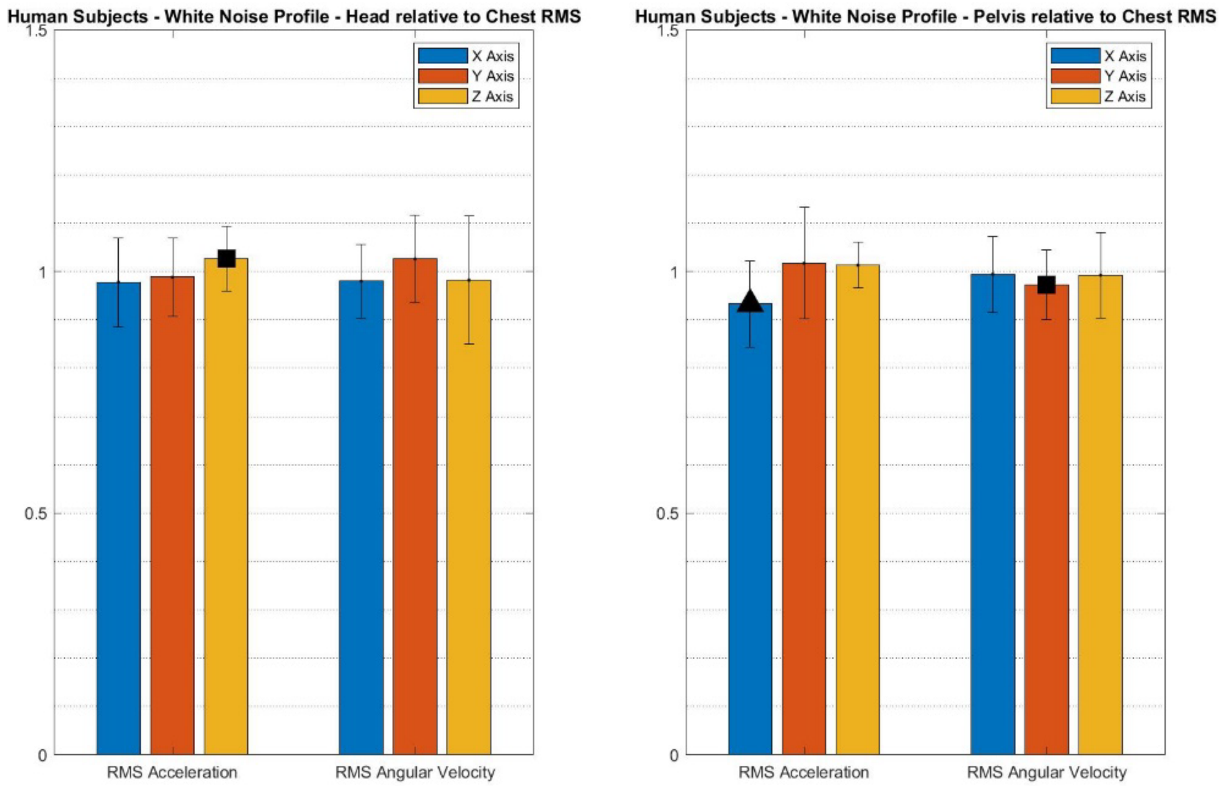

Figure 23: This figure depicts the mean ratio values and corresponding standard deviations of the relative segment motion metrics (RMS Acceleration and RMS Angular Velocity) for White Noise vibration profile. On the left the metrics concerning the motion of the head relative to the chest are shown, and on the right the pelvis relative to the chest. The bar shows the mean ratio, the black brackets show the corresponding standard deviation, the black triangles denote statistically significant results, and the black squares denote results of marginal statistical significance.

Discussion

<u>Overall Takeaways</u>

The major finding from this study is that strap tension impacts how input vibration energy is distributed, amplified/reduced, and focused throughout a subject's body, and the manner of this distribution is dependent on the type of input vibration. When the input vibration is high frequency (such as in the Air profile) the low tension condition exhibits slightly lower MT and AuT than the standard tension condition, but it also permits more relative segment motion. When the input vibration is low frequency (such as in the Ground and White Noise profiles), the low tension case allows vibrational energy to the head, increasing the head's MT (by up to 19% in the bandpass case). Relative segment motion is also increased in the vertical direction, but decreased in the lateral directions. Therefore, it can be said that in general the standard tension condition tends produce to a more clinically-favorable biodynamic response than the low tension condition. Reducing the patient vibration, both in terms of body segment acceleration and relative body segment motion, is desirable when stabilizing trauma patients with severe injuries. This is especially true for head and spinal injuries which can be negatively impacted by head and chest motion. However, the ride conditions, as well as what one determines as the criteria for "clinically-favorable" are, must be considered as well.

The amount of energy in the applied vibration profiles should also be considered (Figure 5). This can be most readily seen in the White Noise vibration profile. While we referred to it above as a "low frequency input", white noise, by definition, has equal power across all frequencies. Therefore, instead of separating the responses based on low and high frequency inputs, it could more accurately be described as inputs that have "enough" power in either the low or high frequency bands. The reason for this is likely that below a certain threshold of vibration energy, motion in the subject is not induce, and effects of differing strap tension cannot manifest. The three chosen vibration profiles struck a good balance between heuristic and practical vibration inputs, but it would be interesting to see the results of profiles that had significant power in the middle frequency ranges.

Finally, while results and corresponding discussion of resonant frequency are presented in this report, caution is recommended in interpreting them. This is primarily due to the stretched out shape of the transmissibility "hump" that the resonant frequency is contained. Often this hump is relatively flat but somewhat noisy. For example, refer to the frequency response seen in Figure 7, specifically the Head body segment, Air vibration profile, and no strap condition. Visual inspection reveals that the resonant frequency could be reasonably placed at any location between 7 – 8.25 Hz, though the numerical maximum (and therefore the resonant frequency) was assigned at 7.75 Hz. The authors believe that magnitude of this uncertainty in identifying the resonant frequency value is of similar magnitude to the difference in resonant frequency resulting from varying the strap tension. Therefore, it is difficult to draw any concrete conclusions from the calculated resonant frequency metrics.

Manikin Results

The manikin testing included not only the two strap conditions used in the human subject testing, but also a no strap condition and three strap conditions. The results of the two strap conditions generally paralleled that of the human subjects, that is the standard tension condition tended to reduce the MT and AuT, especially in the head. This suggests that the no strap and three strap conditions tested on the manikin are indicative of how a human would respond under the same conditions.

Focusing on the three strap conditions, it is interesting to note that the addition of a third strap did not always reduce the transmissibility response. In fact, it tended to increase the transmissibiltiy response more often than not. Furthermore, the addition of a third strap tended to increase the relative segment motion, particularly at the head. This is reasonable, as adding another point of restraint forces the vibrational energy to redistribute to where motion is possible. Overall, the manikin results suggest that the two strap approach results in a more favorable motion response than the three strap approach that has been used in this work. It should be noted that the location of the third strap may play a role in this process, but this was not investigated in this work.

Broad Observations for Contextualization

The vast amount of data collected in this study, and the multitude of processing methods applied to the data, lend themselves to some broad insights that bear discussing before the study's primary comparison on the effect of strap tension is dealt with. Firstly, a large amount of inter-subject variability in calculated transmissibility was expected, but the observed variation was far larger than that. Consider the mean and standard deviation of the MT for the Head segment under standard tension and exposed to the air vibration profile (Table 1). Respectively, these values are 2.43 and 0.74, which means that a range of 1.69 to 3.17 was needed to encompass the max transmissibility of approximately 2/3 of the tested subjects. This is strong evidence that subject anthropometry can greatly impact maximum transmissibility. In addition to the general explanation that anthropometry impacts biodynamic response, another possible explanation for this variability is that there is an interaction between subject anthropometry and strap conditions. That is, anthropometry impacts how straps are applied.

Secondly, transmissibility responses were impacted by the applied vibration profile. Such variation was expected, but it underscores the fact that the observed biodynamic response of a subject is a function of the input vibration spectra. This fact is especially evident in the MT metrics listed in Table 1. This input-dependent biodynamic response should be kept in mind as the effects of varying strap tension are discussed, as the results showed that strap tension impacts subjects differently depending on the input vibration profile.

Transmissibility Metrics

The three vibration profiles used in this experiment exhibit very different spectral responses (Figure 5). The Air profile has energy at higher frequencies (~16-19 Hz), the Ground profile has energy at the lower frequencies (~1-3 Hz), and the White Noise profile has energy distributed uniformly over all frequencies tested (at least in the Z axis). Given these differences, we should expect the transmissibility metrics to be impacted differently by each profile, and the results corroborate this.

Varying strap tension has a negligible impact on the amount of vibratory energy that reaches the subject, as it has no impact on the input. Therefore, it is reasonable to assume that the primary impact of varying strap tension will be to alter how the output energy is distributed over the subject segments rather than altering the total energy. Just as the input vibration spectra influences the subject's biodynamic response, the strap tension also influences it. Furthermore, the straps are not perfectly elastic and may dissipate energy as they stretch and contract as a result of vibration. This may add further complexity to observed biodynamic response.

Max Transmissibility

In terms of the effect of strap tension on MT (Figure 15), the primary result was a statistically significant increase in the MT of the head segment for the Ground and White Noise vibration profiles. For the ground case, the MT in the low tension case was over 15% greater than the standard tension case. Conversely, the MT of the pelvis for the Ground profile was decreased by over 3% for the low tension case compared with the standard tension case . This pattern of increasing the MT of the head segment while decreasing the MT of the pelvis segment can also be seen for the White Noise vibration profile, though the decrease of the Pelvis MT was not statistically significant. Furthermore, something of the inverse of this pattern is evident in the Air vibration profile results (though none were statistically significant). In the Air profile, all three segment experienced reduced MT in the low tension case, but the head segment was reduced the most while the pelvis segment was reduced the least.

Area Under Transmissibility Curve

The AuT metric can be interpreted as an analogue for the amount of total energy reaching the body segment in question. Eight of the nine AuT metrics were statistically significant (only the AuT for the head segment in the Air profile was not). This suggests that AuT is a useful metric in differentiating effects from the low tension case and standard tension case. Where MT and Wn are metrics that target specific characteristics of the transmissibility response, AuT characterizes the entire transmissibility response.

A pattern in AuT distribution is present in all three vibration profiles – the head AuT is the largest, chest AuT is the smallest, and pelvis AuT is in the middle. The inter-segment variation is most pronounced in the Ground profile (low frequency input), least pronounced in the Air profile (high frequency input), and the White Noise profile (broad spectrum input) falls in between. This suggests that redistribution of output energy (per the AuT metric) is inversely related to frequency input (lower frequency inputs yield greater inter-segment energy redistribution). This is reasonable given that humans tend to be more impacted by lower frequency inputs. Low strap tension permits freer subject motion relative to the litter than standard tension straps do. The results of Figure 16, suggest that this freer motion redistributes energy from the chest and pelvis segments to head segment. For lower frequency inputs (Ground profile), this freer motion decreases chest and pelvis AuT by increasing head AuT. At higher frequencies (Air profile), the same general effect is observed, but even the head AuT is lower for the low tension case than the standard tension case.

Resonant Frequency

The effects of strap tension on Wn are difficult to interpret The standard deviations exhibited in Figure 17 are often large when compared to the mean they describe, and even the results deems statistically significant or marginally significant admit little variation (the greatest variation is less than 7%, occurring at the pelvis segment in the White Noise profile). It is difficult to extrapolate if and how these small changes in Wn would manifest in practical applications. Perhaps a more relevant observation is that lower strap tension admits large variations in Wns of the chest and pelvis, but has little impact on the Wn of the head.

Overall Transmissibility Metrics

Examining the transmissibility results (Figure 15, Figure 16, and Figure 17) as a whole, the following generalizations can be made. Comparing the low tension conditions and standard tension conditions, the low tension conditions tend to increase transmissibility, both in terms of MT and AuT, at the head segment (and sometimes the chest segment) when the input spectra consists of lower frequency content (Ground and White Noise profiles). Furthermore, for higher frequency inputs (Air profile) the low tension conditions benefit from both reduced MT and reduced AuT.

All Frequencies vs Band-passed Results
When examining the data at all frequencies (1.1-22 Hz), whether in terms of transmissibility or relative segment motion, many of the metrics showed a statistically significant difference between the low tension and standard tension cases. However, statistical significance only determines how confident we can be that there is a difference in the means of the two datasets – it does nothing to describe the magnitude of the differences. Furthermore, when examining the differences in the low tension and standard tension dataset means, the difference was often quite low (often less than 5%).

Given the large frequency band considered and the smoothing filter applied to the transmissibility results, it seemed plausible that differences between the low and standard tension datasets were being mitigated. Therefore, the same transmissibility and relative segment analysis was repeated after application of a bandpass filter (5-9 Hz) that isolated the segment of greatest transmissibility. The results of this bandpass analysis followed the same pattern as that of full-frequency analysis, however, the differences between the means increased greatly (up to 19% difference).

Segmented Air Vibration Profile

The results exhibited in Figure 18, Figure 19, and Figure 20 show considerable variation in the transmissibility response for the seven segments. Given the variability in the frequency content of the seven segments, this is not surprising. Perhaps the most impactful results is the MT of the head body segment at segment 4, where the MT was 4% higher for the low tension case than the standard tension case. Segment 4 is a high vibration visual approach of the aircraft. Another example is the hip body segment for time segments five and six (each of which contain a high amount of vibration with respect to the other seven segments, with the exception of four). This shows that even though the low tension case produces better motion results for most of the aircraft's motions, when the vibration magnitude is high the standard tension produces better motion results. So while the overall air profile results suggest that the low tension condition reduces vibratory motion, there are certain times in flight when the standard tension condition is preferable.

Relative Segment Motion

Out of the 36 parameters dealing with relative segment motion that were tested, only nine were found to be either statistically significant or marginally significant. Of those nine, only two concerned the motion of the head with respect to the chest (the RMS acceleration in the X axis for the ground profile and the RMS Z acceleration for the White Noise profile). The other seven concerned the motion of the pelvis with respect to the chest. This greater impact on the relative pelvis motion than the relative head motion is reasonable given that strap tension impact the range of motion of the pelvis far more than that of the head.

As seen in the transmissibility results, the frequency content of the input vibration impacted the results. In this case, the higher frequency input (Air profile) exhibited an increase in relative segment motion for the low tension condition. The lower frequency inputs (Ground and White Noise profiles) exhibited either no change or a slight decrease in relative segment motion for the low tension condition.

Limitations

While a large and varied set of test subjects certainly has many merits, the large variability in subject anthropometry could be considered a limitation of this study. Subject weight ranged from 48.2 – 105.7 kg, subject height ranged from 154.2 – 181.2 cm, and both male and female subjects were used. This large variation in subject anthropometry manifested in highly-variable biodynamic responses between subjects, even for the same strap tension and vibration profile. The use of intra-subject normalization that was implemented in the data analysis reduced the anthropometry variability among subjects and provided a sound assessment for the differences between strap tension conditions.

Another potential limitation was the lack of trial repetition – each subject was exposed to each combination of vibration profile and strap tension only once. Multiple repetitions would have made the data collected more robust. This is especially true as subjects may have taken some time to become accustomed to the vibration process. For example, a subject unaccustomed to the vibration process may have tensed their body on the first exposure but have fully relaxed by the sixth. This body tension would certainly impact the vibration response. Exposing subjects to the same conditions multiple times would have both allowed for the investigation of such a relaxation response, as well as improved the quality of the intra-subject normalization. Despite this, it should be noted that the order of application of the combinations of vibration profile and strap tension were randomized between subjects. This would have randomly distributed and reduced the effects of a relaxation response.

Strap tension is another potential limitation. Even assuming that the tension was measured and set perfectly for each trial, straps can shift and change tension under vibration. Also, the interaction between straps and different anthropometries (such as different ratios and distributions of adipose and muscle tissue) adds further complication. However, both of these cases are representative of real-world conditions and might therefore be unavoidable.

Other Considerations

In this study, the subjects were placed directly onto the litter – a rigid spineboard was not placed between the subject and the litter as is sometimes done. The litter is composed of a mesh that conforms to the subject's body. This mesh-conformation phenomenon both changes how and where energy is transferred from the vibration platform to the subject and introduces a multi-faceted spring-damper effect associated with the stretching of the litter mesh. If a rigid spineboard were used, the transfer of energy from the vibration platform to the subject would be more evenly distributed and the spring-damper effect resulting from litter mesh stretching would be simplified and mitigated. For these reasons, future studies in this area should consider placing a spineboard between the subject and the litter.

References and Works Cited

Barazanji K, Jonathan D, Frick E, Rahmatalla S, Kinsler R. "Biodynamically Validated Instrumented Supine Manikin for Evaluation of Patient Systems," oral presentation at Military Health System Research Symposium, Kissimmee, Florida, August 2019.

Conti, C., Kroening, L., Lloyd, A., Kinsler, R., and Molles, J (2019). Effect of Patient Weight as a Factor during Use of an Immobilization System versus No Immobilization System. USAARL Technical Report No. 2020– 004, 2019

DeShaw, J., & Rahmatalla, S. (2012). Comprehensive Measurement in Whole-Body Vibration. *Journal of Low Frequency Noise, Vibration and Active Control*, 31(2), 63-74.

DeShaw, J., Rahmatalla, S. (2015). Predictive discomfort of supine humans in whole-body vibration and shock environments. *Ergonomics*, 59(4), 568-581.

Deshaw, J, Frick, E., Rahmatalla, S., Kinsler, R., and Barazanji, K. (2019). Biodynamically Validated Instrumented Supine Manikin for Evaluation of Patient Systems. Abstract, Military Health System Research Symposium, Kissimmee, FL, August 2019.

International Organization for Standardization, "ISO 7096:2020, Earth-moving machinery – Laboratory evaluation of operator seat vibration," Switzerland, 2020.

International Organization for Standardization, "ISO 2631-1: 1997, Mechanical Vibration and Shock - Evaluation of Human Exposure to Whole-body Vibration," Switzerland, 1997.

International Organization for Standardization, "ISO 2631-5: 1997, Mechanical Vibration and Shock - Evaluation of Human Exposure to Whole-body Vibration – Part 5: Method for evaluation of vibration containing multiple shocks.," Switzerland, 1997.

Kinsler, R. and Barazanji, K. (2011). *Assessment of fixed position litter loading in the HH-60M MEDEVAC helicopter*. Fort Rucker, AL: U.S. Army Aeromedical Research Laboratory. USAARL Technical Memorandum 2011-19.

Kinsler, R., Barazanji, K., Lee, J., Fulton, L., & Hatzfeld, J. (2015). *Analysis of Two Surveys Examining Enroute Care Technologies, Platforms, and Space Requirements.* Poster Presentation at Military Health System Research Symposium, August 2015.

Kinsler, R., Khouri, R., Squire, C., Conti, S., & Wurzbach, J. (2018). [Immobilization and Vibration Mitigation Systems: Test and Evaluation of Current and Developmental Products]. Unpublished report. Fort Rucker, AL: U.S. Army Aeromedical Research Laboratory.

Meusch, J., & Rahmatalla, S. (2014a). 3D Transmissibility and Relative Transmissibility of Immobilized Supine Humans during Transportation. *Journal of Low Frequency Noise, Vibration and Active Control*, 33(2), 125-138.

Meusch, J., & Rahmatalla, S. (2014b). Whole-body vibration transmissibility in supine humans: effects of board litter and neck collar. *Applied Ergonomics,* 45 (3), 677–685.

Ratanalert, S., Phuenpathom, N., Saeheng, S., Oearsakul, T., Sripairojkul, B., Hirunpat, S. (2004). ICP Threshold in CPP Management of Severe Head Injury Patients, Surg Neurol, 61(5):429-34.

Reno, J. (2010). Military aeromedical evacuation, with special emphasis on craniospinal trauma, Neurosurg Focus 28 (5):E12.

S. O. H. Madgwick, A. J. L. Harrison and R. Vaidyanathan, "Estimation of IMU and MARG orientation using a gradient descent algorithm," *2011 IEEE International Conference on Rehabilitation Robotics*, 2011, pp. 1-7, doi: 10.1109/ICORR.2011.5975346.

Appendix

Human Transmissibility Results

The transmissibility results shown in Figure 15, Figure 16, and Figure 17 are better suited to assessing the impact of varying strap tension due to their intra-subject normalization. However, viewing the same data prior to intra-subject normalization provides additional, useful information. The transmissibility curves shown in Figure 24 to Figure 32 are particularly useful for understanding the transmissibility responses of each segment, as well as the magnitude of the inter-subject variability that made intra-subject normalization necessary. Before presenting the aforementioned figures, Table 6 is presented, in which t-tests were applied to the transmissibility metrics before intra-subject normalization.

Table 6: Tabulated p-values for the three transmissibility metrics applied to the human subject data (***not*** subjected to intra-subject normalization). Yellow highlights denote statistically significant values ($p < 0.05$) and green highlights denote marginally statistically significant values ($p < 0.10$).

VIBRATION PROFILE	BODY SEGMENT	MAX TRANSMISSIBILITY	AREA UNDER TRANSMISSIBILITY CURVE	RESONANT FREQUENCY
AIR	Head	0.4390	0.6522	0.0757
	Chest	0.4430	0.1526	0.6383
	Pelvis	0.4695	0.2604	0.8249
GROUND	Head	0.0148	0.0207	0.4793
	Chest	0.9558	0.1658	0.7219
	Pelvis	0.3038	0.3623	0.5074
WHITE NOISE	Head	0.0700	0.1954	0.8346
	Chest	0.7398	0.1981	0.4382
	Pelvis	0.5226	0.3500	0.3721

For the transmissibility plots (Figure 24 to Figure 32), a pair of graphs will shown for each combination of the three body segments (head, chest, and pelvis) and the three vibration profiles (Air, Ground, White Noise). Both graphs in the pair will include three lines, one solid and two dashed. The solid line represents the mean value over all subjects, and the dashed lines encompass an envelope determined by the corresponding standard deviation. Furthermore, the left graph will show the results for the low tension strap case, and the right graph will show the results for the standard tension strap case. For ease of comparison, all graphs will be displayed on axes with the same limits (1-22 Hz for the X axis, and 0 to 3.2 transmissibility magnitude for the Y axis).

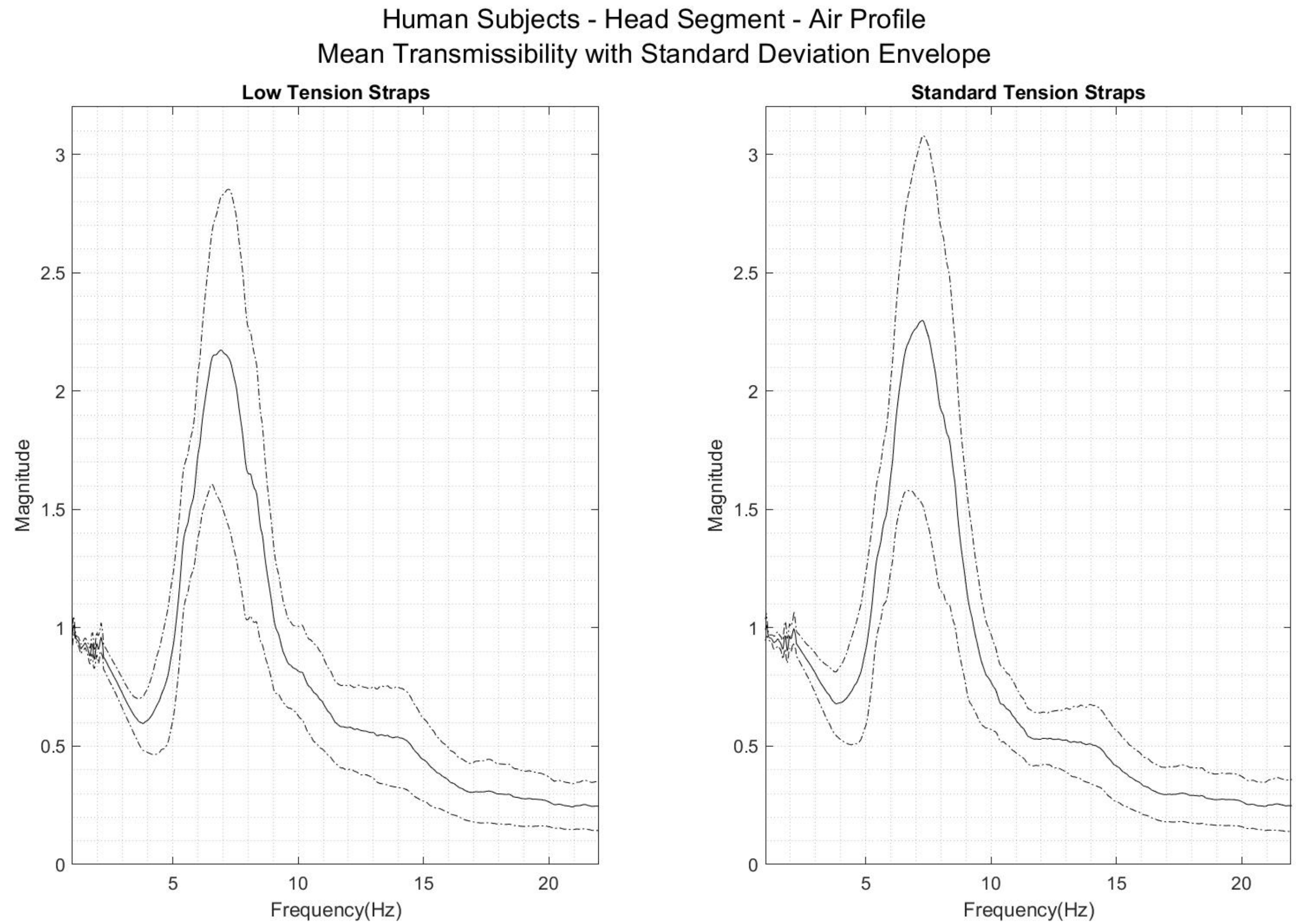

Figure 24: Plots of human subject mean transmissibility (solid line) with the corresponding standard deviation envelope (dashed lines). The results of the head segment in the air vibration profile are shown here. The left graph depicts the low tension strap condition, and the right graph depicts the standard tension strap condition.

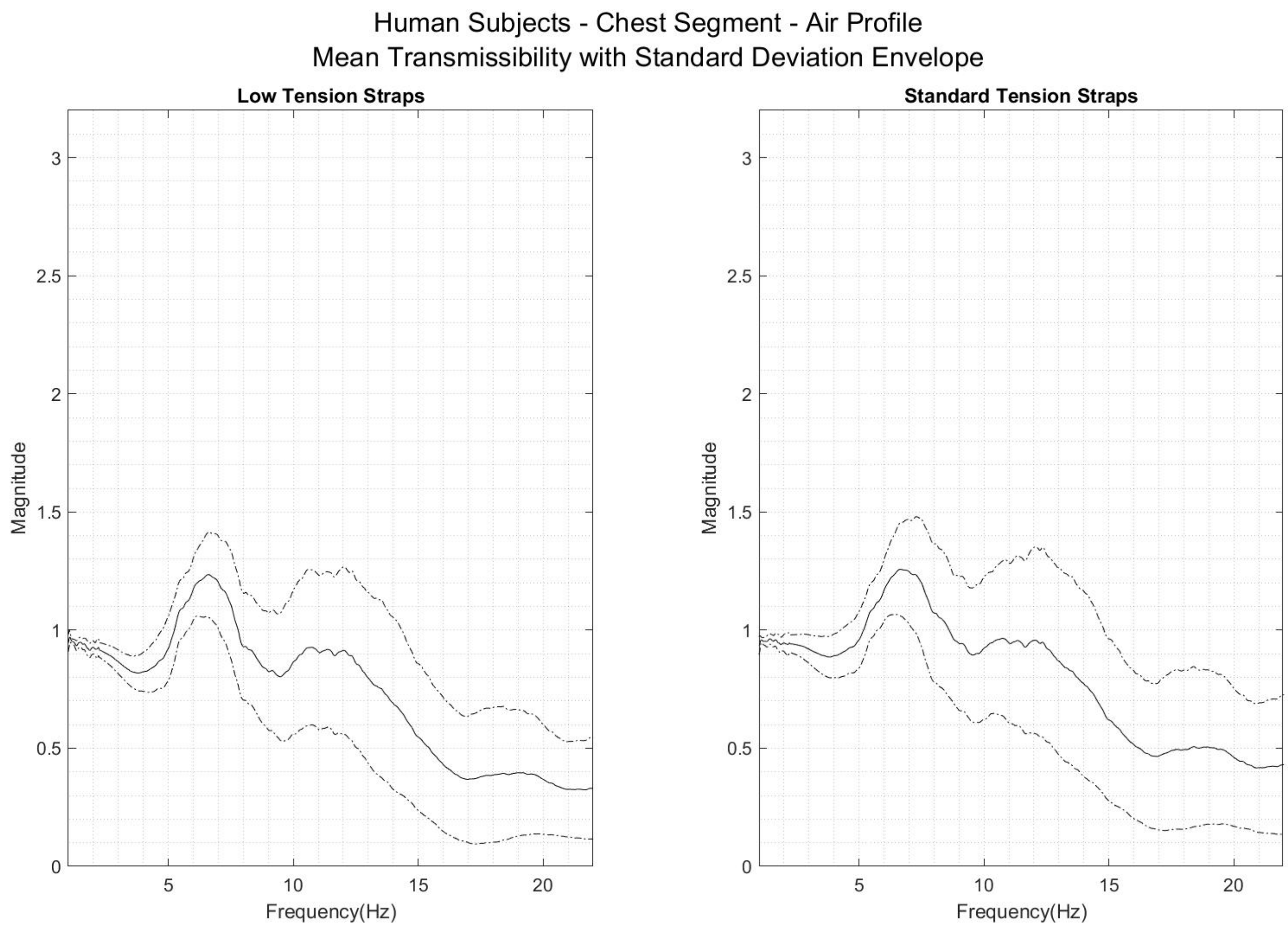

Figure 25: Plots of human subject mean transmissibility (solid line) with the corresponding standard deviation envelope (dashed lines). The results of the chest segment in the air vibration profile are shown here. The left graph depicts the low tension strap condition, and the right graph depicts the standard tension strap condition.

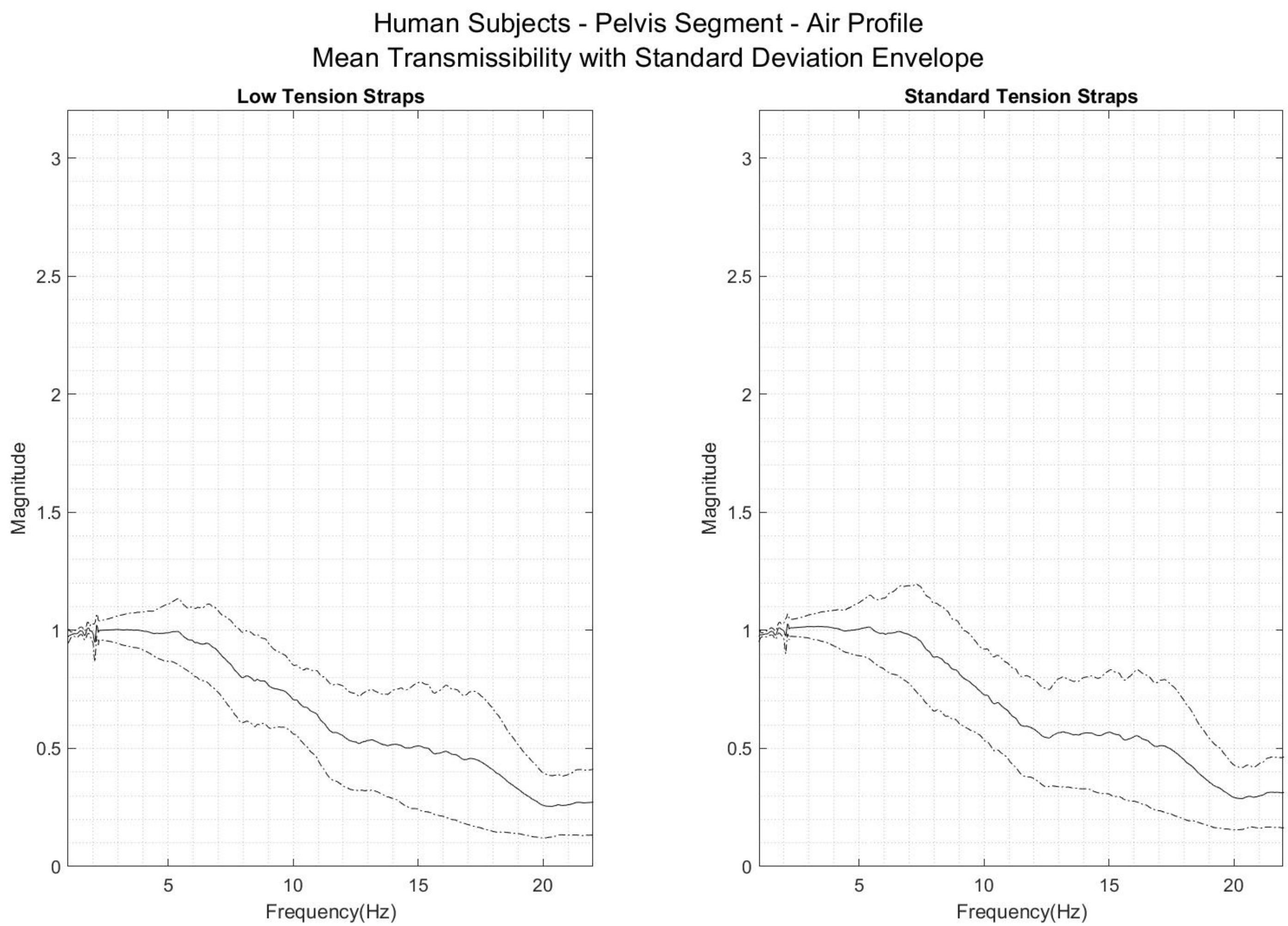

Figure 26: Plots of human subject mean transmissibility (solid line) with the corresponding standard deviation envelope (dashed lines). The results of the pelvis segment in the air vibration profile are shown here. The left graph depicts the low tension strap condition, and the right graph depicts the standard tension strap condition.

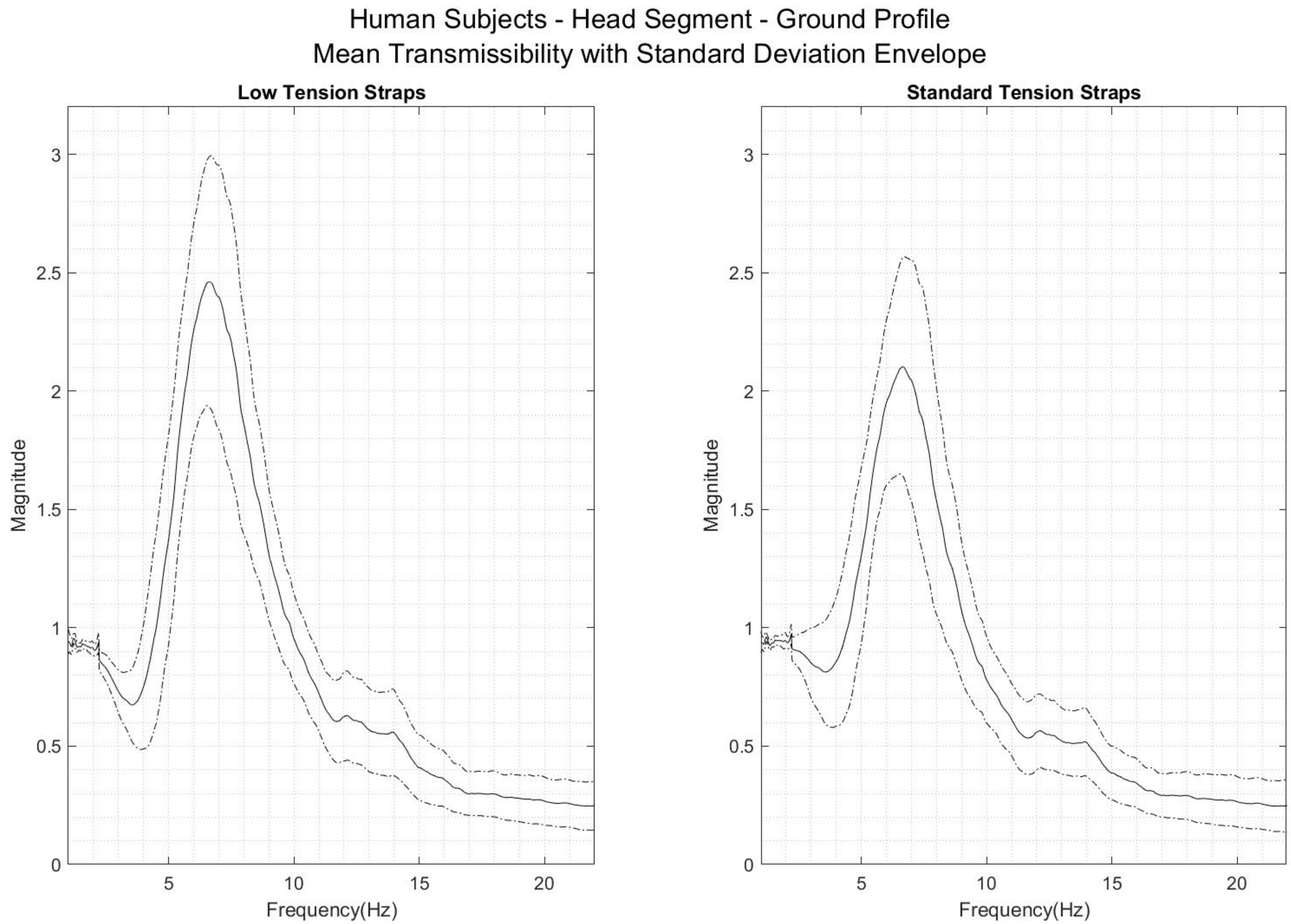

Figure 27: Plots of human subject mean transmissibility (solid line) with the corresponding standard deviation envelope (dashed lines). The results of the head segment in the ground vibration profile are shown here. The left graph depicts the low tension strap condition, and the right graph depicts the standard tension strap condition.

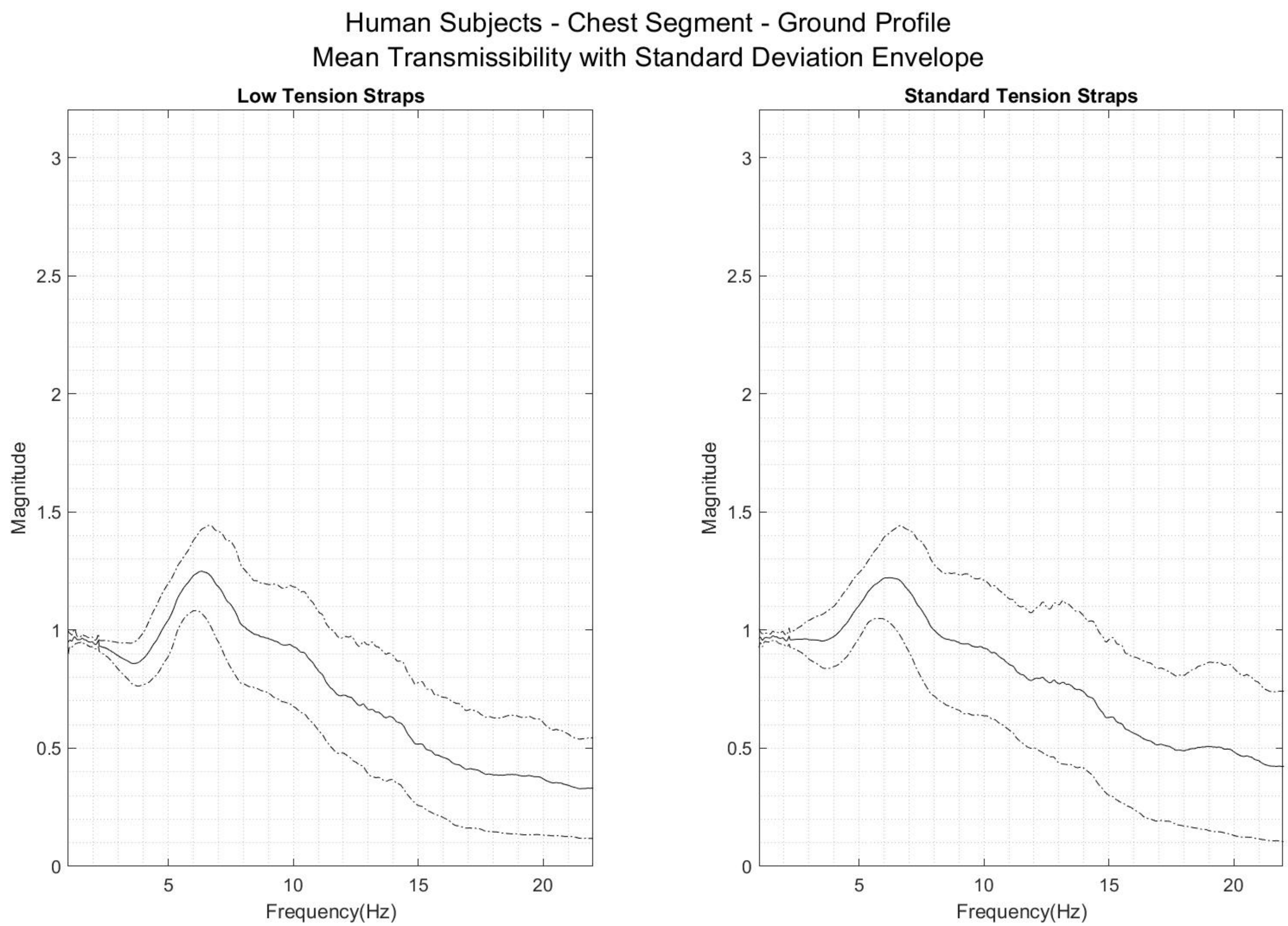

Figure 28: Plots of human subject mean transmissibility (solid line) with the corresponding standard deviation envelope (dashed lines). The results of the chest segment in the ground vibration profile are shown here. The left graph depicts the low tension strap condition, and the right graph depicts the standard tension strap condition.

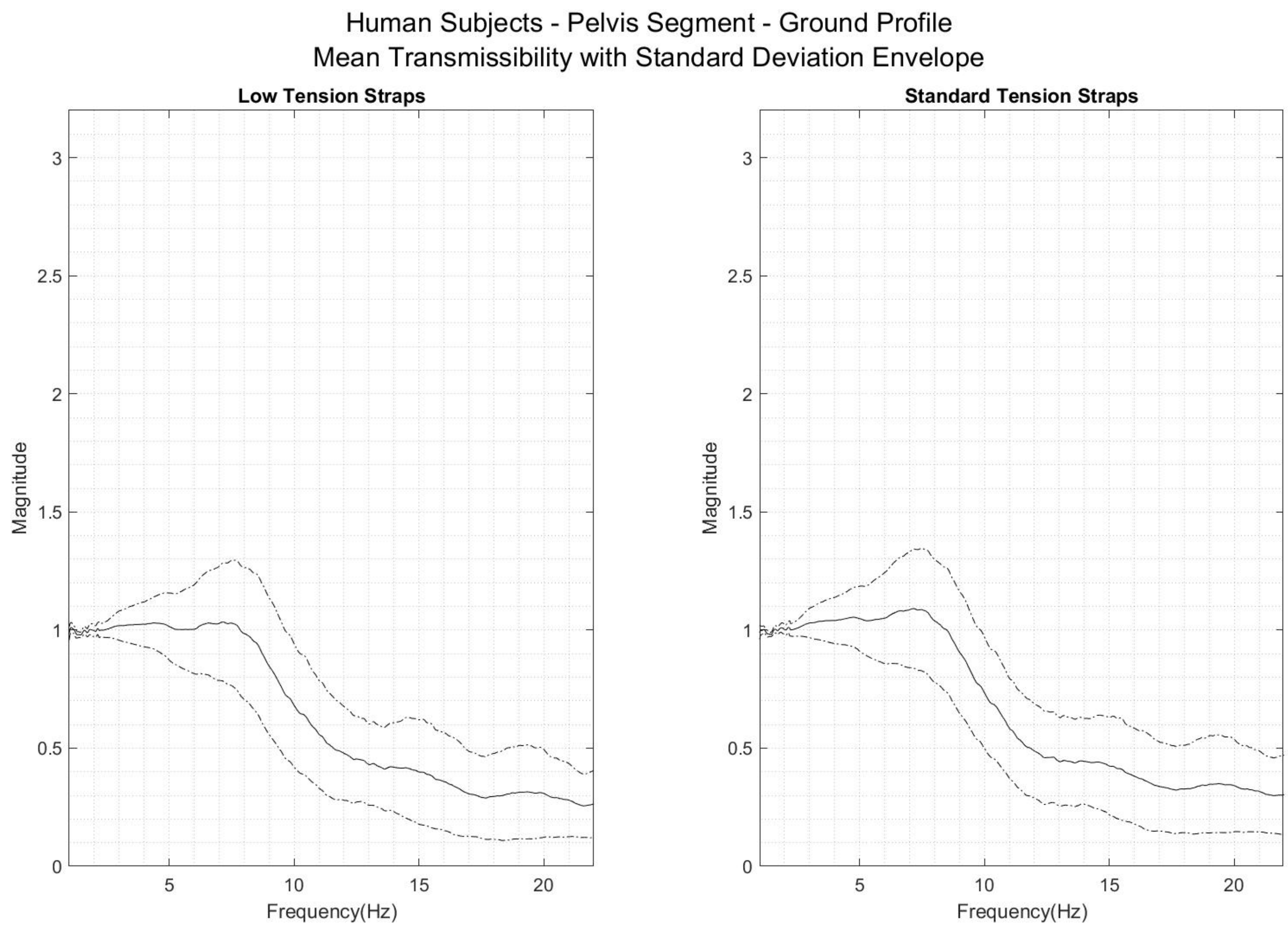

Figure 29: Plots of human subject mean transmissibility (solid line) with the corresponding standard deviation envelope (dashed lines). The results of the pelvis segment in the ground vibration profile are shown here. The left graph depicts the low tension strap condition, and the right graph depicts the standard tension strap condition.

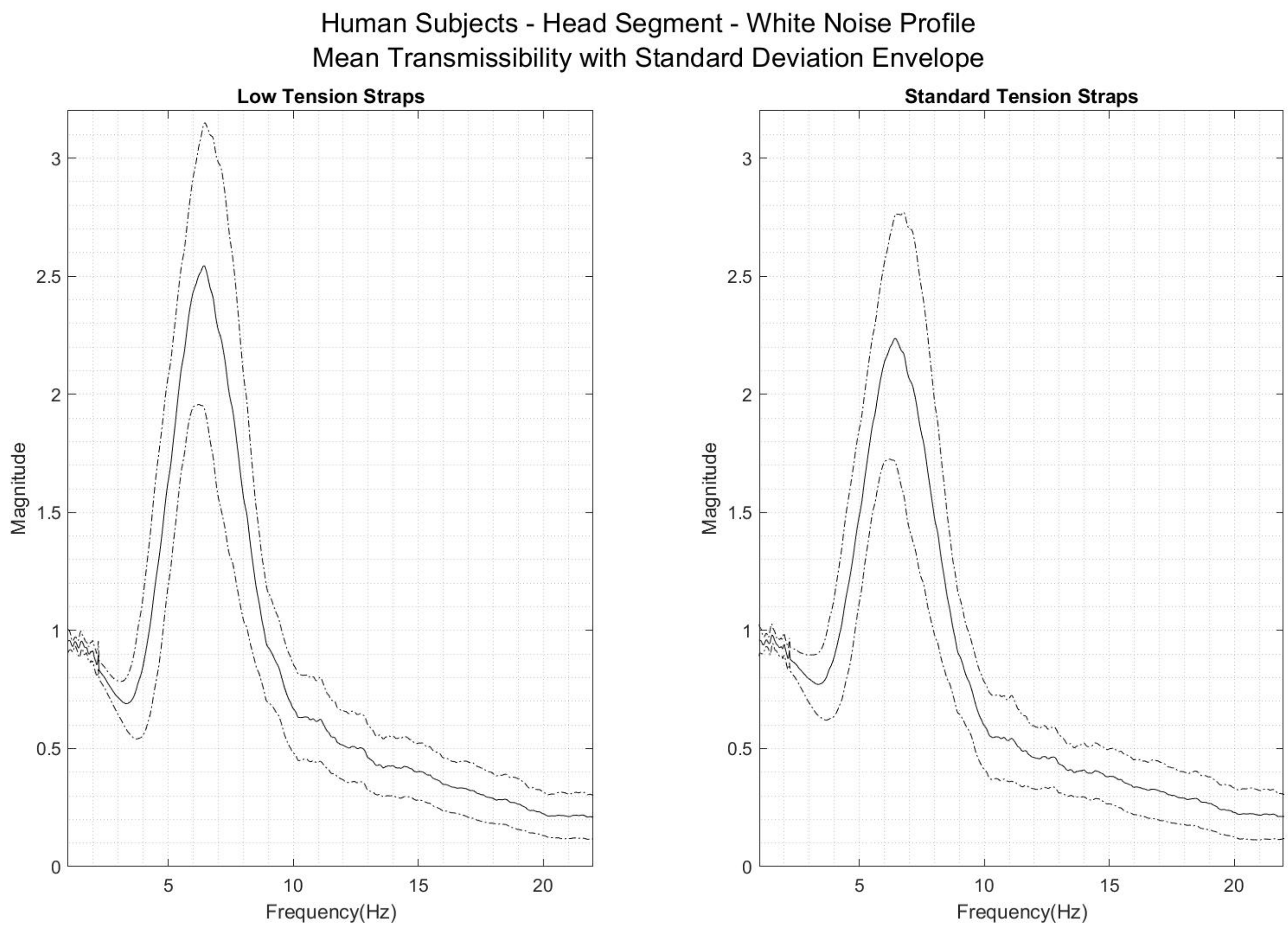

Figure 30: Plots of human subject mean transmissibility (solid line) with the corresponding standard deviation envelope (dashed lines). The results of the head segment in the white noise vibration profile are shown here. The left graph depicts the low tension strap condition, and the right graph depicts the standard tension strap condition.

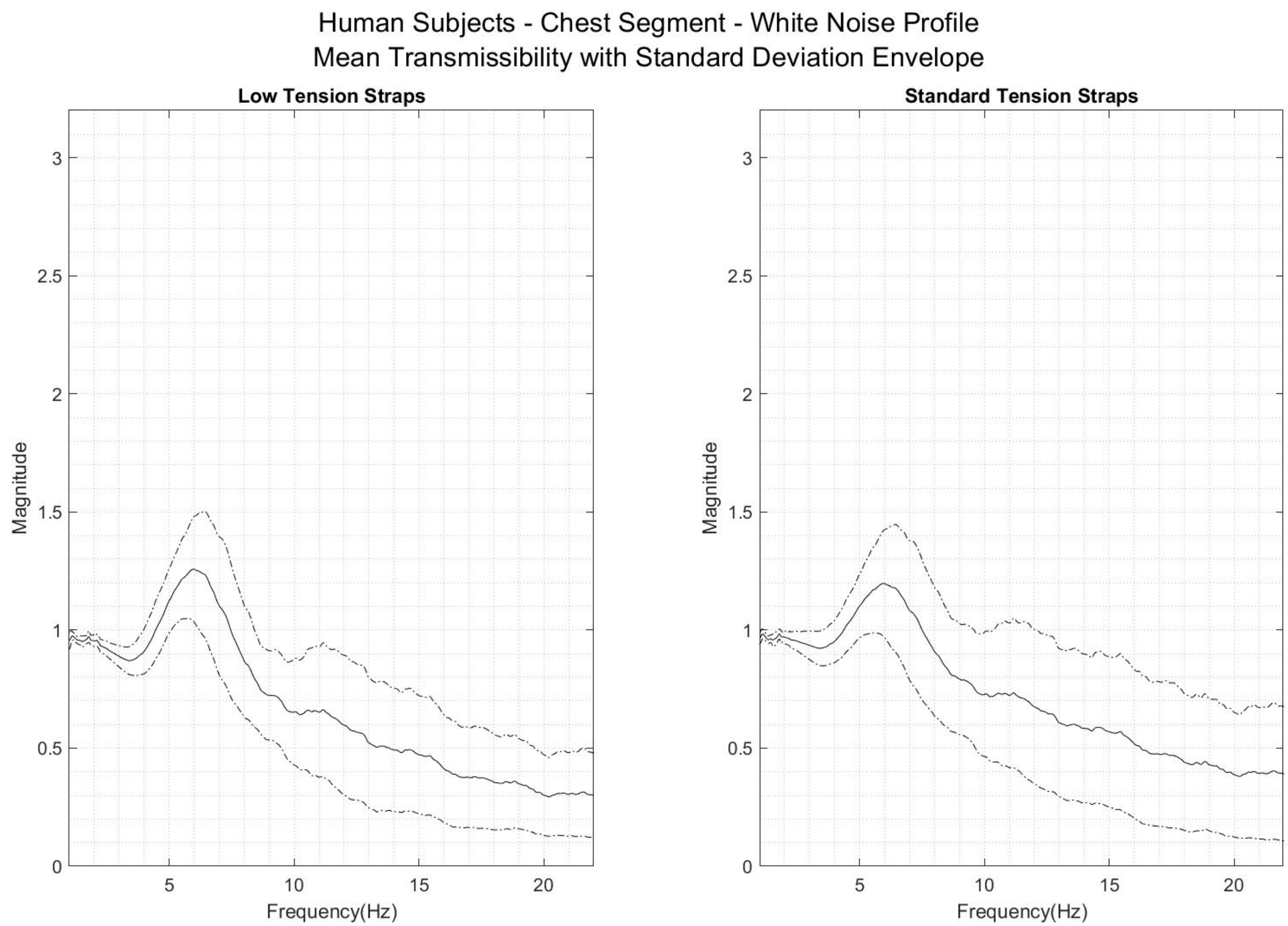

Figure 31: Plots of human subject mean transmissibility (solid line) with the corresponding standard deviation envelope (dashed lines). The results of the chest segment in the white noise vibration profile are shown here. The left graph depicts the low tension strap condition, and the right graph depicts the standard tension strap condition.

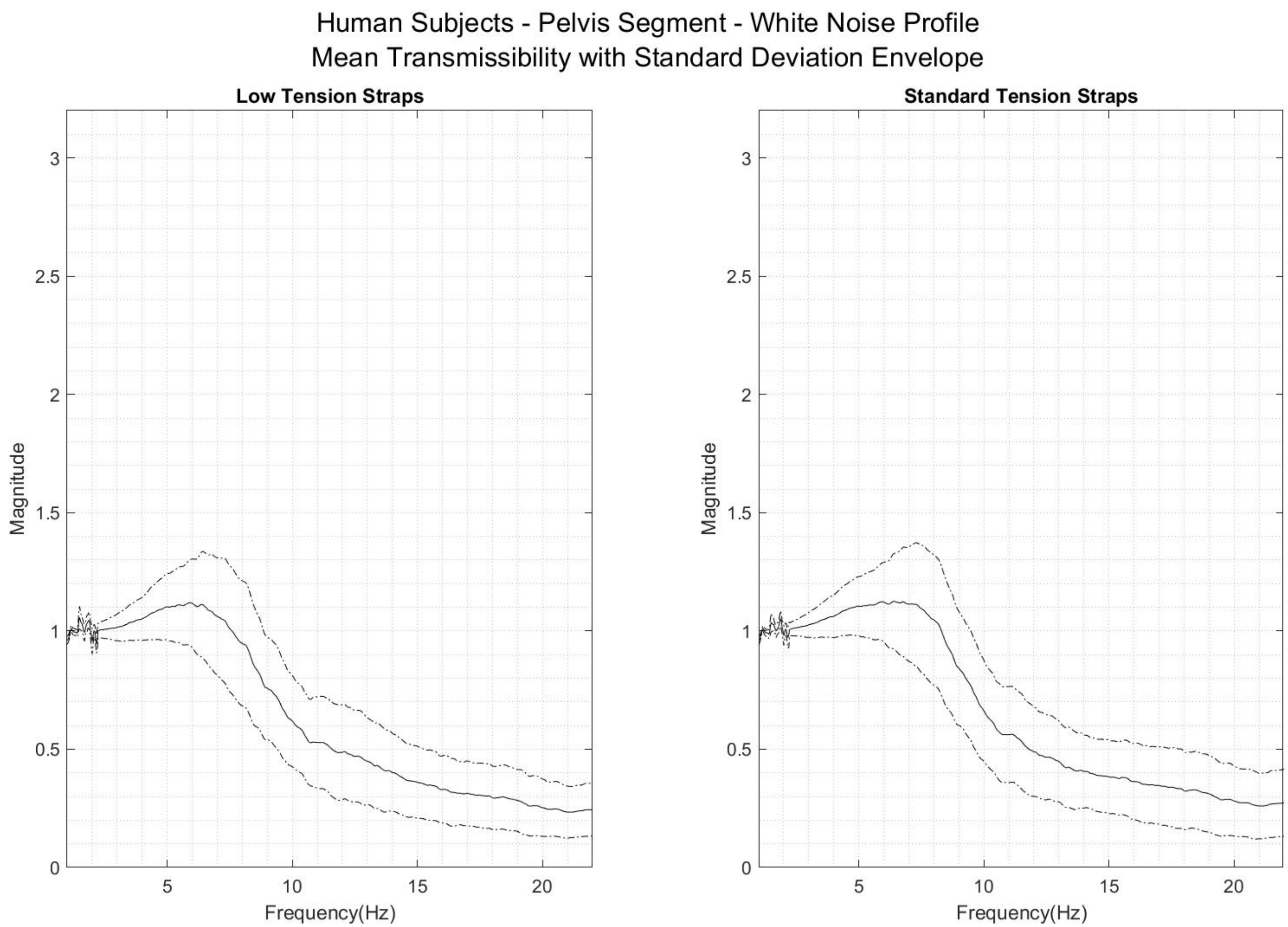

Figure 32: Plots of human subject mean transmissibility (solid line) with the corresponding standard deviation envelope (dashed lines). The results of the pelvis segment in the white noise vibration profile are shown here. The left graph depicts the low tension strap condition, and the right graph depicts the standard tension strap condition.

Table 7: List of the three transmissibility metrics for human subjects one to eleven.

Transmissibility Metric		Max Transmissibility						Area Under Transmissibility Curve						Resonant Frequency					
Vibration Profile		Air		Ground		White Noise		Air		Ground		White Noise		Air		Ground		White Noise	
Strap Tension		Low	Standard	Low	Standard	Low	Standard	Low	Standard	Low	Standard	Low	Standard	Low	Standard	Low	Standard	Low	Standard
Subject 1	Head	3.09	3.74	3.38	3.42	2.87	3.15	499.24	563.70	468.20	469.62	367.22	400.97	4.07	4.34	3.81	3.67	3.97	4.01
	Chest	0.71	0.65	0.72	1.11	0.19	0.18	163.03	155.54	135.88	163.95	56.25	54.11	4.24	4.61	4.44	4.01	4.84	4.84
	Pelvis	1.35	1.35	1.19	1.27	1.42	1.36	278.67	277.56	253.47	277.41	216.62	218.26	3.07	3.30	3.27	3.27	2.24	2.24
Subject 2	Head	1.86	1.86	2.03	2.02	1.60	1.65	316.73	291.54	383.39	376.33	266.76	269.55	6.41	6.44	6.51	6.34	6.01	5.98
	Chest	0.35	0.31	0.30	0.30	0.21	0.22	122.30	120.78	100.97	117.17	58.14	71.45	5.47	9.71	5.31	10.45	6.41	6.94
	Pelvis	1.33	1.35	1.00	1.07	1.26	1.10	324.73	323.38	271.35	286.42	240.37	246.77	3.64	3.97	2.97	3.67	2.24	3.30
Subject 3	Head	1.63	1.57	2.57	2.55	1.84	1.94	316.63	328.61	412.25	434.64	300.28	299.95	5.24	4.87	5.37	5.34	5.04	5.04
	Chest	0.51	0.37	0.50	0.38	0.18	0.15	137.92	134.59	125.25	120.95	65.33	61.77	5.21	5.07	5.24	4.61	5.37	4.74
	Pelvis	1.28	1.10	1.20	1.05	1.57	1.58	238.47	201.33	225.45	188.68	206.22	190.19	3.27	3.24	2.24	2.24	2.24	2.24
Subject 4	Head	1.83	2.08	2.98	3.08	2.14	2.22	397.12	432.89	498.99	520.19	370.07	383.19	4.97	6.38	5.37	5.37	5.84	5.88
	Chest	0.51	0.58	0.55	0.56	0.30	0.25	140.65	158.74	133.33	151.66	70.10	69.86	5.11	5.51	5.24	4.71	4.84	5.07
	Pelvis	1.23	1.27	1.06	1.02	1.21	1.26	282.93	291.50	272.08	267.92	227.46	215.00	3.61	3.67	3.34	3.34	2.24	2.24
Subject 5	Head	1.94	1.36	1.97	2.30	1.60	1.54	373.85	249.93	402.18	453.37	304.72	250.08	6.44	6.64	6.54	6.34	6.34	6.34
	Chest	0.36	0.52	0.51	0.41	0.18	0.15	128.49	138.25	152.21	134.21	58.33	54.49	6.58	5.34	4.71	4.71	6.01	5.21
	Pelvis	0.79	0.98	0.98	1.02	0.75	1.00	205.15	241.63	228.07	244.51	147.63	207.46	3.37	3.97	3.07	3.44	3.41	3.44
Subject 6	Head	2.51	2.49	3.31	3.50	2.47	2.48	373.07	381.42	501.06	524.19	362.80	374.08	6.41	6.38	5.41	5.44	5.84	5.84
	Chest	0.50	0.54	0.62	0.60	0.24	0.29	151.08	153.68	149.12	156.33	61.20	66.31	5.54	6.18	7.04	5.31	5.84	6.01
	Pelvis	1.28	1.17	1.52	1.55	1.20	1.10	297.99	292.63	298.76	302.03	215.98	209.37	3.71	3.74	3.47	3.61	3.20	3.34
Subject 7	Head	2.42	2.61	2.87	2.74	2.22	2.25	427.38	473.78	503.54	534.12	377.76	398.18	6.38	6.38	5.37	5.41	5.51	5.98
	Chest	0.52	0.48	0.56	0.52	0.15	0.20	131.68	143.38	116.27	123.43	45.40	57.54	5.54	5.47	5.04	4.44	5.77	5.81
	Pelvis	2.08	2.06	1.70	1.88	1.80	1.78	442.13	456.85	399.01	416.63	358.32	382.30	3.64	3.64	3.30	3.51	2.24	3.37
Subject 8	Head	2.30	2.29	3.55	3.10	2.41	2.38	428.13	400.52	541.88	499.61	385.35	364.30	4.97	4.94	5.14	5.14	4.84	4.67
	Chest	0.46	0.45	0.49	0.43	0.24	0.18	134.55	140.71	140.32	135.70	76.95	74.71	4.47	4.71	4.71	4.57	4.84	4.87
	Pelvis	1.25	1.31	1.14	1.15	1.08	1.09	293.07	299.24	255.63	274.15	219.45	207.83	3.64	4.41	3.30	3.54	3.17	3.24
Subject 9	Head	1.80	2.01	2.51	2.22	1.70	1.94	355.49	363.21	487.82	428.92	337.57	360.45	7.04	6.44	6.58	6.34	6.38	6.38
	Chest	0.55	0.55	0.63	0.45	0.22	0.21	161.59	168.71	165.42	147.36	66.42	63.84	7.78	7.04	5.24	7.44	5.98	6.01
	Pelvis	1.30	1.00	1.14	0.89	1.05	0.87	316.86	295.10	247.53	243.05	211.94	195.57	3.71	4.04	3.34	4.57	3.74	3.84
Subject 10	Head	2.39	2.31	2.54	3.00	1.75	1.98	447.68	410.22	528.48	524.45	359.36	354.67	6.84	6.41	6.58	6.58	6.08	6.08
	Chest	0.36	0.43	0.55	0.47	0.17	0.15	117.93	134.78	137.11	149.08	53.85	52.06	6.51	6.54	4.71	5.14	6.01	5.41
	Pelvis	1.11	1.23	1.27	1.49	0.88	1.02	219.93	233.05	215.57	231.86	150.30	167.20	4.91	4.87	4.34	4.34	3.54	3.77
Subject 11	Head	2.31	2.51	2.45	2.81	2.09	2.09	411.02	417.02	458.05	488.30	366.94	358.74	6.41	6.44	6.31	6.31	6.04	6.01
	Chest	0.49	0.45	0.54	0.58	0.29	0.27	176.58	189.03	193.38	179.47	82.81	92.23	6.88	6.54	4.71	4.71	6.38	6.78
	Pelvis	1.17	1.33	1.22	1.43	1.03	1.13	202.60	218.46	218.84	242.64	155.03	170.16	4.41	4.41	3.77	4.14	3.47	3.57

Table 8: List of the three transmissibility metrics for human subjects twelve to twenty-five.

Subject 12	Head	2.10	2.20	3.41	3.24	1.97	2.07	426.37	314.04	496.90	507.06	304.51	318.29	4.87	4.87	5.14	5.17	4.74	4.77
	Chest	0.62	0.51	0.73	0.57	0.31	0.27	173.66	151.61	159.01	140.30	67.64	64.45	4.17	5.44	5.04	4.67	4.24	4.21
	Pelvis	1.64	1.63	1.33	1.29	1.49	1.37	363.48	384.69	311.57	335.98	272.99	272.74	3.71	4.01	3.34	3.61	3.34	3.44
Subject 13	Head	1.81	1.57	2.65	2.30	1.80	1.65	334.22	301.98	414.69	402.27	257.10	234.42	4.81	4.91	5.11	4.94	4.64	4.67
	Chest	0.72	0.62	0.72	0.65	0.20	0.20	175.82	181.93	151.74	158.55	76.94	78.13	4.21	4.67	4.04	4.01	3.67	4.11
	Pelvis	0.62	0.55	0.61	0.61	0.37	0.33	160.73	179.08	144.53	152.82	114.24	111.06	4.94	5.01	4.51	4.57	3.61	4.61
Subject 14	Head	3.27	3.27	3.43	3.67	3.08	3.38	487.78	510.56	593.04	632.44	500.43	538.55	6.41	6.44	6.31	6.31	6.01	5.98
	Chest	0.40	0.36	0.46	0.60	0.20	0.23	158.59	142.13	141.06	155.51	66.79	71.09	6.88	5.54	4.74	4.74	5.37	5.84
	Pelvis	1.52	1.56	1.46	1.53	1.28	1.32	355.88	366.09	330.38	350.41	256.95	262.97	4.01	4.01	3.81	3.84	3.57	3.67
Subject 15	Head	2.30	2.39	3.62	3.85	2.49	2.60	366.55	362.98	503.23	488.48	345.04	331.48	4.84	4.81	5.11	5.07	4.84	4.27
	Chest	0.56	0.59	0.92	0.76	0.25	0.23	154.77	168.56	172.51	168.30	61.55	69.87	5.44	4.64	4.97	4.94	5.57	4.57
	Pelvis	1.30	1.19	1.09	1.25	0.98	1.01	303.93	295.94	258.98	266.47	207.49	211.27	3.64	3.97	3.67	3.74	3.51	3.54
Subject 16	Head	2.33	2.69	2.63	2.82	2.16	2.14	399.20	422.70	474.90	494.20	363.01	357.60	6.41	6.44	6.31	6.31	6.04	6.08
	Chest	0.41	0.51	0.64	0.63	0.27	0.25	144.75	155.33	146.80	153.13	57.78	61.26	6.48	6.14	4.71	4.71	6.04	6.01
	Pelvis	1.52	1.42	1.45	1.46	1.62	1.31	291.23	274.74	250.75	264.79	212.19	204.91	3.34	3.57	3.30	3.34	2.24	3.41
Subject 17	Head	2.24	2.41	2.54	2.43	1.90	1.98	481.61	466.76	529.93	491.86	382.98	373.78	6.71	6.44	6.61	6.54	6.04	6.04
	Chest	0.47	0.46	0.80	1.00	0.31	0.26	135.94	136.96	167.80	185.58	73.51	66.52	5.24	5.31	4.71	4.71	6.38	4.97
	Pelvis	1.07	1.03	1.11	1.02	1.17	1.07	245.02	261.57	213.63	235.46	217.02	219.74	3.77	3.77	3.30	3.64	3.27	3.41
Subject 18	Head	2.08	2.21	2.16	2.39	1.67	1.73	377.25	368.31	433.54	444.12	317.27	309.62	6.41	6.78	6.31	6.34	6.01	6.04
	Chest	0.58	0.67	0.74	0.67	0.24	0.23	170.27	170.86	176.69	180.48	71.30	68.17	7.58	7.91	6.41	6.64	6.44	6.84
	Pelvis	1.55	1.30	1.51	1.58	1.18	1.08	310.35	282.35	269.36	295.58	198.76	185.08	4.41	4.91	4.34	4.34	3.77	3.77
Subject 19	Head	1.92	2.02	2.91	3.22	2.13	2.41	344.53	410.63	516.63	542.16	332.93	371.19	6.41	6.44	5.41	5.41	5.81	5.47
	Chest	0.40	0.41	0.53	0.44	0.21	0.23	128.65	123.37	124.12	117.36	54.41	58.54	5.54	5.41	5.21	5.21	5.77	5.61
	Pelvis	1.67	1.47	1.53	1.43	2.33	2.05	318.71	315.92	289.17	295.99	263.91	270.16	3.24	3.07	2.24	3.07	2.24	2.24
Subject 20	Head	1.90	1.94	2.33	2.48	1.83	1.96	365.53	400.13	439.67	459.74	323.05	349.91	6.44	6.41	6.14	6.18	5.98	5.88
	Chest	0.43	0.44	0.68	0.77	0.19	0.20	126.55	138.78	155.51	159.81	53.76	59.46	5.11	5.27	5.17	4.71	6.04	5.57
	Pelvis	1.20	1.07	1.53	1.57	1.48	1.43	299.29	258.74	316.81	319.00	191.16	180.98	3.14	3.27	3.30	3.34	2.24	2.24
Subject 21	Head	1.18	1.17	2.14	2.09	1.28	1.40	234.55	229.60	341.58	341.16	223.39	241.26	6.44	5.27	5.31	5.37	5.04	5.04
	Chest	0.45	0.47	0.57	0.51	0.17	0.21	143.46	140.66	135.01	144.54	54.60	59.73	5.11	5.64	4.74	4.74	5.61	4.84
	Pelvis	1.49	1.31	1.30	0.97	1.15	1.21	284.09	260.41	224.44	230.36	196.47	195.24	2.24	2.24	2.24	2.24	2.24	2.24
Subject 22	Head	1.92	2.00	2.96	2.88	1.95	2.03	482.12	510.90	566.63	561.21	381.81	387.00	6.38	6.48	6.54	6.54	6.01	6.01
	Chest	0.41	0.40	0.61	0.68	0.18	0.19	130.04	130.06	128.42	143.23	49.07	50.36	5.94	5.07	5.27	5.27	5.61	5.57
	Pelvis	1.20	1.11	0.87	0.94	0.94	0.87	318.76	282.65	255.34	265.12	227.13	216.73	4.91	4.44	4.44	4.61	3.47	3.57
Subject 23	Head	1.82	1.82	2.36	2.42	1.92	2.02	305.60	313.56	369.51	390.85	292.82	300.60	5.54	5.54	5.37	5.41	5.07	5.04
	Chest	0.51	0.51	0.58	0.73	0.23	0.22	133.89	151.38	118.17	148.63	58.80	61.09	5.11	4.77	4.47	4.44	4.81	4.84
	Pelvis	1.40	1.39	1.02	1.06	1.16	0.97	282.00	277.83	260.13	260.44	196.59	196.09	3.30	3.64	3.30	3.51	2.24	3.10
Subject 24	Head	1.87	2.17	3.13	3.24	2.26	2.55	313.80	323.38	463.20	431.60	314.38	338.36	4.87	4.97	5.14	5.24	4.84	4.94
	Chest	0.61	0.56	0.76	0.98	0.24	0.19	151.05	153.24	162.69	179.34	59.50	61.73	5.24	5.11	4.84	4.67	4.67	5.81
	Pelvis	1.39	1.28	1.30	1.22	1.31	1.29	286.34	284.26	295.95	302.22	238.01	236.31	3.64	4.04	3.81	4.11	3.54	3.74
Subject 25	Head	2.27	2.36	3.58	2.95	2.22	2.23	493.53	417.61	545.99	484.45	374.66	386.84	6.34	6.44	5.41	6.31	5.81	5.98
	Chest	0.40	0.32	0.48	0.43	0.18	0.20	135.61	135.54	145.44	177.73	61.10	69.42	4.67	20.96	4.71	5.21	5.01	5.37
	Pelvis	0.88	0.74	0.89	0.88	0.82	0.67	232.68	207.21	224.69	240.90	186.46	173.62	4.91	5.64	4.57	4.57	2.24	3.44

Bandpassed Human Transmissibility Results

This report has presented much in the way of transmissibility-based metrics, and many of the results were found to be statistically significant. However, despite this significance, the differences between the low tension and standard tension conditions was generally low (less than 5%). The researchers hypothesized that because such small differences were calculated as statistically significant, greater differences were likely to be found if a more focused approach was used.

In the previous transmissibility calculations, frequencies from 1.1 – 22 Hz were considered, and a filter was used to smooth out numerical artifacts. It was hypothesized that the combination of examining such a wide frequency band and applying a filter was having an "averaging" effect on the results. To mitigate this "averaging" effect the considered frequency band was reduced to 5 – 9 Hz and no filter was applied. The same window size as before, 4000, was used. The 5 – 9 Hz band was chosen as it contained high input power, high transmissibility, or both, across the majority of the cases. The results of these bandpassed calculations can be seen below in Figure 33, Figure 34, and Figure 35.

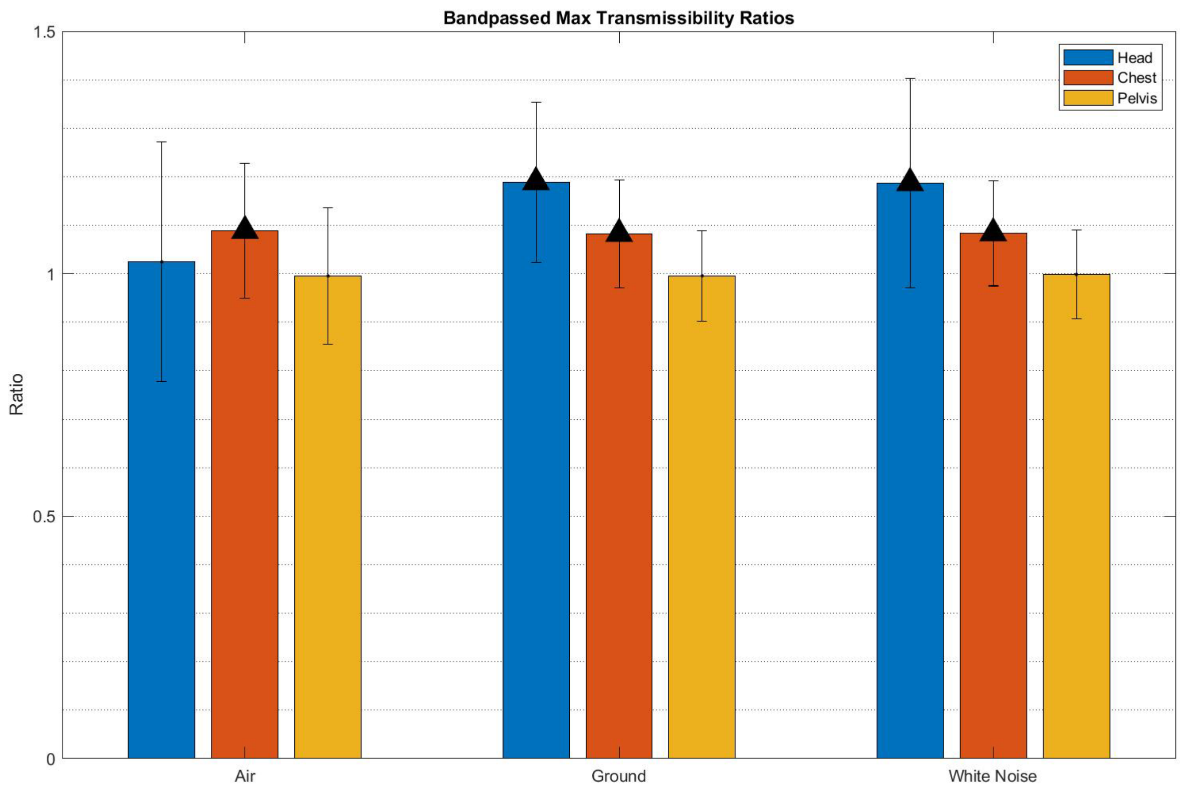

Figure 33: This figure depicts the mean ratio values and corresponding standard deviations of the bandpassed max transmissibility ratios for the head, chest, and pelvis body segments. The bar shows the mean ratio, the black brackets show the corresponding standard deviation, and the black triangles denote statistically significant results.

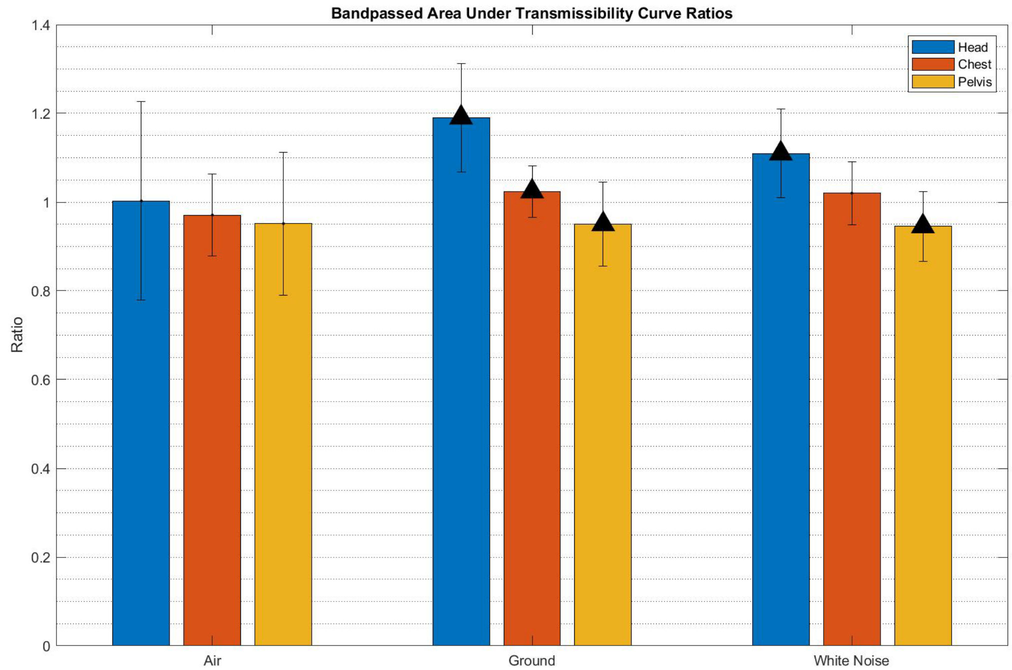

Figure 34: This figure depicts the mean ratio values and corresponding standard deviations of the bandpassed area under the transmissibility curve ratios for the head, chest, and pelvis body segments. The bar shows the mean ratio, the black brackets show the corresponding standard deviation, and the black triangles denote statistically significant results.

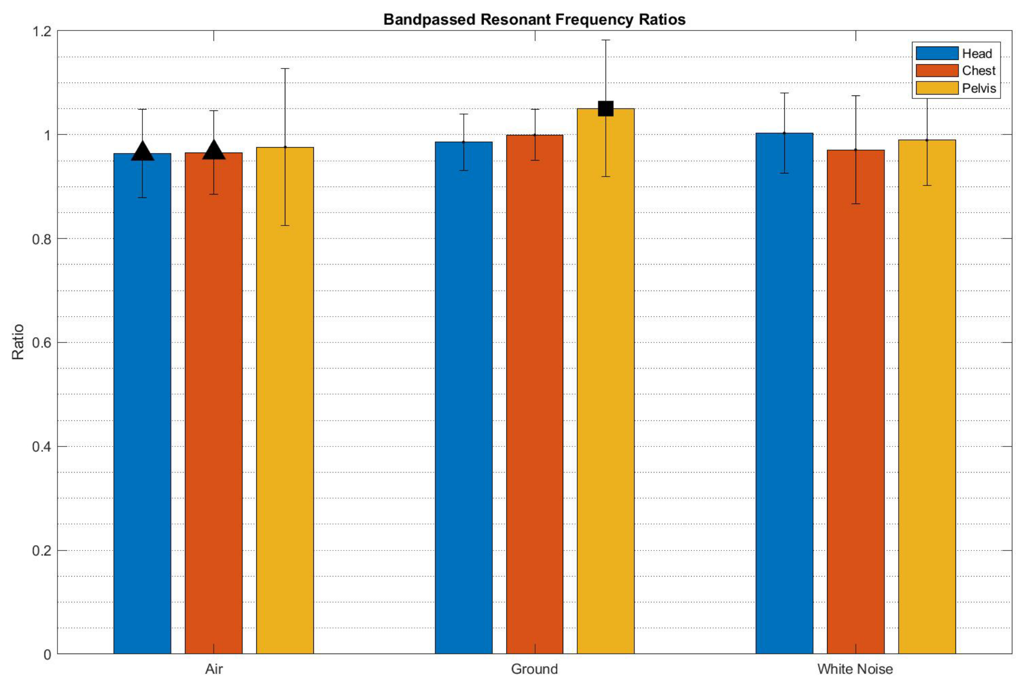

Figure 35: This figure depicts the mean ratio values and corresponding standard deviations of the bandpassed resonant frequency ratios for the head, chest, and pelvis body segments. The bar shows the mean ratio, the black brackets show the corresponding standard deviation, and the black triangles denote statistically significant results.

In the opinions of the researchers, the results of these bandpass calculations confirmed that the original approach did have an "averaging" on the results. The patterns of the original graphs were largely maintained, but the ratios tended to be of greater magnitude. Consider the Head Segment under the AuT Metric applied to the ground profile. Without bandpassing, the ratio was 1.1, but with bandpassing it was 1.19. It should be noted, however, that not all patterns were preserved in the bandpassed results. This is readily seen when comparing the results of the Air profile, likely because the Air profile had a significant amount of energy outside of the 5 – 9 Hz band.

When interpreting the bandpassed results, consider that they were not intended or expected to produce results that exactly followed the original results. Rather, they were intended to mitigate the hypothesized "averaging" effect. The original frequency band of 1.1 – 22 Hz was chosen as the author's wanted to present results covering the vast majority of consequential frequencies. These bandpassed results show that even though the differences in strap tensions can appear small in the original results, they should be take seriously, as narrowing the considered frequency bands can result in a magnification of the differences.

Relative Segment Motion Results

Table 9: List of the relative segment motion (head relative to chest) metrics for all human subjects exposed to the Air vibration profile.

Air Vibration Profile - Head Relative to Chest

Inertial Metric	RMS Acceleration						RMS Angular Velocity					
Axis	X Axis		Y Axis		Z Axis		X Axis		Y Axis		Z Axis	
Strap Tension	Low	Standard	Low	Standard	Low	Standard	Low	Standard	Low	Standard	Low	Standard
Subject 1	0.08	0.08	0.07	0.08	0.06	0.06	9.91	10.37	6.20	5.68	6.16	5.34
Subject 2	0.08	0.07	0.09	0.08	0.04	0.04	7.55	8.05	6.35	6.70	5.74	5.46
Subject 3	0.10	0.10	0.09	0.09	0.05	0.05	12.76	12.58	9.46	9.13	5.61	5.11
Subject 4	0.08	0.09	0.08	0.08	0.05	0.06	8.85	11.43	14.88	18.28	6.25	7.07
Subject 5	0.19	0.07	0.10	0.08	0.05	0.04	12.93	10.86	9.54	9.74	6.87	4.83
Subject 6	0.12	0.12	0.08	0.08	0.05	0.04	10.15	10.88	7.89	7.56	7.61	6.38
Subject 7	0.08	0.08	0.07	0.08	0.06	0.06	10.17	10.98	8.53	8.47	5.87	8.37
Subject 8	0.07	0.06	0.09	0.08	0.07	0.06	10.71	9.33	6.93	6.47	7.47	6.54
Subject 9	0.11	0.10	0.10	0.08	0.06	0.05	15.79	15.33	7.48	7.25	6.27	5.23
Subject 10	0.23	0.15	0.12	0.10	0.08	0.05	15.45	12.92	8.64	10.26	7.78	8.79
Subject 11	0.11	0.12	0.11	0.11	0.07	0.07	18.54	17.46	9.02	9.94	4.94	7.44
Subject 12	0.12	0.11	0.08	0.08	0.06	0.05	13.55	11.45	8.78	8.03	6.62	6.88
Subject 13	0.07	0.06	0.09	0.10	0.08	0.07	10.05	9.30	7.41	7.53	5.77	7.09
Subject 14	0.09	0.09	0.08	0.08	0.05	0.05	9.21	8.21	7.48	7.42	9.47	7.95
Subject 15	0.08	0.07	0.07	0.07	0.06	0.05	5.64	5.59	6.09	6.25	6.17	6.15
Subject 16	0.15	0.15	0.08	0.09	0.05	0.05	11.06	12.02	8.87	9.24	7.72	9.02
Subject 17	0.16	0.14	0.09	0.10	0.04	0.05	10.70	12.44	10.59	9.10	10.69	9.53
Subject 18	0.11	0.11	0.09	0.09	0.06	0.07	7.06	6.71	7.32	8.14	6.00	6.95
Subject 19	0.07	0.07	0.08	0.08	0.04	0.04	9.06	8.50	8.37	8.57	6.73	6.73
Subject 20	0.09	0.09	0.07	0.07	0.05	0.05	8.74	8.18	7.87	6.32	7.31	5.05
Subject 21	0.06	0.06	0.09	0.08	0.04	0.04	12.16	10.40	6.97	6.91	6.51	6.56
Subject 22	0.07	0.07	0.10	0.10	0.06	0.06	8.89	9.03	10.18	8.80	4.94	5.52
Subject 23	0.06	0.08	0.08	0.07	0.05	0.07	9.68	11.71	7.53	7.93	6.19	6.41
Subject 24	0.06	0.07	0.07	0.07	0.05	0.04	7.25	8.56	9.07	8.87	5.63	5.71
Subject 25	0.08	0.07	0.09	0.09	0.07	0.06	10.32	9.38	9.11	8.48	7.82	8.82

Table 10: List of the relative segment motion (pelvis relative to chest) metrics for all human subjects exposed to Air vibration profile.

Air Vibration Profile - Pelvis Relative to Chest

Inertial Metric	RMS Acceleration						RMS Angular Velocity					
Axis	X Axis		Y Axis		Z Axis		X Axis		Y Axis		Z Axis	
Strap Tension	Low	Standard	Low	Standard	Low	Standard	Low	Standard	Low	Standard	Low	Standard
Subject 1	0.05	0.05	0.08	0.08	0.10	0.10	8.64	6.54	11.74	13.37	3.85	4.07
Subject 2	0.05	0.04	0.07	0.06	0.08	0.08	7.27	5.57	9.01	9.13	6.38	6.27
Subject 3	0.05	0.06	0.07	0.06	0.06	0.06	8.09	8.61	9.90	9.22	7.22	5.55
Subject 4	0.06	0.06	0.07	0.06	0.11	0.09	7.27	8.69	7.84	9.38	6.32	6.93
Subject 5	0.05	0.05	0.07	0.06	0.08	0.06	9.18	7.84	9.16	10.13	9.25	6.54
Subject 6	0.07	0.07	0.06	0.07	0.07	0.07	8.09	6.92	11.26	12.27	8.93	8.05
Subject 7	0.09	0.09	0.07	0.07	0.14	0.13	12.22	11.82	10.73	10.95	12.79	12.15
Subject 8	0.05	0.04	0.08	0.08	0.07	0.06	6.47	6.36	9.88	9.45	8.63	8.50
Subject 9	0.05	0.05	0.09	0.06	0.09	0.09	13.85	13.59	6.36	6.18	5.25	5.60
Subject 10	0.05	0.06	0.07	0.07	0.06	0.06	10.98	9.78	6.81	7.19	4.15	6.42
Subject 11	0.03	0.05	0.07	0.06	0.07	0.07	10.83	8.12	9.75	9.80	4.71	7.29
Subject 12	0.06	0.06	0.07	0.06	0.08	0.06	11.98	10.40	7.38	8.22	4.63	4.98
Subject 13	0.05	0.06	0.08	0.07	0.06	0.08	14.13	12.54	7.43	7.96	6.58	7.06
Subject 14	0.05	0.04	0.09	0.09	0.07	0.07	7.23	5.76	8.01	7.93	11.05	9.75
Subject 15	0.07	0.08	0.08	0.08	0.08	0.06	6.40	6.37	7.51	8.05	8.03	7.25
Subject 16	0.05	0.05	0.05	0.07	0.07	0.07	9.24	9.14	12.94	13.40	8.17	7.65
Subject 17	0.07	0.07	0.07	0.08	0.07	0.07	6.60	7.66	9.99	10.54	5.87	7.40
Subject 18	0.05	0.05	0.06	0.06	0.07	0.05	8.63	7.02	9.05	9.60	5.53	4.26
Subject 19	0.06	0.07	0.06	0.07	0.07	0.08	7.56	7.48	12.19	10.90	7.62	7.14
Subject 20	0.11	0.11	0.06	0.05	0.10	0.08	8.13	7.16	19.72	17.81	9.13	8.98
Subject 21	0.07	0.06	0.07	0.06	0.08	0.08	19.53	17.15	19.71	16.14	8.01	8.43
Subject 22	0.05	0.05	0.06	0.08	0.07	0.07	4.73	4.57	11.25	9.30	5.36	4.85
Subject 23	0.04	0.05	0.06	0.06	0.05	0.06	6.55	8.36	6.87	7.61	5.89	5.34
Subject 24	0.04	0.05	0.06	0.05	0.06	0.05	8.38	6.74	7.47	8.22	7.10	5.62
Subject 25	0.05	0.06	0.07	0.07	0.06	0.05	7.43	7.49	7.79	8.46	7.50	8.90

Table 11: List of the relative segment motion (head relative to chest) metrics for all human subjects exposed to the Ground vibration profile.

Ground Vibration Profile - Head Relative to Chest

Inertial Metric	RMS Acceleration						RMS Angular Velocity					
Axis	X Axis		Y Axis		Z Axis		X Axis		Y Axis		Z Axis	
Strap Tension	Low	Standard	Low	Standard	Low	Standard	Low	Standard	Low	Standard	Low	Standard
Subject 1	0.06	0.06	0.10	0.10	0.07	0.08	11.09	10.65	12.26	11.42	9.23	9.39
Subject 2	0.08	0.09	0.12	0.13	0.07	0.07	8.31	8.95	15.14	15.00	10.43	10.98
Subject 3	0.08	0.07	0.13	0.13	0.07	0.05	11.82	12.25	19.32	18.68	8.58	8.33
Subject 4	0.12	0.12	0.12	0.12	0.07	0.08	9.90	10.61	35.44	28.86	8.79	8.40
Subject 5	0.08	0.08	0.13	0.13	0.08	0.08	10.36	11.53	15.41	13.55	6.84	6.62
Subject 6	0.07	0.07	0.14	0.13	0.07	0.07	12.12	11.94	15.65	14.15	8.53	8.51
Subject 7	0.07	0.06	0.12	0.12	0.10	0.09	10.23	10.39	15.31	13.22	7.55	7.67
Subject 8	0.05	0.05	0.12	0.11	0.11	0.10	10.66	10.35	11.52	12.69	8.44	8.37
Subject 9	0.06	0.06	0.12	0.13	0.09	0.08	13.15	12.03	13.61	12.47	7.32	7.87
Subject 10	0.09	0.07	0.11	0.13	0.07	0.08	11.61	12.51	14.82	13.65	7.50	8.03
Subject 11	0.07	0.08	0.11	0.12	0.08	0.10	12.78	14.03	14.50	14.60	7.35	9.37
Subject 12	0.07	0.08	0.13	0.14	0.11	0.10	12.59	13.03	15.04	15.49	9.28	11.05
Subject 13	0.07	0.07	0.12	0.11	0.11	0.10	9.94	10.33	13.81	13.21	6.77	7.47
Subject 14	0.08	0.08	0.19	0.17	0.10	0.10	13.11	12.95	15.97	14.76	9.33	9.27
Subject 15	0.06	0.07	0.12	0.13	0.10	0.10	9.09	9.45	11.74	13.01	10.60	10.68
Subject 16	0.06	0.07	0.13	0.13	0.07	0.07	12.44	13.56	13.22	14.41	7.58	9.13
Subject 17	0.06	0.07	0.15	0.15	0.04	0.05	10.38	11.52	11.21	13.31	10.02	12.76
Subject 18	0.09	0.08	0.12	0.13	0.07	0.08	8.46	8.38	14.06	13.04	10.10	10.42
Subject 19	0.08	0.08	0.16	0.15	0.07	0.07	12.17	11.59	18.63	18.49	9.85	9.40
Subject 20	0.06	0.05	0.11	0.11	0.07	0.06	9.35	10.60	15.09	15.29	10.56	10.19
Subject 21	0.06	0.07	0.16	0.17	0.05	0.05	12.45	14.04	13.86	14.78	9.02	12.09
Subject 22	0.07	0.08	0.12	0.12	0.11	0.11	8.84	9.49	15.33	16.43	6.28	6.18
Subject 23	0.05	0.06	0.12	0.11	0.07	0.09	10.05	10.03	11.67	12.16	7.28	7.76
Subject 24	0.08	0.08	0.10	0.11	0.08	0.07	10.21	11.61	16.36	15.40	7.31	6.81
Subject 25	0.08	0.07	0.12	0.13	0.14	0.13	9.29	10.70	15.36	16.60	8.82	9.42

Table 12: List of the relative segment motion (pelvis relative to chest) metrics for all human subjects exposed to the Ground vibration profile.

Ground Vibration Profile - Pelvis Relative to Chest

Inertial Metric	RMS Acceleration						RMS Angular Velocity					
Axis	X Axis		Y Axis		Z Axis		X Axis		Y Axis		Z Axis	
Strap Tension	Low	Standard	Low	Standard	Low	Standard	Low	Standard	Low	Standard	Low	Standard
Subject 1	0.06	0.06	0.07	0.08	0.06	0.06	7.26	7.28	10.73	10.58	5.42	4.93
Subject 2	0.05	0.05	0.07	0.05	0.07	0.06	9.33	8.53	14.04	14.20	7.78	8.40
Subject 3	0.04	0.04	0.07	0.06	0.07	0.06	8.39	8.07	12.68	14.41	8.46	5.65
Subject 4	0.04	0.04	0.08	0.08	0.07	0.07	6.84	7.70	8.77	10.11	5.83	6.61
Subject 5	0.06	0.07	0.06	0.07	0.10	0.10	11.70	12.85	14.98	14.82	9.07	10.49
Subject 6	0.07	0.07	0.07	0.06	0.08	0.08	10.24	9.42	19.54	19.31	9.48	9.06
Subject 7	0.08	0.08	0.08	0.07	0.11	0.10	13.42	11.72	11.47	11.49	11.24	10.48
Subject 8	0.04	0.04	0.06	0.06	0.06	0.05	8.33	9.94	11.29	12.67	7.13	7.42
Subject 9	0.04	0.05	0.09	0.07	0.09	0.08	13.44	10.19	9.24	10.62	6.54	7.10
Subject 10	0.05	0.06	0.07	0.10	0.08	0.08	11.87	16.74	12.94	13.16	7.53	9.28
Subject 11	0.04	0.05	0.08	0.10	0.11	0.13	10.72	13.77	13.06	13.58	7.14	10.03
Subject 12	0.05	0.05	0.07	0.07	0.07	0.07	10.83	10.70	10.43	10.47	5.58	5.77
Subject 13	0.04	0.04	0.06	0.06	0.06	0.06	16.57	16.70	12.56	11.78	6.64	7.13
Subject 14	0.05	0.05	0.08	0.07	0.08	0.07	10.04	9.51	12.08	11.67	8.37	8.33
Subject 15	0.05	0.05	0.08	0.08	0.07	0.06	8.00	7.97	8.43	8.39	7.10	6.49
Subject 16	0.06	0.07	0.06	0.09	0.08	0.08	10.04	9.84	16.70	18.41	9.56	8.63
Subject 17	0.04	0.05	0.07	0.12	0.05	0.05	7.84	7.60	13.38	13.98	7.33	8.09
Subject 18	0.06	0.07	0.10	0.10	0.08	0.08	11.06	12.15	16.42	16.82	8.79	10.15
Subject 19	0.06	0.06	0.07	0.06	0.06	0.07	7.62	7.40	16.66	15.57	9.41	9.34
Subject 20	0.10	0.12	0.08	0.07	0.10	0.09	8.05	8.82	24.62	24.96	13.34	13.93
Subject 21	0.07	0.08	0.08	0.09	0.08	0.08	14.77	14.14	18.16	19.24	8.87	10.15
Subject 22	0.04	0.03	0.07	0.07	0.07	0.07	5.95	5.72	12.82	11.59	5.66	4.34
Subject 23	0.04	0.04	0.07	0.09	0.05	0.07	5.76	8.18	8.43	8.20	5.69	6.13
Subject 24	0.04	0.05	0.07	0.08	0.07	0.06	8.65	12.61	10.02	16.19	7.42	10.39
Subject 25	0.05	0.06	0.07	0.08	0.08	0.08	13.31	14.83	12.81	14.49	11.65	14.97

Table 13: List of the relative segment motion (head relative to chest) metrics for all human subjects exposed to the White Noise vibration profile.

White Noise Vibration Profile - Head Relative to Chest

Inertial Metric	RMS Acceleration						RMS Angular Velocity					
Axis	X Axis		Y Axis		Z Axis		X Axis		Y Axis		Z Axis	
Strap Tension	Low	Standard	Low	Standard	Low	Standard	Low	Standard	Low	Standard	Low	Standard
Subject 1	0.13	0.14	0.17	0.17	0.14	0.13	19.50	20.74	32.98	33.90	22.50	25.85
Subject 2	0.19	0.21	0.25	0.27	0.13	0.12	21.41	24.57	39.96	38.78	27.39	28.88
Subject 3	0.20	0.20	0.28	0.27	0.11	0.10	32.78	32.05	45.83	44.81	24.80	23.49
Subject 4	0.25	0.24	0.27	0.28	0.15	0.17	27.56	29.92	71.95	65.83	21.02	22.91
Subject 5	0.22	0.21	0.26	0.26	0.15	0.15	29.64	24.78	44.87	47.22	16.40	13.88
Subject 6	0.17	0.26	0.27	0.27	0.14	0.15	26.57	25.80	42.50	40.76	22.16	23.74
Subject 7	0.20	0.23	0.22	0.26	0.17	0.18	24.88	26.56	44.39	47.63	20.67	21.52
Subject 8	0.15	0.14	0.23	0.20	0.20	0.19	26.11	24.39	34.63	32.79	22.12	17.97
Subject 9	0.15	0.16	0.25	0.27	0.14	0.13	34.47	35.07	32.22	30.81	18.70	21.20
Subject 10	0.21	0.20	0.24	0.24	0.14	0.15	27.48	26.32	41.88	38.88	21.51	24.38
Subject 11	0.21	0.21	0.25	0.25	0.18	0.16	35.29	35.81	53.14	46.01	19.68	20.05
Subject 12	0.17	0.19	0.21	0.24	0.17	0.17	28.47	28.83	36.62	37.87	24.37	26.87
Subject 13	0.19	0.19	0.23	0.22	0.20	0.18	22.98	23.95	37.03	36.64	16.62	18.02
Subject 14	0.24	0.24	0.34	0.32	0.19	0.19	29.37	28.24	45.52	42.69	26.63	25.02
Subject 15	0.16	0.16	0.23	0.24	0.16	0.16	19.24	19.54	32.05	31.76	31.28	27.48
Subject 16	0.15	0.15	0.26	0.28	0.15	0.14	28.25	29.38	35.12	36.60	21.90	24.08
Subject 17	0.17	0.17	0.30	0.28	0.11	0.11	24.36	28.18	31.43	36.07	24.27	26.03
Subject 18	0.20	0.17	0.21	0.23	0.13	0.12	17.76	18.77	36.87	37.14	21.59	23.46
Subject 19	0.21	0.23	0.28	0.26	0.13	0.14	26.99	26.08	49.37	51.58	30.22	27.97
Subject 20	0.17	0.18	0.22	0.22	0.15	0.13	22.04	24.68	47.80	47.90	25.28	27.50
Subject 21	0.17	0.17	0.29	0.30	0.09	0.09	25.98	25.45	39.26	37.30	25.69	31.44
Subject 22	0.24	0.24	0.24	0.24	0.22	0.21	24.26	24.73	59.31	58.11	20.14	22.29
Subject 23	0.17	0.17	0.25	0.22	0.13	0.14	23.79	22.57	42.39	37.76	19.60	18.71
Subject 24	0.25	0.23	0.20	0.22	0.16	0.14	21.73	23.94	56.32	42.39	21.30	15.78
Subject 25	0.18	0.22	0.25	0.29	0.23	0.22	27.49	31.89	45.19	49.16	21.39	26.86

Table 14: List of the relative segment motion (pelvis relative to chest) metrics for all human subjects exposed to the White Noise vibration profile.

White Noise Vibration Profile - Pelvis Relative to Chest

Inertial Metric	RMS Acceleration						RMS Angular Velocity					
Axis	X Axis		Y Axis		Z Axis		X Axis		Y Axis		Z Axis	
Strap Tension	Low	Standard	Low	Standard	Low	Standard	Low	Standard	Low	Standard	Low	Standard
Subject 1	0.10	0.11	0.14	0.15	0.12	0.12	14.94	15.03	22.38	23.00	14.42	14.80
Subject 2	0.13	0.14	0.13	0.12	0.12	0.12	19.87	18.55	42.81	44.96	21.50	23.56
Subject 3	0.11	0.11	0.11	0.10	0.14	0.14	23.13	20.51	26.28	25.57	17.60	15.69
Subject 4	0.10	0.10	0.14	0.13	0.15	0.14	21.56	22.50	23.48	23.72	16.36	16.09
Subject 5	0.13	0.17	0.13	0.13	0.16	0.18	24.96	24.66	34.62	47.43	15.71	17.19
Subject 6	0.15	0.15	0.14	0.14	0.17	0.16	27.57	28.28	52.36	52.53	23.33	24.82
Subject 7	0.16	0.17	0.15	0.14	0.22	0.24	35.64	33.27	28.76	29.29	29.42	32.28
Subject 8	0.10	0.10	0.12	0.10	0.13	0.13	23.36	23.66	29.04	28.26	17.37	15.69
Subject 9	0.09	0.10	0.14	0.13	0.16	0.14	22.55	21.98	22.81	23.39	14.28	13.95
Subject 10	0.12	0.16	0.12	0.16	0.14	0.16	26.27	31.22	38.35	38.66	20.27	23.77
Subject 11	0.12	0.15	0.18	0.16	0.21	0.21	28.21	27.02	42.65	40.84	18.83	16.83
Subject 12	0.15	0.15	0.12	0.11	0.15	0.15	21.86	20.82	31.22	32.06	11.58	13.26
Subject 13	0.12	0.13	0.12	0.11	0.11	0.11	33.40	34.07	35.12	36.41	15.35	16.23
Subject 14	0.14	0.15	0.16	0.13	0.16	0.14	23.85	20.34	37.59	36.55	16.61	16.59
Subject 15	0.13	0.14	0.14	0.13	0.14	0.14	21.79	21.75	19.34	20.29	16.85	17.14
Subject 16	0.12	0.14	0.12	0.14	0.16	0.15	27.23	28.26	40.57	43.28	21.23	19.29
Subject 17	0.11	0.12	0.14	0.17	0.10	0.10	19.87	22.58	36.97	43.45	17.09	15.71
Subject 18	0.15	0.15	0.16	0.16	0.16	0.16	21.37	25.10	44.27	45.31	17.11	18.34
Subject 19	0.15	0.15	0.14	0.14	0.15	0.14	17.64	17.75	37.92	36.76	21.90	23.12
Subject 20	0.20	0.21	0.16	0.14	0.18	0.17	19.68	19.57	53.77	53.75	34.54	36.91
Subject 21	0.15	0.14	0.13	0.14	0.16	0.15	27.03	28.92	34.46	37.56	20.95	20.95
Subject 22	0.10	0.10	0.11	0.10	0.13	0.13	17.82	17.87	42.87	40.68	16.06	13.37
Subject 23	0.12	0.11	0.12	0.13	0.13	0.13	16.16	18.43	22.64	23.04	16.40	16.25
Subject 24	0.11	0.14	0.12	0.12	0.14	0.14	24.38	23.63	30.83	35.21	20.57	20.72
Subject 25	0.13	0.16	0.11	0.13	0.15	0.15	29.95	29.62	47.11	44.21	23.47	26.01

Hip Pitch and Roll Comparison

A generalized observation of the effect of low versus standard strap tension was that it caused the vibrational energy entering the subject to be redistributed among the segments. This redistribution was examined in terms of relative segment motion, but not in terms of overall motion. Therefore this section is dedicated to examining the roll (rotation about the global X axis) and pitch (rotation about the global Y axis) motions of the human hip segment. The aforementioned roll and pitch were calculated by taking the root mean square values of the X and Y axis gyroscope measurements respectively. This data was subjected to intra-subject normalization, which is why the results are reported as a ratio. No bandpass filter was applied. The results can be seen below in Figure 36.

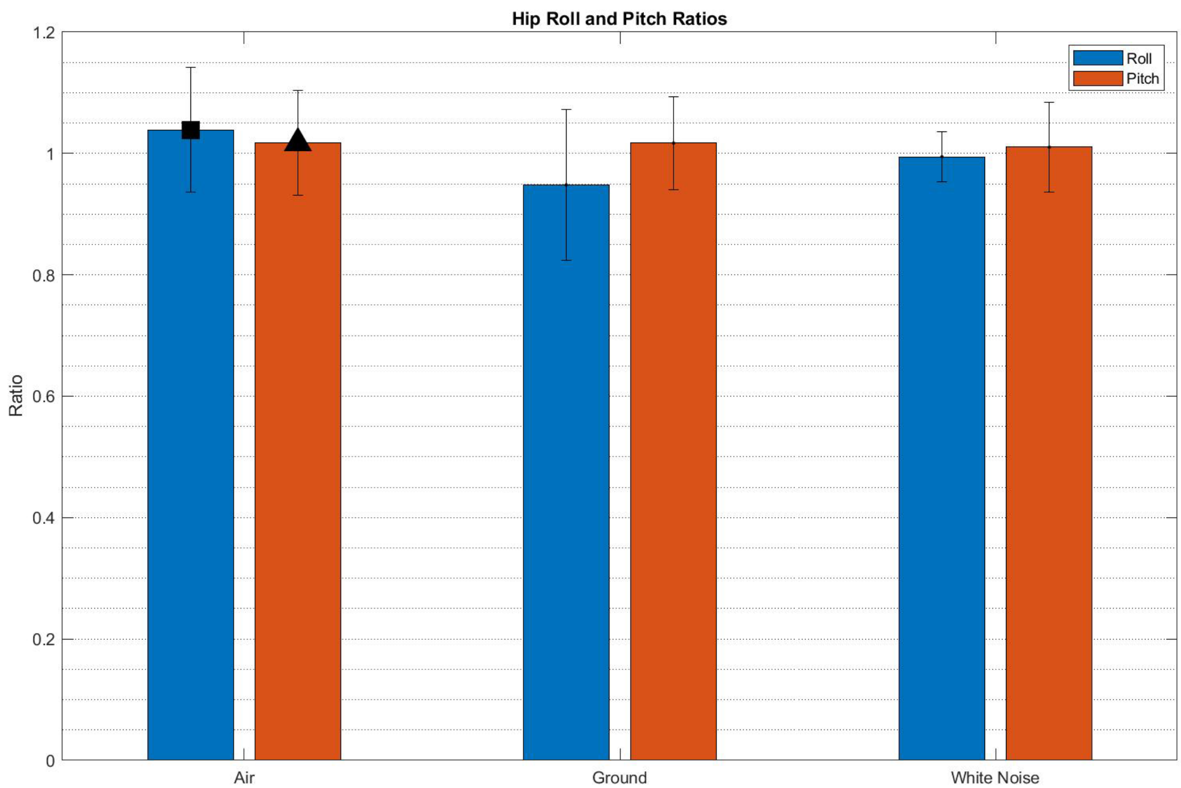

Figure 36: This figure shows how the roll and pitch motion of the hip segment (human) varies across the different vibration profiles. The results are reported as a ratio, as they have been subjected to intra-subject normalization. The black triangle signifies statistical significance and the black square signifies marginal statistical significance.

The results of Figure 36 only admitted two metrics with statistical significance, both associated with the air vibration profile. In both cases, the low tension condition led to ~2.5% roll and pitch motion when compared to the standard tension condition. This is in agreement with the earlier observation that when the input vibration is of high frequency, the relative motion of body segments is increased.

In order to further investigate this data set, it was decided to separate the data based on gender into male and female. Note that this separation was not accounted for in the original subject selection, and its results should be interpreted with that in mind. Only the results of the Ground vibration profile were accounted for, *and no intra-subject normalization was applied*. This reduced the number of parameters examined down to gender (male vs female), strap tension (low vs standard), and rotation type (roll and pitch). The results can be seen below in Figure 37 and Figure 38.

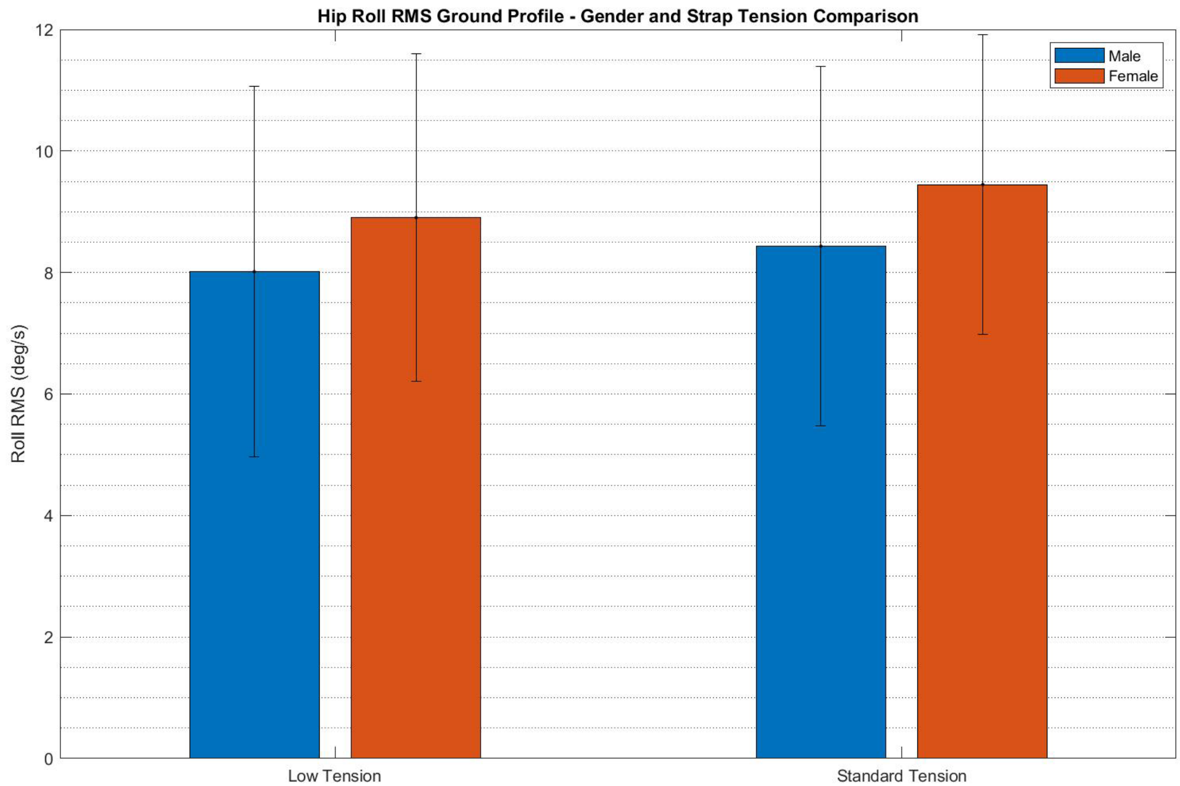

Figure 37: This figure shows how the roll motion of the hip segment in the ground vibration profile varied based on gender and strap tension. The results are reported as root mean square (RMS) values. Intra-subject normalization was no applied. The black triangle signifies statistical significance and the black square signifies marginal statistical significance (this plot shows no statistically significant results).

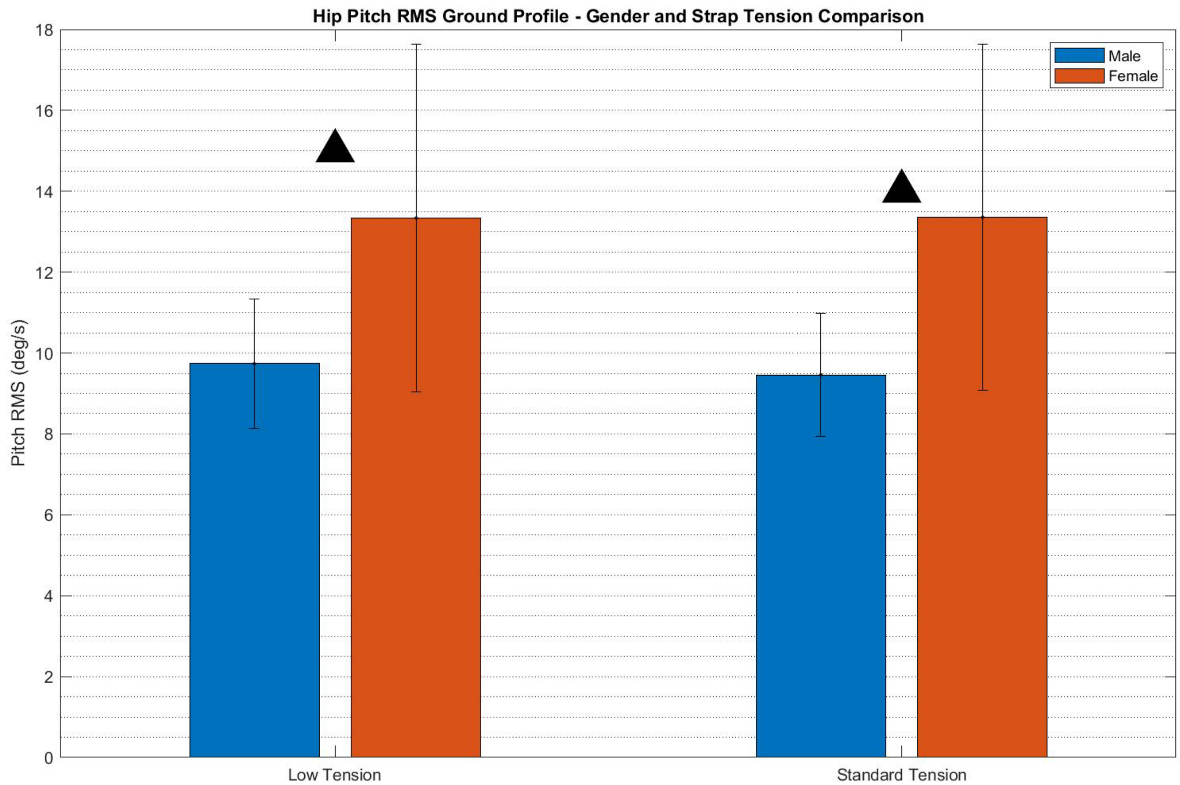

Figure 38: This figure shows how the pitch motion of the hip segment in the ground vibration profile varied based on gender and strap tension. The results are reported as root mean square (RMS) values. Intra-subject normalization was not applied. The black triangle signifies statistical significance, and the black square signifies marginal statistical significance (this plot shows that the male and female data sets differed in a statistically significant manner under both the low and standard tension conditions).

The results of Figure 37 show that the female subjects experienced greater roll motion under both strap tension conditions (differences were ~ 10%), but the differences were not statistically significant. The results of Figure 38 show that the female subjects experienced greater pitch motion under both strap tension conditions (differences were ~ 30%), and both differences were statistically significant.

As previously mentioned, subject selection was not performed in such a manner designed to allow for gender-based comparisons, which should be kept in mind when interpreting these results. However, Figure 37 and Figure 38 suggest that gender has an effect on hip motion during vibration. This is likely due to the differences in the shape of the pelvis between the two genders.

U.S. Army Aeromedical Research Laboratory
Fort Rucker, Alabama

All of USAARL's science and technical information documents are available for download from the Defense Technical Information Center.

https://discover.dtic.mil/results/?q=USAARL

Army Futures Command
U.S. Army Medical Research and Development Command